https://doi.org/10.35662/unine-thesis-3161

University of Neuchâtel, Switzerland

Faculty of Science

Centre for Hydrogeology and Geothermics (CHYN)

And

Chang'an University

School of Water and Environment

Infiltration and recharge processes in semi-arid regions

A thesis presented for the degree of Doctor of Sciences

by

Chengcheng Gong

Prof. Philip Brunner, University of Neuchâtel, Switzerland (Thesis Director)

Prof. Wenke Wang, Chang'an University, China (Thesis Director)

Prof. Harrie-Jan Hendricks-Franssen, Forschungszentrum Jülich, Germany (Rapporteur)

Prof. René Therrien, Université Laval, Canada (Rapporteur)

Prof. Laurel ThomasArrigo, University of Neuchâtel, Switzerland (Rapporteur)

Prof. Vetrimurugan Elumalai, University of Zululand, South Africa (Rapporteur)

Defended on September 5, 2024

unine
Université de Neuchâtel
Faculté des sciences

Rue Emile-Argand 11
CH-2000 Neuchâtel
doctorat.sciences@unine.ch

IMPRIMATUR POUR THESE DE DOCTORAT

La Faculté des sciences de l'Université de Neuchâtel autorise l'impression de la présente thèse soutenue par

Madame Chengcheng GONG

Titre :

"Infiltration and recharge processes in semi-arid regions"

sur le rapport des membres du jury composé comme suit :

- **Prof. Philip Brunner,** directeur de thèse, Université de Neuchâtel, Suisse
- **Prof. Wenke Wang,** co-directeur de these, Chang'an University, Chine
- **Prof. Laurel Thomas Arrigo,** Université de Neuchâtel, Suisse
- **Prof. Harrie-Jan Hendricks-Franssen,** Forschungszentrum Jülich, Allemagne
- **Prof. René Therrien,** Université Laval, Canada
- **Prof. Vetrimurugan Elumalai,** University of Zululand, Afrique du Sud

Neuchâtel, le 28 janvier 2025

Le Doyen, Prof. P. Brunner

Summary

Infiltration and recharge processes play an important role in the hydrological cycle. Robust estimation of recharge is critical for sustainable water resource management, especially in arid and semi-arid regions where surface water is limited and groundwater constitutes the main source of water throughout the year. However, the estimation of recharge remains a challenge as many of the controlling factors are difficult to measure. For example, evaporation and transpiration processes strongly influence recharge dynamics but are difficult to quantify. Moreover, transpiration and evaporation rates are also influenced by the depth to groundwater. The presence of vegetation influences the interception of rainfall, further affecting recharge dynamics, and this influence is difficult to quantify.

The goal of this thesis is to increase the robustness of recharge estimation, with a focus on semi-arid regions. The thesis is based on a combination of lysimeter experiments in Guanzhong Basin and Mu Us Sandy Land with numerical models.

In the first contribution, a systematic assessment of the reliability of four commonly used methods for estimating bare soil evaporation is carried out under consideration of variable depth to groundwater. The results show that the maximum entropy production method performed best for all water table depths. The extinction depth is an important indicator for considering methods for estimating evaporation.

Subsequently, the influence of shrub (*Salix psammophila*) on the infiltration process is investigated under both shallow and deep water table conditions. *Salix psammophila* is a phreatophyte which can absorb water from both groundwater and the vadose zone. In particular, the distribution of root density in response to shallow and deep water table depths was systematically analyzed. We focus our research on this specific species, as in the current, large reforestation projects in Mu Us Sandy Land, China is using this species. The results show that *Salix psammophila* afforestation can cause a decline of the water table, prevent groundwater recharge, and reduce effective infiltration.

In the third contribution, the thesis focuses on investigating whether actual recharge can be uniquely extracted from variably saturated subsurface flow models. As variably saturated subsurface flow models conceptualize and simulate water flow in both the unsaturated and saturated zones, recharge is expected to be reliably extracted from such kinds of models. The results show that actual recharge cannot be uniquely extracted from variably saturated subsurface flow models, as opposed to the potential recharge.

Finally, we evaluated the performances of different methods to estimate specific yield for

estimating recharge under different water table conditions. In particular, the depth-dependency of specific yields was examined for estimating recharge. The results indicate that the estimation of recharge can be enhanced through the utilization of depth-dependent specific yield, contingent upon the acquisition of reliable parameters.

From a methodological point of view, the combination of lysimeter experiments with different water table depths and variably-saturated subsurface flow models constituted a powerful approach for exploring infiltration and recharge processes under natural conditions.

Keywords

Infiltration; Groundwater recharge; Evaporation; Evapotranspiration; Variably-saturated subsurface flow model; Water table fluctuation method; Specific yield; Vegetation; Afforestation; Water table depth; Water resources management; Arid and semi-arid regions

摘要

入渗和补给过程在水文循环中发挥着重要作用。加强地下水补给量的准确估计对于水资源的可持续开发利用至关重要，尤其是在干旱和半干旱地区，地表水资源匮乏，地下水成为全年重要的水源。然而，由于影响补给量估计的因素难以观测，因此精确计算地下水的补给量仍面临挑战。例如，蒸散发过程对补给的动态变化有显著影响，但很难进行定量分析。此外，地下水的埋深也会影响蒸散发速率。植被的存在能够截留降雨，进一步影响补给的动态变化速率，但这种影响同样难以定量化。

论文将在半干旱区关中盆地和毛乌素沙地开展一系列的蒸渗仪实验并结合数值模拟的方法，研究入渗和补给的机理，增强补给计算的可靠性。

论文的第一个贡献是，考虑在影响入渗补给动态方面蒸发的重要性，论文系统评估了四种常用的裸土蒸发量计算方法在不同的地下水位埋深条件下计算蒸发量的可靠性。研究表明最大熵增蒸散法在不同地下水位埋深条件下都能较好地计算蒸发量。极限蒸发深度是选择蒸发量计算方法的重要参考指标。

随后，研究了毛乌素沙地典型的灌木（沙柳，*Salix psammophila*）在浅地下水位埋深和深地下水位埋深条件下对入渗补给过程的影响。沙柳是一种能吸收地下水和包气带水的深根植物。需要重点指出的是，本文系统地分析了在浅水位和深水位深度的条件下根系密度的分布状态。之所以本论文重点研究沙柳是因为在中国毛乌素沙地当前的大规模植树项目中，沙柳被广泛地种植。研究表明种植沙柳会引起地下水位下降，减少地下水的补给和降雨有效入渗量。

第三个贡献，论文重点研究了是否可以从变饱和地下水流模型中得到唯一且可靠的实际地下水补给量。由于变饱和地下水流模型能够同时模拟饱和带和非饱和带水流，因此人们对从该模型中获取可靠的补给量寄予厚望。研究表明，基于变饱和地下水流模型无法获得唯一可靠的实际补给量，但可以获得唯一的潜在地下水补给量。

最后，论文评价了在不同地下水位埋深条件下，采用不同的给水度定义方法计算地下水补给量的可靠性，尤其是系统地分析了与地下水位埋深有关的给水度计算补给量的可靠性。研究结果表明如果可以获得可靠的土壤水分特征曲线参数，采用考虑地下水位埋深的给水度可以提高地下水位补给量计算的精度。

从方法的角度来看，将不同地下水位埋深的蒸渗仪试验与变饱和的地下水流数值模型的方法相结合，能够有效地用于探索自然条件下的入渗和补给过程。

关键词

入渗；地下水补给；蒸发；蒸散发；变饱和地下流模型；水位波动法；给水度；植被；植树造林，地下水位埋深；水资源管理；干旱半干旱区

Résumé

Les processus d'infiltration et de recharge jouent un rôle important dans le cycle hydrologique. Une estimation robuste de la recharge est essentielle pour une gestion durable des ressources en eau, en particulier dans les régions arides et semi-arides où l'eau de surface est limitée et les eaux souterraines constituent la principale source d'eau tout au long de l'année. Cependant, l'estimation de la recharge reste un défi, car de nombreux processus importants sont difficiles à mesurer. Par exemple, les processus d'évaporation et de transpiration influencent fortement la dynamique de la recharge, mais sont difficiles à quantifier. De plus, les taux de transpiration et d'évaporation sont également influencés par la profondeur de la nappe phréatique. La présence de végétation influence l'interception des précipitations, affectant ainsi la dynamique de la recharge, et cette influence est difficile à quantifier.

L'objectif de cette thèse est d'accroître la robustesse de l'estimation de la recharge, en se concentrant sur les régions semi-arides. La thèse s'appuie sur une combinaison de mesures lysimétriques dans le bassin du Guanzhong et dans le désert de Mu Us avec des modèles numériques.

Dans la première contribution, une évaluation systématique de la fiabilité de quatre méthodes couramment utilisées pour estimer l'évaporation du sol nu est réalisée en tenant compte de la profondeur variable de la nappe phréatique. Les résultats montrent que la méthode de la production maximale d'entropie a donné les meilleurs résultats pour toutes les profondeurs de nappe phréatique. La profondeur d'extinction (profondeur maximale d'évapotranspiration) est un indicateur important à considérer pour les méthodes d'estimation de l'évaporation.

Ensuite, l'influence de l'arbuste, Salix psammophila, sur le processus d'infiltration est étudiée dans des conditions de nappe phréatique peu profonde et profonde. Salix psammophila est une phréatophyte capable d'absorber de l'eau à la fois de la nappe phréatique et de la zone vadose. En particulier, la répartition de la densité des racines en réponse à des profondeurs de nappe phréatique peu profondes et profondes a été systématiquement analysée. Nous concentrons notre recherche sur cette espèce spécifique, car dans les projets de reforestation à grande échelle en cours dans le désert de Mu Us, la Chine utilise cette espèce. Les résultats montrent que le reboisement de Salix psammophila peut provoquer une baisse de la nappe phréatique, empêcher la recharge des eaux souterraines et réduire l'infiltration effective.

Dans la troisième contribution, la thèse se concentre sur l'investigation de la possibilité d'extraire de manière unique la recharge réelle à partir de modèles de flux souterrain variablement saturé. Étant donné que les modèles de flux souterrain variablement saturé

conceptualisent et simulent le mouvement de l'eau à la fois dans les zones non saturées et saturées, il est attendu que la recharge puisse être extraite de manière fiable à partir de ce type de modèles. Les résultats montrent que la recharge réelle ne peut pas être extraite de manière unique des modèles de flux souterrain variablement saturé, contrairement à la recharge potentielle.

Enfin, nous avons évalué les performances de différentes méthodes pour estimer la porosité efficace lors de l'estimation de la recharge sous différentes conditions de nappe phréatique. Les résultats indiquent que l'estimation de la recharge peut être améliorée par l'utilisation de porosités efficaces dépendantes de la profondeur, sous réserve de l'acquisition de paramètres fiables.

D'un point de vue méthodologique, la combinaison de mesures lysimétriques avec différentes profondeurs de nappe phréatique et de modèles de flux souterrain variablement saturé constitue une approche puissante pour explorer les processus d'infiltration et de recharge dans des conditions naturelles.

Mots-clés

Infiltration; Recharge des eaux souterraines; Évaporation; Évapotranspiration; Modèle de flux souterrain variablement saturé; Méthode de fluctuation de la nappe phréatique; Rendement spécifique; Végétation; Reforestation; Profondeur de la nappe phréatique; Gestion des ressources en eau; Régions arides et semi-arides.

Acknowledgments

I would like to express my sincere gratitude to all those who have supported me throughout my journey to completing this thesis.

First and foremost, I would like to express my deepest gratitude to my supervisors, Prof. Philip Brunner and Wenke Wang, for their invaluable supervision and support throughout my entire doctoral journey. Your expertise and constructive feedback have played a crucial role in my research. I am especially thankful for your encouragement during challenging times, which motivated me to persevere and strive for excellence. I am grateful to Prof. Brunner for his patience in supervising my research and imparting the principles of rigorous scientific research. Thanks a lot to Prof. Wang for providing an advanced research platform. Without your input and supervision, I would not have been able to complete my thesis.

Secondly, I would like to t express my gratitude to the members of my thesis committee, Prof. Harrie-Jan Hendricks-Franssen, René Therrien, Laurel Thomas Arrigo, and Vetrimurugan Elumalai for their meticulous reading of my thesis and for providing me with invaluable insights and constructive feedback. Meanwhile, many thanks to Prof. Peter Cook for his diverse perspectives and critical insights which have helped me to improve the quality of my recharge paper.

My sincere thanks go to my colleagues and friends, Fabien Cochand, Asame, Maria, Roberta Perio, Saeed Mhanna, Blanc Théo at the University of Neuchatel and Lei Duan, Zhoufeng Wang, Zaiyong Zhang, Peiyuan Yu, Jie Luo, Haizhen Ma at Chang'an University. In particular, thanks a lot to Dr. Fabien Cochand for his support with the HydroGeoSphere model and Zaiyong Zhang for his assistance in revising papers with me. Working alongside you has fostered a collaborative spirit that made my research journey enjoyable. Of course, I am particularly grateful to Yoshiko Sudo-Brunner, Taline Cochand, as well as Fabien's parents for their help and companionship in my life, which has made my life colorful and not lonely.

I appreciate the support from the administrative staff in Neuchatel, particularly Sabine Erb, Corinne Carraux, Carine Erhard, Roberto Costa, as well as Marie-France Farine for their assistance with the logistics and organization of my study. Their contributions were essential to the completion of my research.

I would also like to acknowledge the financial support from the China Scholarship Council (201906560022) and the Short-Term Study Abroad Program for Postgraduate students (No.0021/300203110004).

Lastly, I would like to express my gratitude to my family. To my parents and my husband, thank you for your unwavering support and belief in me. Your encouragement is the driving force that keeps me going.

Thank you all for your contributions, supervision, and support. This thesis would not have been possible without you.

Contents

Chapter 1 General Introduction

1.1 Context and Motivation

Groundwater constitutes the largest freshwater resource in the world, which is vitally important for drinking water production, irrigated agricultural water consumption, industrial water use, as well as water consumed by ecosystems (Aeschbach-Hertig and Gleeson, 2012; Taylor et al., 2012). In arid and semi-arid regions, groundwater is often the only available perennial water resource (Aeschbach-Hertig and Gleeson, 2012; de Vries and Simmers, 2002; Kinzelbach et al., 2010; Wang et al., 2021). In the context of climate change, the surface area of arid and semi-arid regions is expanding globally (Huang et al., 2015). The demand for groundwater resources continues to increase (Scanlon et al., 2023; Scanlon et al., 2006). The concomitant growth in population and climate change-induced increases in water usage, further increase the need for sustainable groundwater management.

The sustainable management of groundwater resources necessitates the maintenance of a sustainable yield, which is contingent upon achieving a long-term equilibrium between the volume of groundwater extracted and the rate at which it is naturally replenished. This is different from the concept of safe yield, which only considers the maximum amount of groundwater that can be extracted without causing significant depletion or adverse environmental impacts in the short term (Alley and Leake, 2004). The implementation of sustainable yield and management practices can ensure the long-term ecological health and resource availability of groundwater resources. Groundwater recharge is an important consideration for sustainable groundwater management (Healy, 2010; Healy and Cook, 2002; Nimmo et al., 2006; Scanlon et al., 2006; Sophocleous, 2005). Estimation of groundwater recharge rates accurately is not only considered to be vital for the sustainable development of groundwater resources management and protection of ecosystems, but also provides essential information for contaminant transport (Dassargues, 2018; Healy and Cook, 2002). In addition, recharge is often used as an input parameter in groundwater modeling approaches (Sanford, 2002).

Precipitation and the subsequent infiltration is one of the main contributions to groundwater recharge. Despite the large number of studies focusing on recharge, the relation between infiltration and recharge remains uncertain, as it is influenced by evapotranspiration, intensity and duration of precipitation, land use and cover, the thickness of the vadose zone, as well as soil properties (Scanlon et al., 2002; Scanlon et al., 2005; Wang et al., 2015; Zhang et al., 2021). Moreover, climate change affects groundwater recharge through changes in

precipitation patterns, the occurrence of droughts, and the frequency of such events. Additionally, an increase in temperature results in increasing evaporation rates, which subsequently reduce groundwater recharge. Furthermore, elevated evaporation rates can impact the quantity and quality (including an increase in salinity) of groundwater (IPCC, 2014). Meanwhile, the impact of climate change on vegetation growth and physiological states, such as leaf area index (LAI), can indirectly influence groundwater recharge through alterations in evapotranspiration (Anurag et al., 2021; Chen et al., 2010). As a consequence of all these complexities, recharge varies greatly in both time and space (Healy, 2010). In addition, recharge is difficult to measure directly (Scanlon et al., 2002). Therefore, recharge is still one of the least understood hydrological processes (Healy, 2010).

1.2 Qualitative description of infiltration and groundwater recharge processes

Infiltration is the water transport from the surface to the subsurface (Figure 1.1). Factors such as soil properties, land use and land cover, initial soil water content, water table depths as well as climatic conditions can influence the infiltration and recharge rates (Zhang et al., 2023) as above mentioned. If the ground is covered by vegetation, the canopy also intercepts water and reduces infiltration. Meanwhile, plant roots can uptake infiltrating water and transpirate through stems and leaves. However, the presence of roots may facilitate the preferential flow of water through the unsaturated zone to the water table, particularly in low-permeability soils. This can lead to an increase in recharge (Le Maitre et al., 1999).

In arid and semi-arid regions, groundwater-dependent vegetation plays an important role in water, soil, and land management. For example, to prevent desertification and increase carbon sequestration, large-scale afforestation programs have been implemented in Mu Us Sandy Land, China (Zhao et al., 2020). Vegetation cover prevents desertification by reducing wind erosion and soil hardness. An increase in vegetation cover can increase the roughness and friction of the surface and thus reduce the wind speeds and erosion close to the soil surface (Li et al., 2003). However, Zhao et al. (2020) pointed out that the total terrestrial water storage significantly declined after the land restoration in Mu Us Sandy Land, China. Huang et al. (2020) highlighted that large-scale land use and cover change can influence infiltration, and they concluded that the estimation of recharge rates decreased under vegetated conditions. However, several important aspects remain poorly understood in this context, and the uncertainties of the previously employed methods are significant, thus undermining efficient and sustainable water and land management. For example, how the vegetation reacts to declining water tables remains unclear.

During the infiltration process, water can also be lost to the atmosphere through

evaporation. If, however, water infiltrates below the so-called zero flux plane, it can no longer be lost to the atmosphere through evaporation or be taken up by plants, and thus eventually will contribute to the groundwater system. The infiltrated water below the root zone or extinction depth is called potential recharge. Potential recharge passes through the vadose zone and arrives at the saturated zone. There is a time lag between potential recharge and groundwater reaching the saturated zone. Especially in arid and semi-arid regions, the lag time can be quite long due to the thick vadose zone (Nazarieh et al., 2018; Rossman et al., 2014). However, the lag effects arising from the vadose zone are often neglected in evaluating the groundwater resources (Wang et al., 2021).

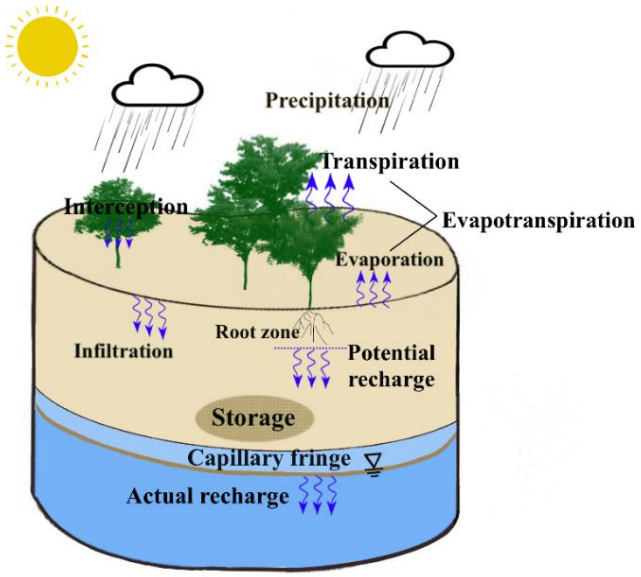

Figure 1.1 Schematic diagram of infiltration and groundwater recharge processes

1.3 Definitions of infiltration and recharge

Infiltration is defined as "*the entry of water into the soil surface and its subsequent vertical motion through the soil profile*" (Brutsaert, 2005). As opposed to the clear definition of infiltration, recharge has not been defined uniquely. For example, Healy (2010) defined groundwater recharge as "*the downward flow of water reaching the water table, adding to groundwater storage*", which referred to actual recharge. Freeze and Cherry (1979) defined recharge as "*the entry of water to the saturated zone*". However, Delleur (2006) claimed that "*Deep soil water percolation, often referred to as groundwater recharge by soil scientists, is the water that has moved past the evaporative and root zones in the vadose zone and is no longer available to plants.*" Scanlon et al. (2002) pointed out that water movement below the zero flux plane or root zone cannot evaporate or transpire is referred to as percolation, drainage, or net infiltration, corresponding to potential recharge. In addition, other definitions of recharge are implicit in approaches that quantify recharge through the response of the system to

infiltration and drainage. For example, the water table fluctuation (WTF) method relates a rise in the water table to groundwater recharge (Healy and Cook, 2002). In the context of sustainable water management, obtaining an accurate and unique recharge value is necessary. Although the above-mentioned recharge definitions have been proposed, it is still not clear whether a reliable recharge value can be obtained based on the existing definitions.

1.4 Methods for Estimating Groundwater Recharge

Many methods have been proposed for estimating groundwater recharge, such as numerical models, the water table fluctuation method, the water budget method, tracer methods, as well as the use of lysimeters.

1.4.1 Water budget method

The water budget method quantifies recharge as a residual of precipitation and runoff as well as evapotranspiration (ET) (Healy, 2010). In arid and semi-arid regions, ET plays an important role in the hydrological cycle (Figure 1.1), as the rate of ET is nearly equal to precipitation (Dassargues, 2018; Kurc and Small, 2004). Brandes and Wilcox (2000) pointed out that ET accounts for around 95% of annual precipitation in arid and semi-arid regions. Dassargues (2018) highlighted that the uncertainty of the estimation of ET can affect decision-making. Therefore, the estimation of ET accurately is critical for evaluating recharge (Van Camp et al., 2016).

Bare soil evaporation is an important component of ET. Although there are many methods available for estimating soil evaporation, such as the water level fluctuation method (Cheng et al., 2013), Darcy's law method (Chen et al., 2018), maximum entropy production (Wang and Bras, 2011), and numerical modeling methods (Jefferson and Maxwell, 2015) or soil moisture balance methods (Zhang et al., 2018), quantifying soil evaporation remains challenging as it is concurrently influenced by climatic conditions, surface temperature, soil properties, water table depth, to mention just a few (Allen et al., 1998; Hellwig, 1973; Zhang et al., 2018). While laboratory studies and numerical tests indicated that the water table depth is important for the estimation of soil evaporation (Ma et al., 2019; Hellwig, 1973), the water table position is rarely considered in approaches employed in the field. In fact, the performance of different methods for estimation of bare soil evaporation under different water table conditions still needs to be explored.

Transpiration is the other component of ET. Canopy can intercept precipitation and reduce infiltration (Figure 1.1). Moreover, the roots of vegetation can uptake infiltrating water and transpire through stems and leaves. Costa et al. (2023) pointed out that groundwater is tightly associated with soil water content through the water table depth. The soil water status is critical

for the plant water uptake and its growth (Vanderborght et al., 2023). O'Connor et al. (2019) also highlighted that the water table depth strongly influenced the ET in vegetated areas, and that shallow water table depths can promote water uptake compared to deep water table depths. Therefore, considering the water table depth is critical for quantifying ET (Soylu et al., 2011).

1.4.2 Numerical modeling approaches

Groundwater models can simulate the movement of groundwater. "Classical" groundwater models such as MODFLOW (Harbaugh, 2005) can simulate saturated groundwater flow only, and do not explicitly take the vadose zone into account (Sanford, 2002). For such a conceptualization, recharge is required as an input boundary condition. On the other hand, variably-saturated subsurface flow models such as HydroGeoSphere (Aquanty, 2018) simulate water movement in both the unsaturated and saturated zones. One might expect that recharge can be easily extracted using such models. In fact, there are some studies which have used such models to estimate potential recharge, such as Hu et al. (2019) and Hou et al. (2016) simulating lysimeter settings. Few studies have used variably saturated subsurface flow models to estimate actual recharge, and there is no generally accepted methodology for extracting groundwater recharge from such models.

1.4.3 Water level fluctuation method

A simple and commonly used method to estimate actual recharge is the water level fluctuation method (Crosbie et al., 2005; Cuthbert, 2010; Sophocleous, 1991). It only needs data about the change in the water table and a parameter of specific yield. A difficulty in using this method is estimating the specific yield. The specific yield is influenced by many factors, such as water table depth, soil properties, time, and vegetation (Logsdon et al., 2010; Lv et al., 2021), resulting in high uncertainty (Crosbie et al., 2019). Depending on the water table depth and time, the specific yield can be classified into three types, which are the so-called ultimate specific yield, the apparent specific yield (depth-dependent specific yield), and the transient specific yield (time-dependent specific yield) (Lv et al., 2021). The ultimate specific yield is a constant, representing situations in which a static equilibrium is achieved and the soil is fully drained by gravity. Zhang et al. (2020) and Crosbie et al. (2005) point out that recharge was overestimated based on the ultimate specific yield. Estimation of recharge rates based on depth-dependent specific yield has been used, such as Crosbie et al. (2019) and Fan et al. (2014). However, few studies have compared the estimated results to actual recharge, and the performances of the depth-dependent specific yield for estimation recharge remain unclear.

1.4.4 Lysimeters method

Lysimeters are a useful tool for quantifying recharge for different soil types and

landcovers under natural climatic conditions (Healy, 2010; Pütz et al., 2018). There are different types of lysimeters. Zhang et al. (2023) used the weighing lysimeter to explore the dynamics of potential recharge under bare ground conditions in Mu Us Sandy Land, China. The weighing lysimeter is supported on a load cell or a scale that can continuously measure the total weight of the soil, water, and any vegetation present. The weighing system is of critical importance for the calculation of water loss. A drainage system may be included at the bottom of the lysimeter, allowing excess water to escape. By measuring the drainage flux at the bottom of the lysimeter (representing potential recharge), allows to estimate evapotranspiration using a water balance approach. The advantage of weighing lysimeter is that the discharge can be directly observed and the soil in the lysimeter remains undisturbed. However, the cost of purchasing and installing a weighing lysimeter is considerable. Furthermore, the cost associated with maintaining this equipment over time is also not cheap. Alternatively, non-weighing lysimeters can be used to study recharge. For example, Zhang et al. (2020) investigated the influence of temperature on groundwater recharge in a semi-arid region in China using a large non-weighing lysimeter. The bottom of the non-weighing lysimeter is sealed, and there is a sensor inside the lysimeter which can measure the dynamics of the water table depth in response to rainfall and evaporation. Non-weighing lysimeters are cheaper than weighing lysimeters. The disadvantage of non-weighing lysimeters is that recharge cannot be measured, but is determined indirectly through soil moisture and groundwater dynamics.

1.5 Research gaps and Objectives

1.5.1 Research gaps

Based on the above literature review, several interesting research gaps can be identified. Firstly, there are many methods for estimating bare soil evaporation, but the performances of different methods to estimate evaporation under dynamic water table depths remain unexplored. This is a major shortcoming, given that the depth of groundwater can vary significantly over time. Secondly, quantifying the influence of the plants, in particular phreatophytes, on infiltration and recharge processes remains unclear and challenging. These questions are of particular importance for afforestation projects. Finally, the applicability of variably-saturated subsurface flow models to estimate recharge remains largely unexplored and should be investigated. Further study is required to gain a deeper understanding of the performance of different determination methods for specific yield based on the water level fluctuation method to estimate recharge under different water table depths.

1.5.2 Objectives

The main objectives of this thesis are as follows:

(1) Evaluate the performances of four commonly used methods, including the FAO-56 method with skin evaporation enhancement, maximum entropy production method, groundwater level fluctuation method, and Darcy's law method, for estimating bare soil evaporation under different water table depths conditions in a semi-arid region.

(2) Quantify the influence of plants on infiltration and recharge processes under different hydrological conditions. The threshold of minimum precipitation for increasing the soil water content on the surface ground will be quantified. How the plant grows adaptively under deep and shallow water table depths will be systematically analysed.

(3) Explore whether a unique value of actual recharge can be extracted based on the variably-saturated subsurface flow models.

(4) Assess the performances of estimation of recharge obtained from different methods for calculating the specific yield under different water table depth conditions. In particular, we evaluate recharge results based on depth-dependent specific yield in contrast with actual recharge under different water table depths.

1.6 Research area

To accomplish the objectives of this thesis, we carried out field experiments in the Guanzhong Basin and Mu Us Sandy Land, China, which are semi-arid regions (Figure 1.2). Mu Us Sandy Land is one of the four main sandy lands in China where large-scale afforestation programs were implemented with a view to addressing ecological and environmental concerns (Huang et al., 2020). The geomorphic features of the Mu Us Sandy Land include fixed dunes, semi-fixed dunes, and well-vegetated inter-dune wetlands, and the topography of the sandy land is slightly undulating from southwest to northeast (Liang and Yang, 2016). The Guanzhong Basin is characterized by a northwest-oriented valley between the Qinling Mountain Range in the south and the Beishan Mountain Range in the north. The basin transitions from a pluvial plain to a loess tableland and valley terrace on both the north and south sides of the valley (Wang et al., 2018). Since the water table depth is an important influencing factor for the infiltration process and recharge, it is necessary to explore the infiltration and recharge process under different water table depth conditions. Taking the cost of the instruments and the cost of installation and maintenance into account, the non-weighing lysimeters with different water table depths were designed and used in this thesis. In the two field experimental sites, four lysimeters were built at each site. In the Guanzhong Basin, the four lysimeters represent bare soil with different water table depths, and in Mu Us Sandy Land, the four lysimeters are two pairs, and one pair being bare ground, and the other pair being vegetated ground. The thesis is focused on *Salix psammophila*, the dominant vegetation type

in Mu Us Sandy Land. *Salix psammophila* is a phreatophyte, which can absorb water from both groundwater and the vadose zone (Huang et al., 2016). A detailed description of the field experiments will be introduced in the following chapters.

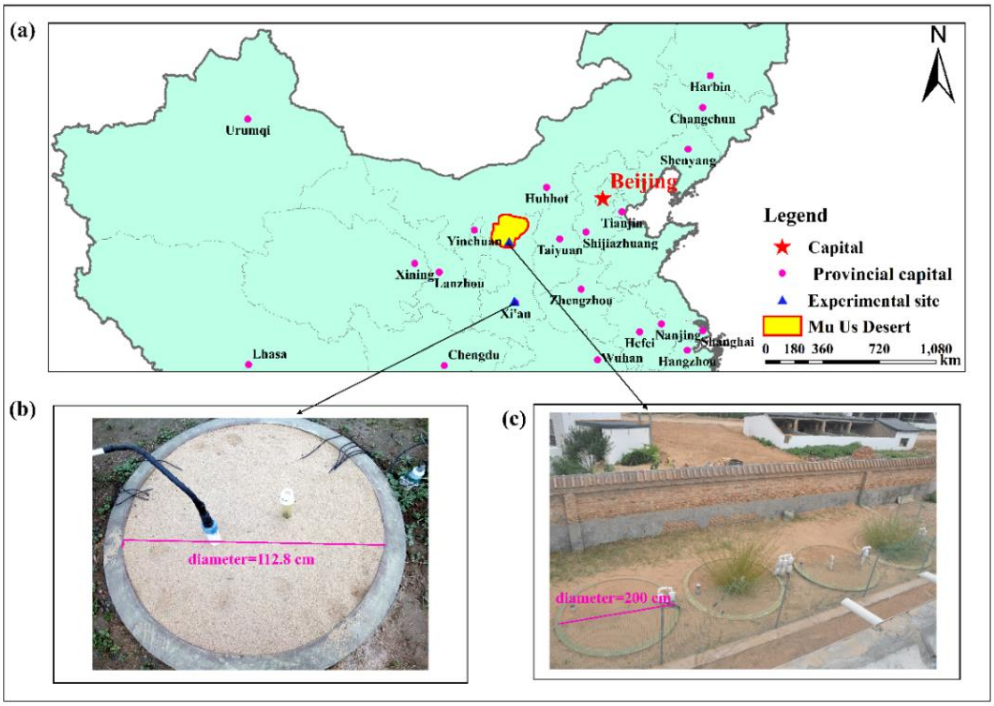

Figure 1.2 Location of field experimental sites, (a) the location of two field experimental sites in Northwest China; (b) lysimeter experiments in the Guanzhong Basin; (c) lysimeter experiments in the Mu Us Sandy Land.

1.7 Structure of the Thesis

Chapter 1 provides the general introduction and clarifies the objectives and structure of the thesis.

Chapter 2 evaluates the performance of four commonly used methods for estimating bare soil evaporation under different water table depths systematically in the Guanzhong Basin. The estimation of evaporation rates is compared to the actual evaporation. The results will provide references for choosing methods to estimate evaporation and improve the accuracy of calculating potential recharge. (This chapter was published in the Journal of Hydrology)

Chapter 3 focuses on exploring how the *salix psammophila* influences the infiltration and recharge processes. We systematically analyze the root adaptability of *salix psammophila* under shallow and deep water table condition, and propose the conceptual model of *salix psammophila* rooting density. Quantify the influence of *salix psammophila* on the groundwater and soil water based on the lysimeter data in Mu Us Sandy Land. In addition, the minimum precipitation for increasing the soil water content on the surface ground is quantified. (This

chapter was published in Science of the Total Environment)

Chapter 4 explores whether the actual recharge can be uniquely extracted based on the variably-saturated subsurface flow models. We set up the simplest one-dimensional models to simulate the infiltration process. The cases used in this chapter covered all possible lower boundary conditions. We deliberately use simple models is that if the extraction of recharge cannot be obtained reliably from these simplest models, it will also be impossible to do so in more sophisticated conditions. (This chapter was published in Water Resources Research)

Chapter 5 evaluates the performances of different methods to calculate the specific yield for estimating recharge in contrast with actual recharge using lysimeter data in the Guanzhong Basin. In particular, we used depth-dependent specific yield to estimate recharge, and the estimation of recharge from depth-dependent specific yield is contrasted with actual recharge. (This chapter was published in Science of the Total Environment)

Chapter 6 summarizes the main findings of the thesis and the outlook for future studies.

References

Aeschbach-Hertig, W., Gleeson, T., 2012. Regional strategies for the accelerating global problem of groundwater depletion. Nature Geoscience, 5(12): 853-861.

Allen, R.G., Pereira, L.S., Raes, D., Smith, M., 1998. FAO Irrigation and drainage paper No. 56. Rome: Food and Agriculture Organization of the United Nations, 56(97): e156.

Alley, W.M., Leake, S.A., 2004. The journey from safe yield to sustainability. Groundwater, 42(1): 12-16.

Anurag, H., Ng, G. H. C., Tipping, R., and Tokos, K. (2021). Modeling the impact of spatiotemporal vegetation dynamics on groundwater recharge. Journal of Hydrology 601.

Aquanty Inc. (2018). HydroGeoSphere: A three-dimensional numerical model describing fully-integrated subsurface and surface flow and solute transport. Waterloo. Retrieved from https://www.aquanty.com/hgs-download.

Brandes, D., Wilcox, B.P., 2000. Evapotranspiration and soil moisture dynamics on a semiarid ponderosa pine hillslope. Journal of the American Water Resources Association, 36(5): 965-974.

Brutsaert, W., 2005. Hydrology: An introduction. Cambridge University Press, United Kingdom. DOI:https://doi.org/10.1017/CBO9780511808470.

Chen, C., Wang, E., and Yu, Q. (2010). Modelling the effects of climate variability and water management on crop water productivity and water balance in the North China Plain. Agricultural Water Management 97, 1175-1184.

Chen, L., Wang, W., Zhang, Z., Wang, Z., Wang, Q., Zhao, M., Gong, C., 2018. Estimation of bare soil evaporation for different depths of water table in the wind-blown sand area of

the Ordos Basin, China. Hydrogeology Journal, 26(5): 1693-1704. DOI:10.1007/s10040-018-1774-6.

Cheng, D.H., Li, Y., Chen, X., Wang, W.K., Hou, G.C., Wang, C.L., 2013. Estimation of groundwater evaportranspiration using diurnal water table fluctuations in the Mu Us Desert, northern China. Journal of Hydrology, 490: 106-113. DOI:10.1016/j.jhydrol.2013.03.027.

Costa, F.R.C., Schietti, J., Stark, S.C., Smith, M.N., 2023. The other side of tropical forest drought: do shallow water table regions of Amazonia act as large-scale hydrological refugia from drought? New Phytol, 237(3): 714-733. DOI:10.1111/nph.17914.

Crosbie, R.S., Binning, P., Kalma, J.D., 2005. A time series approach to inferring groundwater recharge using the water table fluctuation method. Water Resources Research, 41(1). DOI:10.1029/2004wr003077.

Crosbie, R.S., Doble, R.C., Turnadge, C., Taylor, A.R., 2019. Constraining the magnitude and uncertainty of specific yield for use in the water table fluctuation method of estimating recharge. Water Resources Research, 55(8): 7343-7361.

Cuthbert, M.O., 2010. An improved time series approach for estimating groundwater recharge from groundwater level fluctuations. Water Resources Research, 46(9). DOI:10.1029/2009wr008572.

Dassargues, A., 2018. Hydrogeology: groundwater science and engineering. CRC Press.

de Vries, J.J., Simmers, I., 2002. Groundwater recharge: an overview of processes and challenges. Hydrogeology Journal, 10(1): 5-17. DOI:10.1007/s10040-001-0171-7.

Delleur, J.W., 2006. The handbook of groundwater engineering. CRC press.

Fan, J., Oestergaard, K.T., Guyot, A., Lockington, D.A., 2014. Estimating groundwater recharge and evapotranspiration from water table fluctuations under three vegetation covers in a coastal sandy aquifer of subtropical Australia. Journal of Hydrology, 519: 1120-1129. DOI:10.1016/j.jhydrol.2014.08.039

Freeze, R.A., Cherry, J.A., 1979. Groundwater.

Harbaugh, A. W. 2005. MODFLOW-2005, the US Geological Survey modular ground-water model: The ground-water flow process. US Department of the Interior, US Geological Survey.

Healy, R.W., 2010. Estimating groundwater recharge. Cambridge University Press.

Healy, R.W., Cook, P.G., 2002. Using groundwater levels to estimate recharge. Hydrogeology Journal, 10(1): 91-109. DOI:10.1007/s10040-001-0178-0.

Hellwig, D., 1973. Evaporation of water from sand, 4: The influence of the depth of the water-table and the particle size distribution of the sand. Journal of Hydrology, 18(3-4): 317-327.

Hou, L., Wang, X.-S., Hu, B.X., Shang, J., Wan, L., 2016. Experimental and numerical investigations of soil water balance at the hinterland of the Badain Jaran Desert for

groundwater recharge estimation. Journal of Hydrology, 540: 386-396. DOI:10.1016/j.jhydrol.2016.06.036.

Hu, W., Wang, Y.Q., Li, H.J., Huang, M.B., Hou, M.T., Li, Z., She, D.L., Si, B.C., 2019. Dominant role of climate in determining spatio-temporal distribution of potential groundwater recharge at a regional scale. Journal of Hydrology, 578. DOI:10.1016/j.jhydrol.2019.124042.

Huang, J., Yu, H., Guan, X., Wang, G., Guo, R., 2015. Accelerated dryland expansion under climate change. Nature Climate Change, 6(2): 166-171. DOI:10.1038/nclimate2837.

Huang, J., Zhou, Y., Wenninger, J., Ma, H., Zhang, J., Zhang, D., 2016. How water use of Salix psammophila bush depends on groundwater depth in a semi-desert area. Environmental Earth Sciences, 75(7). DOI:10.1007/s12665-016-5376-0.

Huang, T., Pang, Z., Yang, S., Yin, L., 2020. Impact of Afforestation on Atmospheric Recharge to Groundwater in a Semiarid Area. Journal of Geophysical Research: Atmospheres, 125(9). DOI:10.1029/2019jd032185.

IPCC, 2014. Climate Change 2014: impacts, adaptation and vulnerability, part A: global and sectoral aspects. Contribution of Working Group II (WG2) to the Fifth Assessment Report (AR5) of the Intergovernmental Panel on Climate Change (IPCC).

Jefferson, J.L., Maxwell, R.M., 2015. Evaluation of simple to complex parameterizations of bare ground evaporation. Journal of Advances in Modeling Earth Systems, 7(3): 1075-1092. DOI:10.1002/2014ms000398.

Kinzelbach, W., Brunner, P., von Boetticher, A., Kgotlhang, L., Milzow, C., 2010. Sustainable water management in arid and semi-arid regions, 119-130 pp. DOI:10.1017/CBO9780511760280.009.

Kurc, S.A., Small, E.E., 2004. Dynamics of evapotranspiration in semiarid grassland and shrubland ecosystems during the summer monsoon season, central New Mexico. Water Resources Research, 40(9). DOI:10.1029/2004wr003068.

Le Maitre, D. C., Scott, D. F., and Colvin, C. (1999). Review of information on interactions between vegetation and groundwater.

Li, F.-R., Zhang, H., Zhang, T.-H., and Shirato, Y. (2003). Variations of sand transportation rates in sandy grasslands along a desertification gradient in northern China. Catena 53, 255-272.

Liang, P., and Yang, X. (2016). Landscape spatial patterns in the Maowusu (Mu Us) Sandy Land, northern China and their impact factors. Catena 145, 321-333.

Logsdon, S., Schilling, K., Hernandez‐Ramirez, G., Prueger, J., Hatfield, J., Sauer, T., 2010. Field estimation of specific yield in a central Iowa crop field. Hydrological Processes: An International Journal, 24(10): 1369-1377.

Lv, M., Xu, Z., Yang, Z.L., Lu, H., Lv, M., 2021. A Comprehensive Review of Specific Yield in Land Surface and Groundwater Studies. Journal of Advances in Modeling Earth

Systems, 13(2). DOI:10.1029/2020ms002270.

Ma, Z., Wang, W., Zhang, Z., Brunner, P., Wang, Z., Chen, L., Zhao, M. and Gong, C., 2019. Assessing bare-soil evaporation from different water-table depths using lysimeters and a numerical model in the Ordos Basin, China. Hydrogeology Journal, 27(7): 2707-2718.

Nazarieh, F., Ansari, H., Ziaei, A.N., Izady, A., Davari, K., Brunner, P., 2018. Spatial and temporal dynamics of deep percolation, lag time and recharge in an irrigated semi-arid region. Hydrogeology Journal, 26(7): 2507-2520. DOI:10.1007/s10040-018-1789-z.

Nimmo, J.R., Healy, R.W., Stonestrom, D.A., 2006. Aquifer recharge. Encyclopedia of hydrological sciences.

O'Connor, J., Santos, M.J., Rebel, K.T., Dekker, S.C., 2019. The influence of water table depth on evapotranspiration in the Amazon arc of deforestation. Hydrology and Earth System Sciences, 23(9): 3917-3931. DOI:10.5194/hess-23-3917-2019.

Pütz, T., Fank, J., Flury, M., 2018. Lysimeters in Vadose Zone Research. Vadose Zone Journal, 17(1). DOI:10.2136/vzj2018.02.0035.

Rossman, N.R., Zlotnik, V.A., Rowe, C.M., Szilagyi, J., 2014. Vadose zone lag time and potential 21st century climate change effects on spatially distributed groundwater recharge in the semi-arid Nebraska Sand Hills. Journal of Hydrology, 519: 656-669. DOI:10.1016/j.jhydrol.2014.07.057.

Sanford, W., 2002. Recharge and groundwater models: an overview. Hydrogeology Journal, 10(1): 110-120. DOI:10.1007/s10040-001-0173-5

Scanlon, B.R., Fakhreddine, S., Rateb, A., de Graaf, I., Famiglietti, J., Gleeson, T., Grafton, R.Q., Jobbagy, E., Kebede, S., Kolusu, S.R., 2023. Global water resources and the role of groundwater in a resilient water future. Nature Reviews Earth & Environment, 4(2): 87-101.

Scanlon, B.R., Healy, R.W., Cook, P.G., 2002. Choosing appropriate techniques for quantifying groundwater recharge. Hydrogeology Journal, 10(1): 18-39. DOI:10.1007/s10040-001-0176-2.

Scanlon, B.R., Keese, K.E., Flint, A.L., Flint, L.E., Gaye, C.B., Edmunds, W.M., Simmers, I., 2006. Global synthesis of groundwater recharge in semiarid and arid regions. Hydrological Processes, 20(15): 3335-3370. DOI:10.1002/hyp.6335.

Scanlon, B.R., Reedy, R.C., Stonestrom, D.A., Prudic, D.E., Dennehy, K.F., 2005. Impact of land use and land cover change on groundwater recharge and quality in the southwestern US. Global Change Biology, 11(10): 1577-1593. DOI:10.1111/j.1365-2486.2005.01026.x.

Sophocleous, M., 2005. Groundwater recharge and sustainability in the High Plains aquifer in Kansas, USA. Hydrogeology Journal, 13(2): 351-365. DOI:10.1007/s10040-004-0385-6.

Sophocleous, M.A., 1991. Combining the soilwater balance and water-level fluctuation

methods to estimate natural groundwater recharge: practical aspects. Journal of hydrology, 124(3-4): 229-241.

Soylu, M.E., Istanbulluoglu, E., Lenters, J.D., Wang, T., 2011. Quantifying the impact of groundwater depth on evapotranspiration in a semi-arid grassland region. Hydrology and Earth System Sciences, 15(3): 787-806. DOI:10.5194/hess-15-787-2011.

Taylor, R.G., Scanlon, B., Döll, P., Rodell, M., van Beek, R., Wada, Y., Longuevergne, L., Leblanc, M., Famiglietti, J.S., Edmunds, M., Konikow, L., Green, T.R., Chen, J., Taniguchi, M., Bierkens, M.F.P., MacDonald, A., Fan, Y., Maxwell, R.M., Yechieli, Y., Gurdak, J.J., Allen, D.M., Shamsudduha, M., Hiscock, K., Yeh, P.J.F., Holman, I., Treidel, H., 2012. Ground water and climate change. Nature Climate Change, 3(4): 322-329. DOI:10.1038/nclimate1744.

Van Camp, M., de Viron, O., Pajot-Métivier, G., Casenave, F., Watlet, A., Dassargues, A., Vanclooster, M., 2016. Direct measurement of evapotranspiration from a forest using a superconducting gravimeter. Geophysical Research Letters, 43(19): 10,225-10,231. DOI:10.1002/2016gl070534.

Vanderborght, J., Leitner, D., Schnepf, A., Couvreur, V., Vereecken, H., Javaux, M., 2023. Combining root and soil hydraulics in macroscopic representations of root water uptake. Vadose Zone Journal, 23(3). DOI:10.1002/vzj2.20273.

Wang, J., Bras, R., 2011. A model of evapotranspiration based on the theory of maximum entropy production. Water Resources Research, 47(3).

Wang, T., Franz, T.E., Zlotnik, V.A., 2015. Controls of soil hydraulic characteristics on modeling groundwater recharge under different climatic conditions. Journal of Hydrology, 521: 470-481. DOI:10.1016/j.jhydrol.2014.12.040.

Wang, W., Zhang, Z., Yin, L., Duan, L., Huang, J., 2021. Topical Collection: Groundwater recharge and discharge in arid and semi-arid areas of China. Hydrogeology Journal, 29(2): 521-524. DOI:10.1007/s10040-021-02308-0.

Wang, W., Zhang, Z., Duan, L., Wang, Z., Zhao, Y., Zhang, Q., Dai, M., Liu, H., Zheng, X., and Sun, Y. (2018). Response of the groundwater system in the Guanzhong Basin (central China) to climate change and human activities. Hydrogeology Journal 26, 1429-1441.

Zhang, X., Wang, N., Cao, L., Ran, B., Wang, W., Xiao, Y., Zhang, Z., Xu, D., Wang, Z., 2023. Analysis of the contribution of rainfall to recharge in the Mu Us Desert (China) based on lysimeter data. Hydrogeology Journal, 32(1): 279-288. DOI:10.1007/s10040-023-02750-2

Zhang, Z., Wang, W., Gong, C., Zhang, M., 2020. A comparison of methods to estimate groundwater recharge from bare soil based on data observed by a large‐scale lysimeter. Hydrological Processes, 34(13): 2987-2999. DOI:10.1002/hyp.13769.

Zhang, Z., Wang, W., Gong, C., Zhao, M., Franssen, H.J.H., Brunner, P., 2021. Salix

psammophila afforestations can cause a decline of the water table, prevent groundwater recharge and reduce effective infiltration. Science of the Total Environment, 780. DOI:10.1016/j.scitotenv.2021.146336.

Zhang, Z., Wang, W., Wang, Z., Chen, L., Gong, C., 2018. Evaporation from bare ground with different water-table depths based on an in-situ experiment in Ordos Plateau, China. Hydrogeology Journal, 26(5): 1683-1691. DOI:10.1007/s10040-018-1751-0.

Zhao, M., A, G., Zhang, J., Velicogna, I., Liang, C., Li, Z., 2020. Ecological restoration impact on total terrestrial water storage. Nature Sustainability, 4(1): 56-62. DOI:10.1038/s41893-020-00600-7.

Chapter 2 Comparison of field methods for estimating evaporation from bare soil using lysimeters in a semi-arid area

Chapter 2 has been published as **Gong C**, Wang W, Zhang Z, Wang H, Luo J, Brunner P. Comparison of field methods for estimating evaporation from bare soil using lysimeters in a semi-arid area[J]. Journal of Hydrology, 2020, 590: 125334. DOI 10.1016/j.jhydrol.2020.125334.

Abstract

Evaporation from bare soil is an important component of a catchment water balance. However, it is arguably one of the most challenging hydrological processes to estimate and measure accurately. Several approaches to estimate soil evaporation exist, but their performance for specific water table conditions remains unclear. This study investigated the performance of four commonly used approaches and several ways on how to implement them: the energy-balanced based FAO-56 method with the skin evaporation enhancement (FAO-56 skin), hydraulic methods based on groundwater level fluctuation (GLF), Darcy's law, and the maximum entropy production (MEP) method based on non-equilibrium thermodynamics theory. Three lysimeters with different water table depths were used at a research site in the Guanzhong Basin of China. The lysimeters were equipped with soil moisture probes. Water table fluctuations were also measured. The data allow us to accurately estimate evaporation rates using a water balance approach and are used to assess the performance of the analysed methods. The results show that: (1) The MEP method performed best for all water table conditions, but tends to overestimate evaporation if the water table is below the extinction depth. The extinction depth is the depth of the water table were there the contribution of groundwater to bare-soil evaporation is zero. In our case, the extinction depth was 78 cm. (2) The FAO-56 skin method underestimated evaporation where the water table was above the extinction depth, and vice versa. (3) The groundwater level fluctuation method significantly overestimated the evaporation if the specific yield was estimated using hydraulic methods. The groundwater level fluctuation method should be combined with a soil water balance, independent of water table conditions. The method can only be applied if the water table is above the extinction depth. (4) Conceptually, Darcy's law was suitable for estimating evaporation. However, the estimation of the required parameters is challenging. A good fit could only be obtained through calibration to measured evaporation rates.

Keywords: Bare soil evaporation, FAO-56 skin method, Groundwater level fluctuation method, Maximum entropy production, Phreatic evaporation, Semi-arid

2.1 Introduction

Evapotranspiration is one of the dominant processes in the soil-vegetation-atmosphere continuum (Lawrence et al. 2007). Brandes and Wilcox (2000) found that evapotranspiration could account for 95% of the total annual rainfall in arid regions. Despite the importance of evaporation from bare soil, Davarzani et al. (2014) reported that "Even though decades of research have improved our understanding of bare soil evaporation, many knowledge gaps still exist in the current science on how the soil water in the shallow subsurface close to the land surface interacts with the air in the atmosphere."

Reliable information on evapotranspiration is critical for irrigation scheduling, weather forecasting, and water resources management (Liu et al. 2017). Evapotranspiration also plays an important role in groundwater management. Worldwide, groundwater contributes to about 20% of freshwater consumption (Kinzelbach et al. 2003). In China, groundwater accounts for more than 60% of freshwater consumption (Ministry of Water Resources of China, 2010), and agricultural irrigation relies heavily on groundwater, especially in Northwest China (Yang et al. 2010).

Phreatic evaporation from groundwater causes soil salinity, especially in arid and semi-arid regions (Brunner et al. 2007; Brunner et al. 2008) and diminishes water resources unproductively (Li et al. 2009; Zhang et al. 2018). Phreatic evaporation rates depend on the soil type and the depth to groundwater (Wang et al. 2017; Zhang et al. 2019) and therefore are difficult to determine for large spatial scales (Henderson‐Sellers et al. 2003).

Many laboratory studies to estimate evaporation were conducted (Smits et al. 2012; Tran et al. 2015; Trautz et al. 2015; Wang et al. 2011). Early laboratory experiments included Veihmeyer and Brooks (1954), Gardner and Fireman (1958), Shih (1983). Hellwig (1973a, 1973b) investigated the influences of the weather forcing, the depth of the water table, and the particle size distribution on the soil evaporation. He found that if the groundwater level was kept at the surface ground, the coarseness of the sand did not affect evaporation. However, he also pointed out that the water table depth and coarseness of the sand had a significant effect on the evaporation once the water table drops below the surface. More recent laboratory experiments mainly focused on the effect of the atmospheric conditions on actual evaporation (Lehmann et al. 2008; Shahraeeni et al. 2012; Shokri et al. 2008; Smits et al. 2012; Tran et al. 2015). However, a majority of these laboratory studies only tested one water table depth. These results are therefore difficult to apply to field conditions where the water table depth varies in space and time.

Complementary to these laboratory experiments, several field methods to estimate actual bare soil evaporation were proposed. The Bowen ratio-energy balance (BREB) is a widely applied method for estimating evaporation in the field (Bonan 2008; Shanafield et al. 2015). BREB has the advantage of being applicable to almost any type of terrain. The BREB method is based on an energy balance and requires data such as vapor pressure gradient and temperature profiles. However, the application of the method is challenging in arid and semi-arid regions, because the gradient of vapor pressure is typically small (Shanafield et al. 2015). Isotopic profiles in the unsaturated zone have also been used to investigate evaporation, e.g. Brunner et al. (2008). Extracting isotopic profiles from the unsaturated zone are very laborious and yields point values only. In addition, numerical models are also employed to simulate evaporation from the bare soil (Bittelli et al. 2008; Li et al. 2008; Saito et al. 2006). However, the models are often based on conceptual assumptions such as homogeneity of the soil, and are therefore associated with major uncertainties.

The FAO-56 method is widely used to estimate evapotranspiration due to its straightforward implementation (Liu et al. 2017; Mutziger et al. 2005; Valipour et al. 2017). It can be applied for estimating bare soil evaporation using a crop coefficient and reference evapotranspiration (Allen et al. 1998). Rianna et al. (2018) used the FAO-56 method to estimate actual and potential bare soil evaporation over silty pyroclastic soils. Their result showed that the literature-based parameter values led to poor predictions of estimated evaporation rates. Quinn et al. (2018) evaluated the suitability of the FAO-56 method for bare sand evaporation under falling water table conditions. They found a satisfactory agreement between the field experiments and the water balance model based on the FAO-56 method. However, the experiments lasted for about 20 days only and the lysimeters were 60 cm deep. The results therefore cannot represent deep water table conditions, nor seasonal changes of atmospheric forcing.

Mutziger et al. (2005) applied a three-stage application of the FAO-56 method developed by Allen et al. (1998) to predict bare soil evaporation. The results showed that the FAO-56 approach could yield reliable results provided that site-specific information on soil parameters is available. However, Allen (2011) pointed out that the FAO-56 method underestimated evaporation when light rainfall events (less than 5 mm) occurred.

Given the practical difficulties and uncertainties of the above-mentioned approaches, alternative methods or improvement to existing approaches have been developed: (1) the semi-empirical FAO-56 method with the skin evaporation enhancement (FAO-56 skin). (2) the groundwater level fluctuation method (GLF), (3) the maximum entropy production method

(MEP), and (4) Darcy's law method. The focus of this paper is on these four methods and variations of their implementation.

To overcome the issues described above with the classic FAO-56 method, a 'skin' layer enhancement to the FAO-56 evaporation method (FAO-56 skin method) was proposed by Allen (2011). FAO-56 skin method differs from the original FAO-56 method. It accommodates for wetting events which increase the soil water content near the surface. He found that the FAO-56 skin method could obtain satisfactory results compared to numerical and experimental data.

The groundwater level fluctuation method is also widely used to calculate evapotranspiration. The diurnal dynamics in evaporation rates can cause a sinusoidal response in the groundwater level. In addition to estimating evaporation rates, these variations have been used to estimate the transpiration rates of phreatophytes (Lautz 2008). It only requires data on the fluctuation of the water table, as well as an estimation of the specific yield. However, it is very sensitive to the specific yield, which is hard to accurately obtain (Chinnasamy et al. 2018; Crosbie et al. 2005). Moreover, the specific yield can be influenced by hysteresis (Nachabe 2002), plant activity (Logsdon et al. 2010), and antecedent soil moisture (Loheide 2008; Loheide et al. 2005).

An approach based on the theory of maximum entropy production (MEP) was proposed by Wang and Bras (2011) and is increasingly being used (Kornejady et al. 2017). The MEP method is an unconventional, dynamic-statistical model built on non-equilibrium thermodynamics theory and the maximum entropy postulates (Dewar 2005). The MEP has similar advantages to the BREB, for example, its robstuness and the ease of implementation almost everywhere. The MEP method requires few input data, such as soil temperature of the surface ground and net radiation, and doesn't require observations of air temperature and vapor gradients. It is therefore easier to apply than the BREB approach. As for all field-based methods, a disadvantage of the MEP is the point-scale nature of its assessment.

Finally, Darcy's law is an additional method to estimate evaporation using hydraulic conductivity and the hydraulic head gradient in the soil (Qiao and Wang 2014). Many analytical solutions based on Darcy's law have been developed for estimating steady-state evaporation, for example, Gardner (1958) proposed steady-state analytical solutions to quantify the influence of the water table on evaporation. Salvucci (1993) derived an analytic equation to calculate evaporation rates based on pressure gradients in the soil profile. However, Shokri and Salvucci (2011) pointed out that analytical solutions did not consider the discontinuity of capillary force at the drying front, thus inducing bias in the estimates. The application of Darcy's law to estimate bare soil evaporation requires high-quality data of pressure head and

soil water content (Cooper et al. 1990). To the best of our knowledge, the reliability of Darcy's law to estimate evaporation has so far not been assessed outside of laboratory settings.

Comparative studies of different methods for estimating bare soil evaporation are rare. Shanafield et al. (2015) found that land surface energy balance methods, such as MEP, are especially suitable for shallow water table depths. Rianna et al. (2018) assessed the abilities of several simplified models (for example Penman method, Penman-Monteith method, and Penman-Shuttleworth method) in estimating potential and actual evaporation for silty pyroclastic soils. They concluded that the methods performed well, provided the model parameters were calibrated using lysimeter data. The application of literature-based parameters produced biased estimates of actual evaporation.

The above mentioned comparative studies did not systematically assess the performance of the methods under different water table conditions. Given that the water table can significantly influence evaporation rates, this is an important unexplored factor. Also, few field studies integrated measurements of actual evaporation, a prerequisite to assess the performance of the different methods in absolute terms. In this study, we used data from lysimeters installed in the Guanzhong Basin of China to evaluate the performance of four approaches: the FAO-56 skin method, the groundwater level fluctuation method, MEP and Darcy's law. The novelty of the study lies in the different water table depths considered. Our study includes conditions where the water table is above- as well as below the extinction depth. The extinction depth is an important factor for soil evaporation: if the water table falls under the extinction depth, no contribution from groundwater to bare soil evaporation takes place. The study also goes beyond the previous inter-comparisons studies as accurate data of evaporation rates are available through the lysimeters.

2.2 Materials and methods

A field experiment was carried out in the Guanzhong Basin, Shaanxi Province, China with a latitude of 34°22′14″N and a longitude of 108°54′11″E (Figure 2.1). The climate is characterized by large seasonal dynamics. The mean annual air temperature was between 12 and 16 ℃ during the period of 56 years from 1951 to 2006 (Gao et al. 2009), the average annual actual precipitation was about 590 mm during the period of 60 years from 1951 to 2010 (Wang et al. 2018), and average potential annual evaporation was 961 mm based on 50 years of data from 1959 to 2008 (Zuo et al. 2011). Integrated cylinder-shaped lysimeters with the same surface area (1.0 m^2) and diameter (1.128 m) were installed. These lysimeters were made from glass fiber reinforced plastics with 1.2, 2.2, 3.2 m depth (Figure 2.2) which prevent leakage and reduce lateral soil heat fluxes. It is very important to test different water table

conditions to account for the wide range of water table depths that occur in the field.

Identical, homogenous material (sand) was used in all lysimeters. The sand was obtained from the Mu Us Desert in the northwest of China. To ensure homogenous packing, the lysimeters were filled by adding 10cm of material at a time until the lysimeter was fully packed (Zhang et al. 2018). The initial water table depths (from the surface ground to the water table) were at approximately 0.6 m (lysimeter 1), 1.5 m (lysimeter 2), and 2.5 m (lysimeter 3) on November 1, 2016. The lower ends were sealed to prevent water leakage and infiltration from the underlying aquifer.

Soil water content and temperature were measured at 3, 10, 20, 40 and 80 cm, 3, 10, 20, 40, 80, 130 and 180 cm, and 3, 10, 20, 40, 80, 130, 180, 230 and 280 cm below the surface for lysimeter 1, lysimeter 2 and lysimeter 3 using ECH$_2$O-5TM (Decagon Inc, Washington State, USA), and data were automatically recorded by the EM50 (Decagon Inc, Washington State, USA). The sensors were calibrated before installation, following the protocol of Cobos and Chambers (2010). The heat fluxes were measured with heat-flux plates (Hukesflux Inc., Delft, Netherlands, Figure 2.2) at the depth of 3 and 10 cm in lysimeter 1 and lysimeter 3. The data were automatically recorded by a data logger (CR-1000, Campbell Scientific, Utah, USA). Groundwater levels were recorded with a DI271 CTD-Diver (Van Essen Instruments, Delft, Netherlands). Another Diver DI500 (Van Essen Instruments, Delft, Netherlands) sensor was installed to log the air pressure for correcting the groundwater levels for atmospheric changes. A standard meteorological station was installed, and air temperature, relative humidity, precipitation, net radiation, atmospheric pressure, wind speed/direction were measured. The meteorological parameters were collected by a CR-3000 logger (Campbell Scientific, Utah, USA). All data were automatically recorded and averaged every five minutes. The lysimeters were installed in August, 2014. The experiment took place from November 1, 2016 to October 31, 2017.

To obtain the soil-water characteristic curve (the relationship between soil water content and pressure head) of the soil in the lysimeter, an undisturbed soil sample was obtained at the surface of one lysimeter (lysimeter 1) using a ring knife. The soil-water characteristic curve was measured using the Ku-pF apparatus (Germany, UGT) in the laboratory. We used the van Genuchten (1980) model to fit the experimental data.

$$\begin{cases} \frac{\theta-\theta_r}{\theta_s-\theta_r} = [1+|\alpha\varphi|^n]^{-m} & \varphi < 0 \\ \theta(\varphi) = \theta_s & \varphi \geq 0 \end{cases} \quad (2.1)$$

Where θ_s [cm^3/cm^3] and θ_r [cm^3/cm^3] are saturated and residual soil water content,

respectively. φ [cm] is pressure head. α [cm^{-1}] and n [-] are two parameters, m [-] is equal to 1-1/n (Mualem 1976).

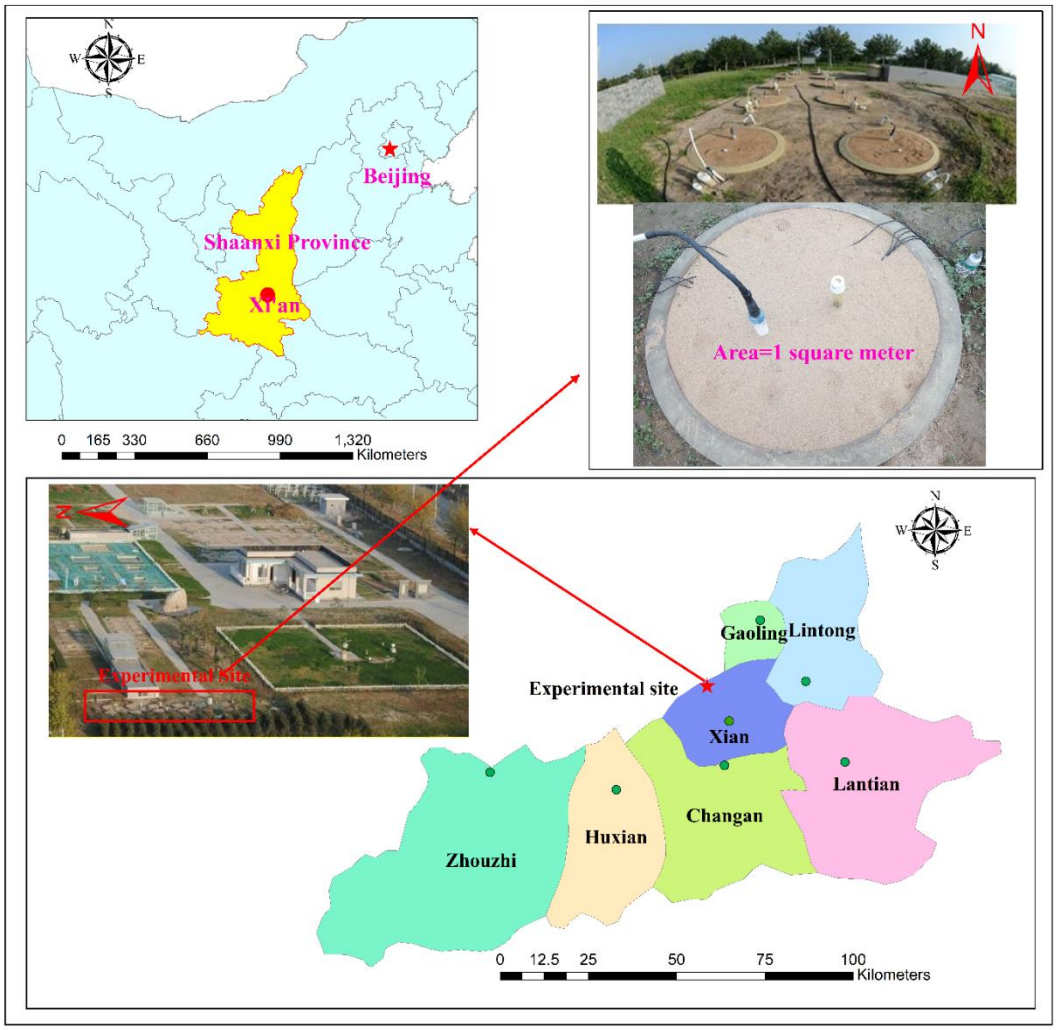

Figure 2.1 Location of the field experiment in the Guanzhong Basin, China.

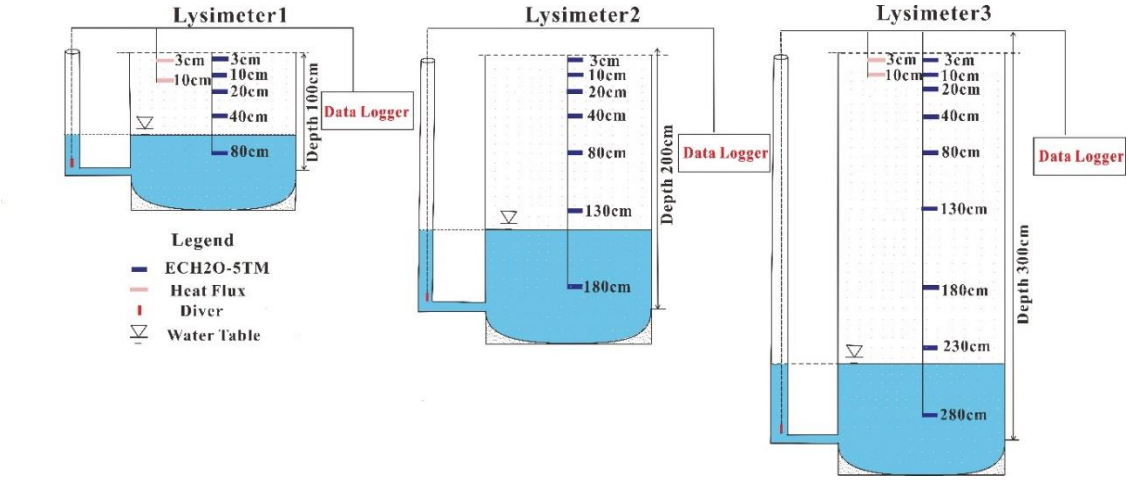

Figure 2.2 Schematic diagram of the lysimeters with different water table depths.

2.2.1 Water balance method

This study used non-weighing lysimeters to determine evaporation using the water balance method:

$$E_a = P_e - R - \frac{dS}{dt} \tag{2.2}$$

Where E_a [cm/d] is the actual evaporation rate, P_e [cm/d] is the effective rainfall, R [cm/d] is the surface runoff, $\frac{dS}{dt}$ [cm/d] is the total water storage change in the lysimeter. Total water storage change is composed of change in both the saturated (S_s) and the unsaturated zone (S_u), which can be calculated according to equation 2.3 (see also Figure 2.3 for an illustration).

$$\frac{dS}{dt} = \frac{dS_u}{dt} + \frac{dS_s}{dt} \tag{2.3}$$

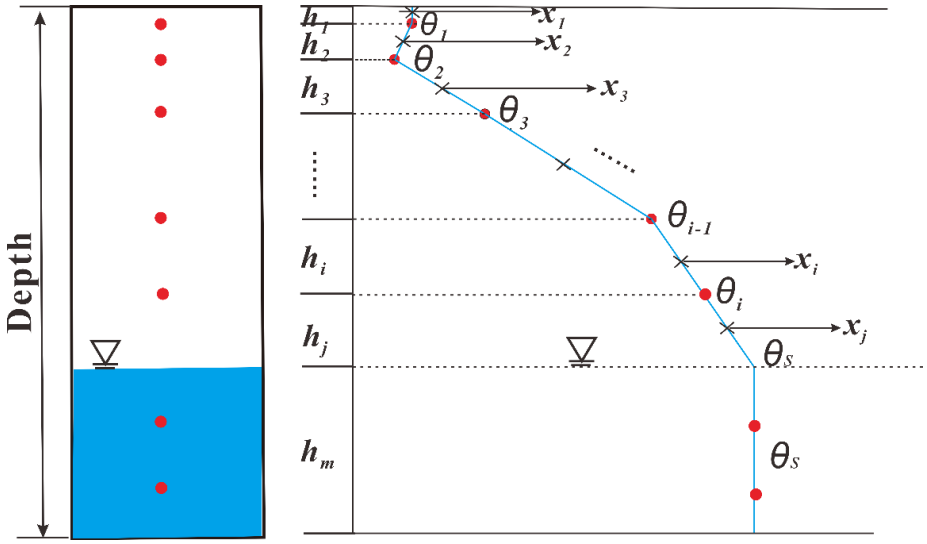

Figure 2.3 Schematic diagram of water balance method to calculate evaporation. The water storage change and evaporation can be estimated by comparing the soil moisture profiles and the groundwater levels between two periods in time (five days, in this case). To calculate the water content on a specific day, the average values between two sensors (indicated with x_i in the diagram) were weighted by the distance between sensors (h_i).

2.2.2 FAO-56 method with the skin evaporation enhancement (FAO-56 Skin method)

Stage 1 evaporation (energy limited stage). In this stage, the evaporation rate is controlled by the availabile energy:

$$E_1 = K_{e\,max} ET_{ref} \tag{2.4}$$

where E_1 [cm/day] is the evaporation rate during stage 1. ET_{ref} [cm/day] is the reference evapotranspiration, typically equated to the grass reference evapotranspiration (ET_0). ET_0 was calculated by the FAO-56 Penman-Monteith equation (Allen et al. 1998). A value $K_{e\,max}$ [-] of 1.2 is recommended for estimating evaporation from bare soil. The duration

of stage 1 and the beginning of stage 2 can range from one to several days, depending on the amount of water that infiltrated and soil properties such as the albedo, porosity, and the hydraulic conductivity.

Stage 2 evaporation (falling rate stage or soil limited stage). The rate of evaporation is controlled by the moisture content in the upper soil layer. Evaporation is thus limited by both soil hydraulics and $K_{e\,max}ET_{ref}$ (Allen 2011). The original FAO-56 model for E_2 was:

$$E_2 = K_e ET_{ref} \tag{2.5}$$

where K_e [-] is the evaporation coefficient.

$$K_e = K_r(K_{c\,max} - K_s K_{cb}) \tag{2.6}$$

such that

$$K_e \leq f_{ew} K_{c\,max} \tag{2.7}$$

where the dual K_c model estimates *ET* as:

$$ET = (K_s K_{cb} + K_e) ET_{ref} \tag{2.8}$$

where K_e [-] is the soil evaporation coefficient, K_{cb} [-] is the basal crop coefficient, $K_{c\,max}$ is the maximum value of K_c [-] depending on the amount of rain or irrigation per wetting event, K_s [-] is a reduction coefficient to account for reduced transpiration under soil water shortage (0 for bare soil) and K_r [-] is a dimensionless evaporation reduction coefficient [0-1]. The parameter f_{ew} [-] represents the fraction of soil surface from which most of the evaporation occurs. With the skin evaporation enhancement K_e [-] is reformulated for bare soil only, i.e. in the absence of vegetation:

$$K_e = f_w[F_t + (1 - F_t)K_r]K_{e\,max} \tag{2.9}$$

$$F_t = \min\left[\frac{REW - D_{REW_{i-1}}}{K_{e\,max}ET_{ref}}, 1.0\right] \tag{2.10}$$

where $D_{REW_{i-1}}$ [cm] is the depletion of the skin layer at the end of the previous time step (day or hour), *REW* [cm] is readily evaporable water, which is the maximum depth of water that can be evaporated from the topsoil layer without restriction during stage 1 (Allen et al. 1998). f_w [-] is the fraction of the wetted surface.

$$0.0 \leq D_{REW_i} = D_{REW_{i-1}} - \left[(1 - f_b)\left(P_i - RO_i + \frac{I_i}{f_w}\right) + f_b\left(P_{i+1} - RO_{i+1} + \frac{I_{i+1}}{f_w}\right)\right] C_{eff} + \frac{E_i}{f_{ew}} \leq REW \tag{2.11}$$

$$REW = \min\left(2 + \frac{TEW}{3}, 0.8TEW\right) \tag{2.12}$$

$$TEW = 1000(\theta_{FC} - 0.5\theta_{WP})z_e \tag{2.13}$$

Where TEW [mm] is the total amount of evaporated water, which is equal to the

maximum depth of water which can be evaporated from the surface soil layer when the layer has been initially completely wetted. f_b [-] is the fraction of the precipitation and irrigation during a time step [hour or day] that contributes to evaporation during that same timestep. θ_{FC} [cm^3/cm^3] is field capacity, θ_{WP} [cm^3/cm^3] is the wilting point. z_e [cm] is the effective depth of soil, with a recommended value of 0.10-0.15m by FAO-56. P_i [cm] is precipitation and RO_{i+1} [cm] is runoff during timestep i. I_i [cm] is the irrigation depth in timestep i that infiltrates the soil. C_{eff} [-] is a spatial infiltration efficiency factor that represents the effectiveness of the skin layer in capturing precipitation and irrigation additions. C_{eff} is estimated as

$$C_{eff} = \min\left(C_0 + C_1\left(1 - \frac{D_{e_{i-1}}}{TEW}\right), 1.0\right) \tag{2.14}$$

C_{eff} is expressed as a fraction (0-1), $D_{e_{i-1}}$ [cm] is the depletion depth through the total evaporation, C_0 and C_1 are the fitted offset and slope of the function (Allen 2011).

Mutziger et al. (2005) evaluated three different methods to obtain the soil parameters: (1) general soil parameters from FAO-56 (see Table 7 in (Mutziger et al. 2005)); (2) the application of literature values obtained in case studies and (3) the calibrated soil parameters to obtain the best fit between the measured and estimated rates of evaporation. This requires, however, observations of evaporation, which in most cases are not available. Therefore, we used the most commonly used approach and based our estimates on reported literature values, specifically Suleiman et al. (2007) who suggested a TEW of 15 mm, REW of 6 mm, z_e of 15 cm, θ_{FC} of 0.12 cm^3/cm^3, and θ_{WP} of 0.04 cm^3/cm^3 for sandy soils, as is the case for our study.

2.2.3 Maximum entropy production model of evaporation

The MEP method proposed by Wang and Bras (2011) only requires net radiation R_n [W/m^2], surface temperature T_s [K], and specific humidity q_s [kg/kg] to obtain the sensible heat flux H [W/m^2], the ground heat flux G [W/m^2], and evaporation rates E [W/m^2] simultaneously.

$$E + H + G = R_n \tag{2.15}$$

$$G = \frac{B(\sigma)I_s}{\sigma I_0} H|H|^{-\frac{1}{6}} \tag{2.16}$$

$$E = B(\sigma)H \tag{2.17}$$

where I_s [$Jm^{-2}K^{-1}s^{-1/2}$] and I_0 [$Jm^{-2}K^{-1}s^{-1/2}$] are the thermal and apparent thermal inertia of the soil and air respectively. $B(\sigma)$ [-] is the reciprocal of the Bowen ratio:

$$B(\sigma) = \left(6\sqrt{1 + \frac{11}{36}\sigma} - 1\right) \tag{2.18}$$

The dimensionless parameter σ [-] is characterizing the phase-change related state of the evaporating surface and can be calculated using the following equation:

$$\sigma(T_s, q_s) = (\frac{\theta}{\theta_s})^{\beta} \frac{\lambda^2 q_s}{c_p R_v T_s^2} \quad (2.19)$$

c_p [J kg^{-1} K^{-1}] is the specific heat of the air under constant pressure (1004 Jkg^{-1}K^{-1}), λ [J/kg] is the vaporization heat of liquid water (2500 J/kg), R_v [J kg^{-1}K^{-1}] is the gas constant for water vapor (461.5 J kg^{-1}K^{-1}). θ [cm^3/cm^3] is the soil moisture content near the surface ground, θ_s [cm^3/cm^3] is the saturated soil moisture content. T_s [K] is the near-surface ground temperature (below surface ground 3cm). β [-] is an empirical parameter dependent on soil texture. Deardorff (1977) suggested a value of 1.0. Alternatively, β [-] also can be obtained using equation (2.19) by fitting the results of MEP to the observed heat or evaporation fluxes (Huang and Wang, 2016; Li et al., 2020). This requires either measurements of the heat flux or measurements of evaporation from e.g. a lysimeter. q_s [kg/kg] is the specific humidity. In this study, the specific humidity was approximated as the air specific humidity near the soil surface, which was calculated using the surface temperature and relative humidity measured near the soil surface (Buck 1996):

$$E_s = 6.1121 * \exp\left(\left(18.678 - \left(\frac{T_a}{234.5}\right)\right) * \left(T_a/(257.14 + T_a)\right)\right) \quad (2.20)$$

$$E_{atm} = (RH * E_s)/100.0 \quad (2.21)$$

if $E_{atm} < E_s$,

$$q_s = \frac{0.622 * E_{atm}}{P - E_{atm} * (1 - 0.622)} \quad (2.22)$$

If $E_{atm} > E_s$

$$q_s = \frac{0.622 * E_s}{P - E_s * (1 - 0.622)} \quad (2.23)$$

In this equation, P [kpa] is the air pressure, T_a [℃] is the air temperature, RH [%] is the relative humidity, E_s [hpa] is the saturation water vapor pressure, and E_{atm} [hpa] is the water vapor pressure.

2.2.4 Groundwater level fluctuation

Evaporation can be estimated using diurnal patterns of groundwater level change at low cost (Cheng et al. 2013). Groundwater level fluctuations result from changing evaporation rates during the course of the day. The groundwater fluctuation method is a daily water balance, with recharge by rainfall and discharge by the evaporative flux (Shanafield et al. 2015). This is well suited to our lysimeters, as the daily groundwater level variations are controlled only by rainfall and evaporation. The following formula to calculate the evaporation *E* [cm/day] was used:

$$E = S_y \frac{dh}{dt} \tag{2.24}$$

where S_y [-] is the specific yield, and $\frac{dh}{dt}$ [cm/day] is the decline rate of the groundwater table. The specific yield is an important parameter for the calculation of groundwater recharge or evaporation using the water table fluctuation method (Chinnasamy et al. 2018; Hill and Durchholz 2015; Shah and Ross 2009). The specific yield is defined as the volume of water that can be released from storage per unit surface area of porous material per unit decline of the water table (Freeze and Cherry 1979). It can be expressed with the following equation (2.25).

$$S_y = \frac{V_w}{A\Delta z} \tag{2.25}$$

In this equation, V_w [cm^3] is the volume of water that can be released from storage, A [cm^2] is the surface area of the lysimeter, Δz [cm] is the decline of the water table. To obtain an estimation of the specific yield, we used two methods: a pumping test, and a water balance method (Sophocleous 1991) considering soil moisture changes in the unsaturated zone- as opposed to the pump test which simply considers changes of the vertical extent of the saturated zone. Pump tests were carried out using a peristaltic pump to extract water at a constant rate (2000 ml/min) in all three lysimeters. The pump inlet was placed at the bottom of the lysimeters. Moreover, we measured the volume of the water at the outlet in order to get an accurate measurement of volume of abstracted water. The test was carried during the period from April 28, 2018 to May 12, 2018. To avoid the influence of precipitation and evaporation during the pump tests, the surface of the lysimeters were covered by plastic. The specific yield based on the pumping is subs2.uently called GLF-G1 method.

An alternative approach to estimating the specific yield was proposed by Sophocleous (1991). This “hybrid water-fluctuation method” combines observations of soil water content along the profile to estimate recharge. By combining groundwater level rises with precipitation and by associating the estimation of recharge using soil water balance with the subsequent water table rise, a specific yield can be estimated. We associated the evaporation using water balance with water table declining to estimate a specific yield and subsequently called it GLF-G2 method.

2.2.5 Darcy’s law method

Darcy’s law (downward positive) can be expressed by equation (2.26):

$$q = -K(\varphi)\frac{\partial H}{\partial z} \tag{2.26}$$

$$H = \varphi + z \tag{2.27}$$

$$K(\varphi) = K_s(1 - (\alpha|\varphi|)^{n-1}[1 + (\alpha|\varphi|)^n]^{-m})^2[1 + (\alpha|\varphi|)^n]^{(-\frac{m}{2})} \quad (2.28)$$

where q [cm/day] is the volumetric water flux through the soil-atmosphere interface (corresponding to evaporation if the flux is upward-moving), $K(\varphi)$ [cm/day] is the hydraulic conductivity for unsaturated conditions according to e.g. the van Genuchten model (1980), K_S [cm/day] is the saturated hydraulic conductivity, z [cm] is the axis of coordinates and coordinate origin is on the surface, and H [cm] is the total head. φ [cm] is the pressure head which can be calculated based on soil moisture measurements and the soil water retention (equation (2.1)).

The vertical upward flux close to the soil represents evaporation (Stephens and Knowlton 1986). We used a numerical approach to solve Darcy's law. This required a vertical discretization. There are many methods to calculate the effective hydraulic conductivity between two nodes, for example, a harmonic average, arithmetic average, geometric average or a weighted average. A commonly used approach employing the geometric average (e.g. Chen et al. (2018)). We applied the geometric average to calculate the unsaturated hydraulic conductivity. In a discretized scheme, the vertical flux between two nodes was thus calculated as follows:

$$q_{z_i} = \sqrt{K_n K_{n-1}}(\frac{H_{n-1} - H_n}{z_{i-1} - z_i}) \quad (2.29)$$

where K_n and K_{n-1} are the unsaturated hydraulic conductivities below and above the node z_i, respectively. H_n and H_{n-1} are the hydraulic heads below and above the node z_i, respectively.

Two different implementations were tested. We first used the soil parameters based on the laboratory analysis (see Table 2.2). To further explore the conceptual suitability of this approach, to reproduce evaporation dynamics, we calibrated the van Genuchten parameters by minimizing the root-mean-square error between the cumulative evaporation of Darcy's law and actual cumulative evaporation.

2.3 Results

2.3.1 Soil properties and parameters

The particle size distribution is shown in Table 2.1, and the estimated van Genuchten parameters in Table 2.2. The saturated hydraulic conductivity, obtained using a permeameter, was 450 cm/day.

Table 2.1 Particle size of the soil in the lysimeter

Particle size [mm]	0.075	0.075-0.25	0.25-0.5	0.5-1
Composition [%]	2.5	73.6	23.4	0.5

Table 2.2 The van-Genuchten parameters

θ_s [cm^3/cm^3]	θ_r [cm^3/cm^3]	α [cm^{-1}]	n	RMSE	R^2
0.32	0.022	0.022	4.14	8.2E-12	0.999

2.3.2 Air temperature, rainfall and water table depth

The daily averaged values of air temperature, rainfall and water table depth are displayed in Figure 2.4. A total of 96 rainfall events with an average value of 0.65 cm occurred during the experimental period. Daily rainfall rates less than 2 cm are common. Rainfall mainly occurred in April, August, September, and October (Figure 2.4). The average daily air temperature can be seen in Figure 2.4 during the experimental period.

The fluctuations of the water table depth for every lysimeter are shown in Figure 2.4b. The extinction depth can be graphically identified in Figure 2.4b, which was 78 cm. The water table cannot drop below this level, despite the evaporative forcing at the soil surface. In this case, evaporation is depleting storage from the unsaturated zone. The water table in lysimeter 1 is above the extinction depth throughout the experiment. Water table depths in lysimeter 2 and 3 are below the extinction depth before June 4, 2017 and before October 9, 2017 in lysimeter 3 respectively. The dynamics of the groundwater level were quite different for each lysimeter. The distributions of the water table depth could be divided into two periods: the first period from November 1, 2016 to March 11, 2017 with little change of the water table and a second period from March 12 to October 31 where the water table increased rapidly, except for lysimeter 1. The water table depth of lysimeter 2 and 3 increased rapidly with rates of 0.48 and 0.76 cm/day in this second period. Because the vadose zone was shallow in lysimeter 1, a large portion of infiltration was lost to evaporation.

Net radiation kept stable from November to January 2017. It subsequently increased from February to June and decreased from July to October (Figure 2.4c). Reference evaporation (ET_0) is shown in Figure 2.4d. The variations were similar to net radiation.

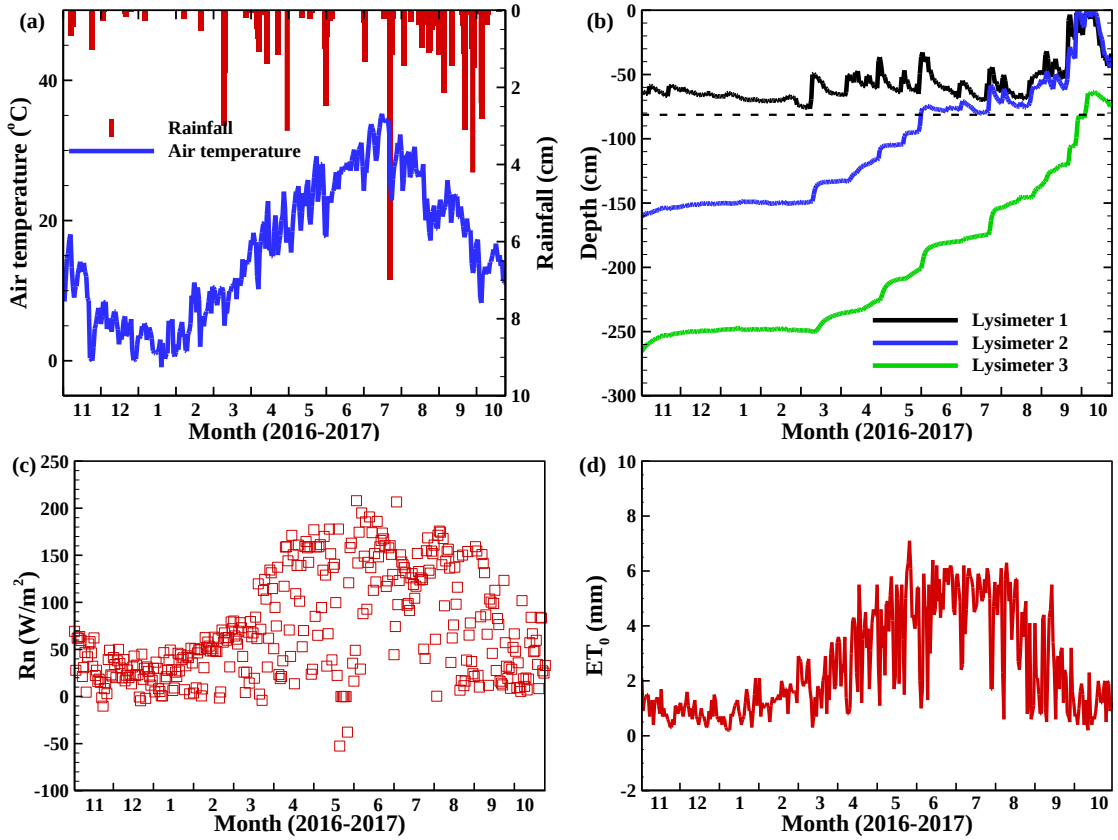

Figure 2.4 (a) Rainfall and air temperature; (b) water table depth in each lysimeter. (The dashed line represents the extinction depth. If the water table depth falls below this depth, evaporation from the water table is no longer occurring); (c) net radiation and (d) Reference evaporation (ET_0) estimated using the Penman-Monteith equation.

2.3.3 Calculation of actual evaporation and intercomparison of different methods

The cumulative monthly evaporation rates are presented in Figure 2.5 for all methods. The water balance method provides actual soil evaporation rates. The cumulative actual evaporation during the experimental period was 44.1 cm for lysimeter 1, 35.8 cm for lysimeter 2, 22.7 cm for lysimeter 3. Besides relative humidity, wind speed, radiation, the actual evaporation rates can, to a certain extent, be explained with air temperature, too. For example, evaporation rates were low during winter and as the air temperature increased, evaporation rates increased, too. Clearly, air temperature alone cannot explain the evaporation dynamics, the influence of the water table (Figure 2.4b) on actual evaporation needs to be examined, too.

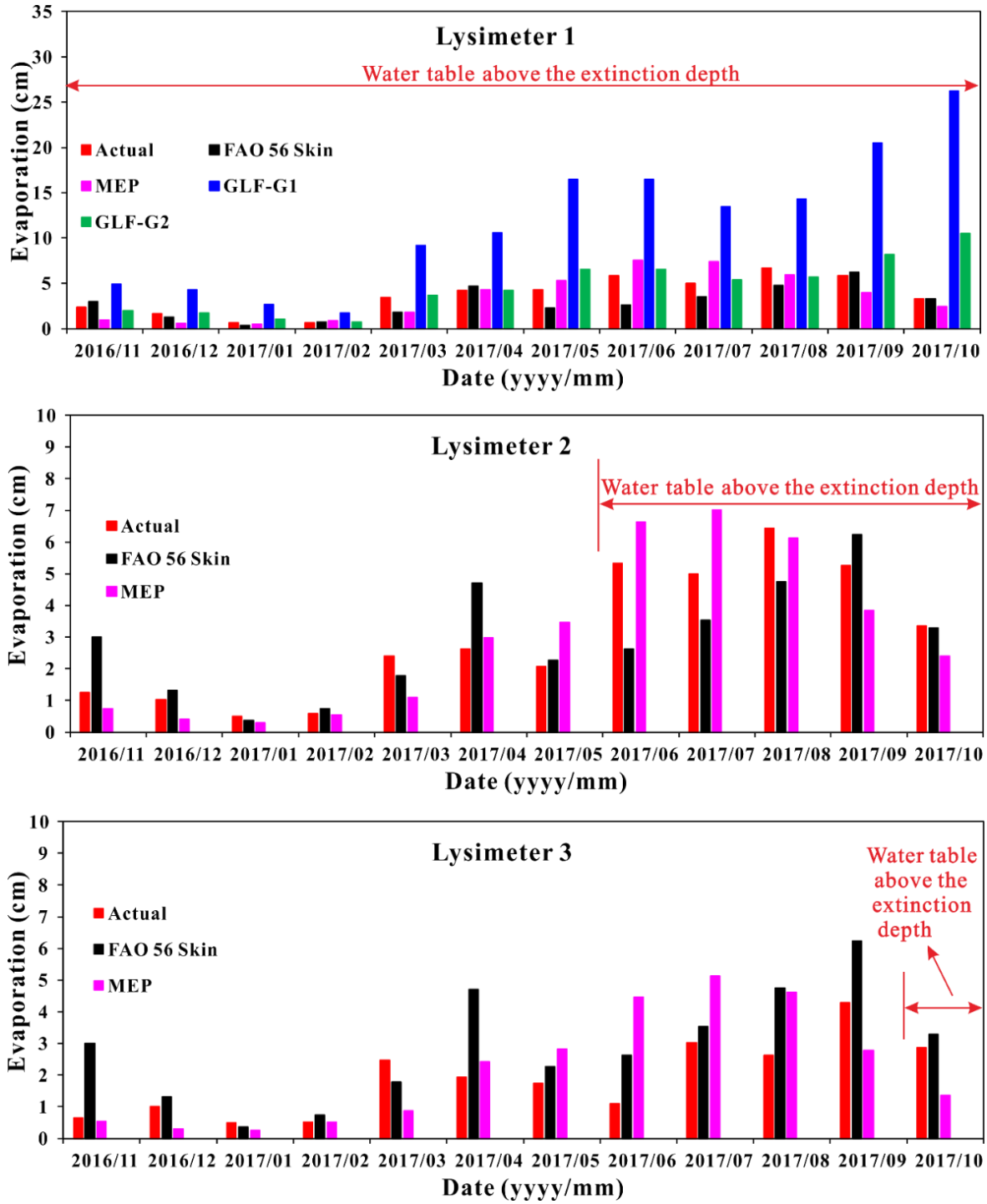

Figure 2.5 Comparison of monthly evaporation rates for the methods. GLF stands for the groundwater level fluctuation method. In GLF-G1, the specific yield was obtained by a pumping test, GLF-G2 uses an estimate of the specific yield based on the approach of Sophocleous (1991). During the experimental period, the groundwater levels in lysimeter 2 and 3 increased, therefore the GLF method can only be applied to lysimeter 1. Evaporation based on Darcy's law method is not shown in this graph (see section 2.3.7).

Evaporation rates in lysimeter 2 and 3 were basically the same from November 2016 to May 2017, while evaporation in lysimeter 1 and 2 were almost identical from June to October, 2017 (Figure 2.5). A reasonable suggestion is to relate these different dynamics to the water table. The position of the water table has a large influence to what extent the evaporation is controlled by the available energy (atmosphere-controlled) or the soil properties. In this context, evaporation can be divided into two distinct stages for bare soil (Allen et al. 2005; Ritchie and Johson 1990), see section 2.2. The first stage is an "energy limited" stage, and the second stage is a "falling rate" or "soil stage" (Allen et al. 2005). A comparison between potential and actual evaporation can indicate at which stage the system is. This is illustrated with an example in Figure 2.6 covering a period of 20 days. Initially, after a strong rainfall event, the actual and potential evapotranspiration were nearly identical, indicating atmospherically controlled conditions (stage 1). As the water evaporates, the soil properties and the soil water content began to control the evaporation processes. Flammini et al. (2018) proposed a simple procedure to identify the first two stages of the evaporation process which we employed here, too. If the soil water content drops below the field capacity, the system is considered to be in stage 2. This analysis was carried out for all lysimeters over the entire period. We found that for the conditions analyzed here, only for 17 % of the time for lysimeter 1, 10% for lysimeter 2, and 0% for lysimeter 3 the systems were controlled by the atmosphere. For the remaining time, the water availability and the soil properties controlled the evaporation rates.

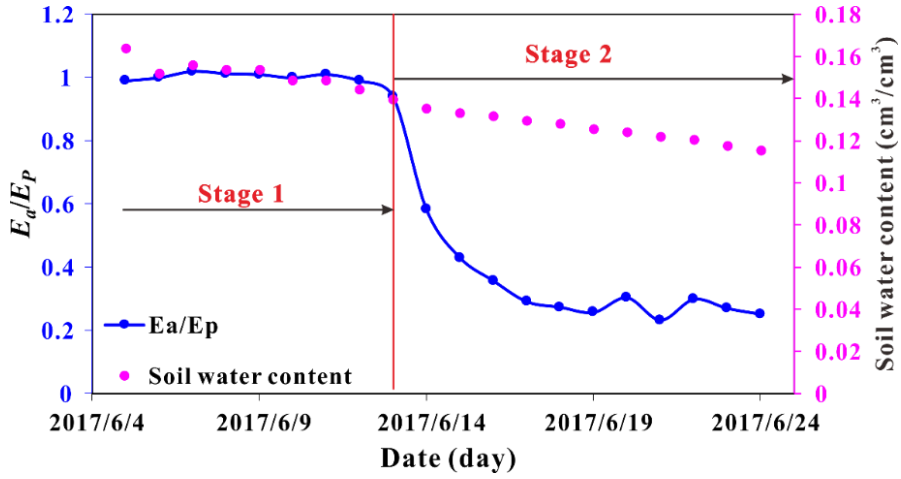

Figure 2.6 Example of the identification of the different stages of evaporation. In Stage 1, energy limits the evaporation rates. The boundary between stage 1 and 2 can be identified through the soil water content in the topsoil (measured at 3 cm in our case). Once stage 2 is reached, the evaporation rate rapidly declines in comparison to the potential evaporation rate.

2.3.4 Comparison of actual evaporation with the FAO-56 skin method

The values of monthly, cumulative evaporation are compared in Figure 2.7 with the FAO-

56 skin method.

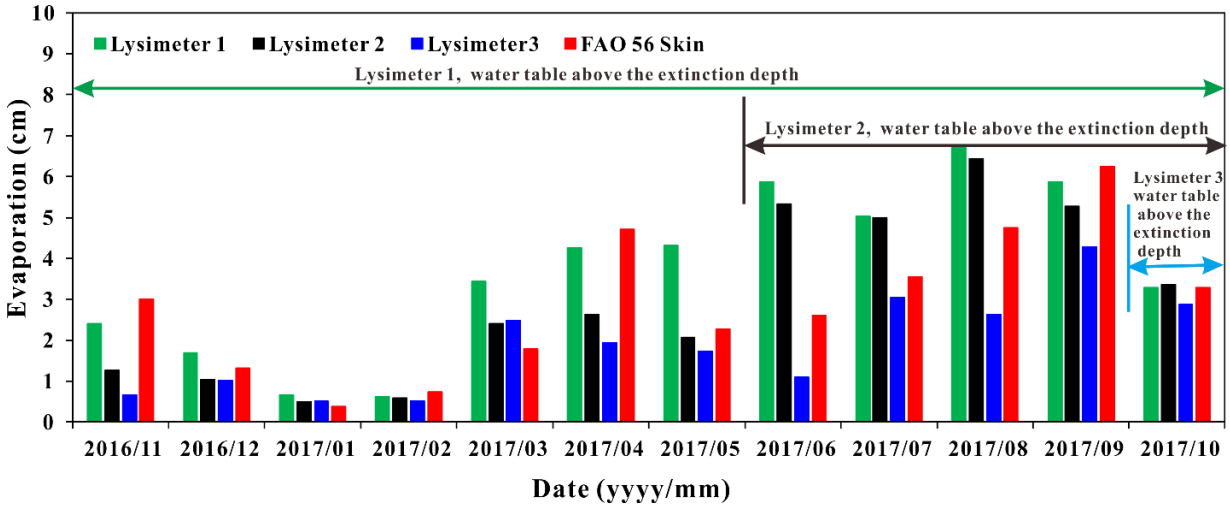

Figure 2.7 Comparison of monthly evaporation rates based on the FAO-56 skin method with actual evaporation in lysimeter 1, lysimeter 2 and lysimeter 3. The extinction depth is 78 cm. The water table in lysimeter 1 was consistently above the extinction depth. In lysimeter 2, extinction depth was exceeded in the month of June. In lysimeter 3 the water table is above the extinction depth for a period of only 23 days (from October 9 to October 31, 2017).

The cumulative amount of evaporation during the experimental period using the FAO-56 skin method was 34.6 cm. On the annual scale, the FAO-56 skin method underestimated 21% of cumulative evaporation in lysimeter 1 (44.1 cm), and underestimated around 3% of cumulative evaporation in lysimeter 2 (35.8 cm), while overestimated 52% of cumulative evaporation in lysimeter 3 (22.7 cm). From November, 2016 to May, 2017, the FAO-56 skin method overestimated 36% of actual evaporation in lysimeter 2, and underestimated 19 % evaporation after May. A more detailed overview of this comparison is compiled in Table 2.3. The cumulative evaporation rates over the entire period, as well as the number of months where evaporation was either over- over underestimated, as well as the % of under- and overestimation during these periods is shown.

Table 2.3 Comparison of FAO-56 skin method with actual evaporation. E_{fcum} is the cumulative evaporation from the FAO-56 skin method, E_{acum} is the cumulative actual evaporation. N_{over}, N_{under} indicate how many months the method over- or underestimated evaporation. We also indicate by how many % evaporation was over ($\%_{over}$) – or underestimated ($\%_{under}$) during these periods.

	Lysimeter 1	Lysimeter 2	Lysimeter 3
E_{fcum}/E_{acum} [%]	79	97	152
N_{over} [-]	5	6	10
($\%_{over}$)	9	42	64
N_{under} [-]	7	6	2
($\%_{under}$)	40	29	28

2.3.5 Comparison with the actual evaporation and the results of the MEP method

The comparison between MEP with actual evaporation for lysimeter 1, lysimeter 2 and 3 are shown in Figure 2.8. As opposed to the FAO-56 skin method (Figure 2.7), the MEP results were closer to the actual evaporation for all lysimeters. On an annual scale, the result of MEP (41.5 cm) was close to the actual evaporation (44.1 cm) in lysimeter 1. MEP underestimated the annual actual evaporation by 6%. The cumulative evaporation of MEP was 35.5 cm in lysimeter 2, which is 99.2% of the actual evaporation (Table 2.4). The cumulative evaporation of MEP for lysimeter 3 was 26.1 cm, which was larger than the actual value of 22.7 cm. MEP overestimated the annual actual evaporation in lysimeter 3 by 14.8%. The very good performance on an annual basis is, however, related to the fact that some months are over- while other months are underestimated. Table 2.4 provides a detailed analysis of the monthly performance.

Table 2.4 Comparison of the MEP method with actual evaporation. E_{Mcum} *is* the cumulative evaporation from the MEP method, E_{acum} is the cumulative actual evaporation. N_{over} , N_{under} indicate how many months the method over- or underestimated evaporation. We also indicate by how many % evaporation was over ($\%_{over}$) – or underestimated *(*$\%_{under}$) during these periods.

	Lysimeter 1	Lysimeter 2	Lysimeter 3
E_{Mcum}/E_{acum} [%]	94	99.2	114.8
N_{over} [-]	5	4	6
$\%_{over}$	26	33.8	82.71
N_{under}[-]	7	8	6
$\%_{under}$	32.7	25.8	48.1

On a monthly scale, MEP overestimated evaporation for all lysimeters from April to July, especially during June and July. Besides that, MEP overestimated evaporation during August for lysimeter 3. Soil moisture content near the surface ground was still low in lysimeter 3 in August (the mean soil water content at 3cm of the surface ground in August is 0.068 cm^3/cm^3). From November to January, March, and August to October, MEP underestimated evaporation for all lysimeters (except for August in lysimeter 3). In addition, our result showed that MEP underestimated evaporation when R_n was lowest from November to January.

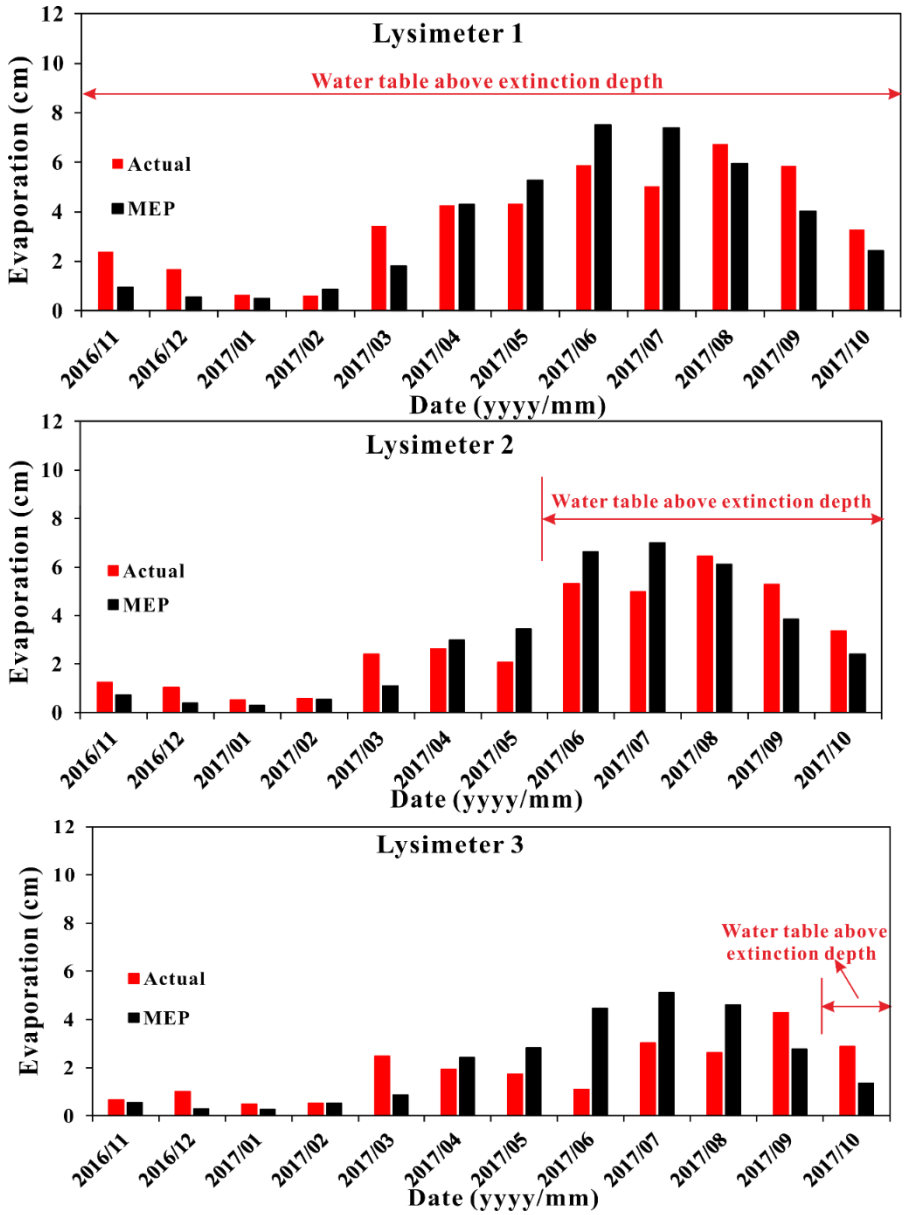

Figure 2.8 Comparison between monthly evaporation rates based on MEP with actual evaporation in lysimeter 1 (a), lysimeter 2 (b) and lysimeter 3 (c). During the period from August to October, the amount of rainfall was 29.6 cm, which accounted for 47.6% of the annual rainfall during the experimental period.

2.3.6 Comparison of actual evaporation with the groundwater level fluctuation method

According to the pumping tests, the specific yields of the three lysimeters were 0.30, 0.31 and 0.30, the average value is 0.30. The second approach to estimate specific yield was based on Sophocleous (1991). The approach from Sophocleous results in estimates of the specific yield equaled to 0.12. The significant differences in the estimation of this crucial parameter are further discussed in section 4. The application of the GLF method requires declining water tables. As lysimeters 2 and 3 are, most of the time, below the extinction depth, the analysis

must be limited to lysimeter 1.

Figure 2.9 shows the results of the GLF. The GLF-G1 approach significantly overestimated actual evaporation every month, especially from March to October 2017 (Figure 2.9). The cumulative evaporation based on the GLF-G1 was 140.6 cm. This implies that the GLF-G1 method significantly overestimated evaporation, by 227.0% for one year. Table 2.5 provides a detailed analysis of the monthly performance.

Table 2.5 Comparison of GLF method with actual evaporation in lysimeter 1. E_{Gcum} is the cumulative evaporation from the GLF method, E_{acum} is the cumulative actual evaporation. N_{over}, N_{under} indicate how many months the method over- or underestimated evaporation. We also indicate by how many % evaporation was over ($\%_{over}$) – or underestimated ($\%_{under}$) during these periods.

	GLF-G1	GLF-G2
E_{Gcum}/E_{acum} [%]	318.61	127.44
N_{over} [-]	12	9
$\%_{over}$	218.61	44.18
N_{under}[-]	0	3
$\%_{under}$	0	11.06

Compared with the GLF-G1 method, the GLF-G2 method yields more accurate results. On a monthly scale, the results of GLF-G2 were consistent with the actual evaporation, except for July and October, 2017. The cumulative evaporation of GLF-G2 was 56.3 cm, as compared to 44.1 cm of actual evaporation. This implies that the GLF-G2 method was a reliable method for estimating evaporation from shallow water table depth.

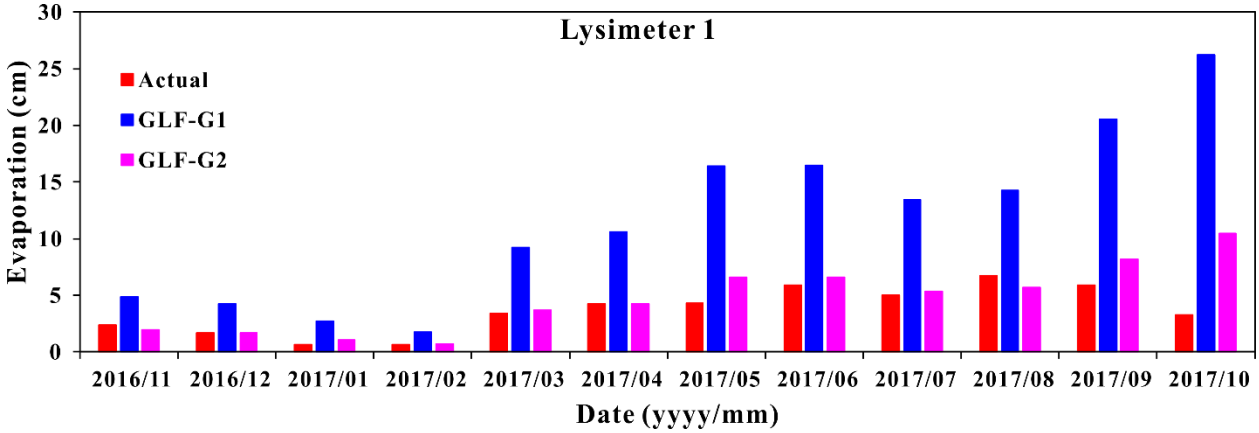

Figure 2.9 Comparison of monthly evaporation rate using GLF-G1 and GLF-G2 in lysimeter 1. GLF-G1(specific yield obtained by pumping test) and GLF-G2 (specific yield obtained by the soil water balance).

2.3.7 Comparison of the actual evaporation with Darcy's law

The laboratory-based van Genuchten parameters do adequately represent the real field conditions. This could, for example, be related to hysteresis. The results (not shown) were not satisfactory as the fluxes are often negative, even during periods where no precipitation occurred. To explore to what extent this method can reproduce evaporation dynamics, we calibrated the soil parameters by minimizing the difference between the observed and calculated evaporation rates. The calibrated parameters are shown in Table 2.6. The values of cumulative evaporation were 43.5, 34.6 and 24.1 cm for lysimeters 1, 2 and 3, respectively. The cumulative evaporation was very good for all three lysimeters. However, as opposed to lysimeter 1 and 2, lysimeter 3 had periods of over-and underestimation. Figure 2.10 displays the cumulative evaporation based on Darcy's law.

Table 2.6 Calibrated parameters for Darcy's law. See table 2.2 for a comparison with the laboratory-based values. The largest changes to the laboratory data are for α.

Lysimeter	θ_s [cm^3/cm^3]	θ_r[cm^3/cm^3]	α[cm^{-1}]	n[-]	K_S[cm/d]
1	0.32	0.02	0.092	1.43	450
2	0.32	0.01	0.06	2.22	450
3	0.32	0.01	0.01	1.66	450

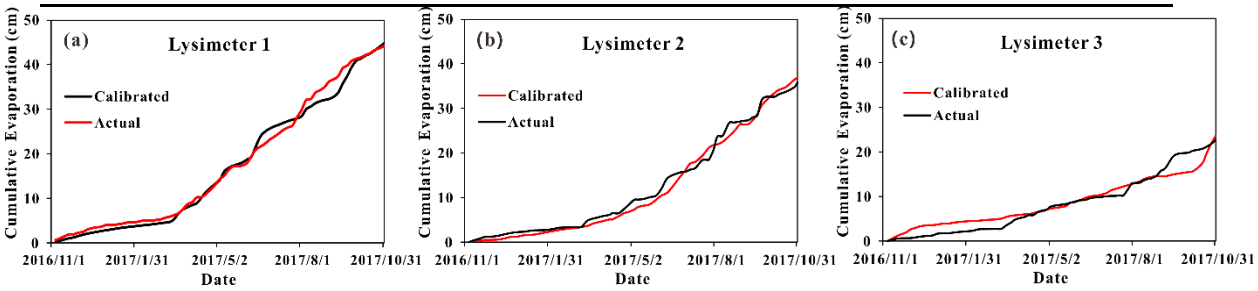

Figure 2.10 Comparison of monthly evaporation rate using Darcy's law method in lysimeter 1(a), lysimeter 2 (b) and lysimeter 3 (c). Calibrated means that the cumulative evaporation from Darcy's law method using calibrated parameters in Table 2.6, and actual means that actual cumulative evaporation.

2.4 Discussion

Multiple methods to estimate evaporation were compared and different implementations of several of these methods were tested. While several studies comparing different methods to estimate bare soil evaporation exist, we are not aware of a study comparing the different methods to accurate, lysimeter based measurements of actual evaporation.

An initial analysis of the meteorological and soil conditions showed that most of the time our system was not controlled by the atmosphere, but rather by soil water availability and the

soil properties. This is a typical situation for arid-and semi-arid regions. Nevertheless, the experimental setup we chose allowed us to explore significantly different hydrological conditions: owing to the instrumentation and different initial conditions of our lysimeters, our study could systematically explore the performance of the different methods in relation to the water table depth. The extinction depth could be graphically identified, in this case it was 78 cm. If the water table is below this depth, no evaporation from groundwater takes place and all evaporation originates from rainfall. Lysimeter 1 was above the extinction depth throughout the experiment, therefore groundwater contributed to evaporation. In lysimeter 3, on the other hand, groundwater contributed only for the last 23 days of the experiment. Lysimeter 2 was between the two extremes, with 5 months below the extinction depth. As our lysimeters are disconnected from the regional groundwater table, the water table in these lysimeters cannot fall below this level. Lysimeters are therefore very well suited to identify the extinction depth for a given soil. However, a clear separation between the contribution of groundwater and rainfall to the total evaporation requires a more detailed analysis and it not the focus of this study.

Our data suggest that across one year and for all lysimeters, MEP performed significantly better than all other methods. Nevertheless, a monthly analysis suggests that MEP can over- or underestimate the evaporation significantly. Alves et al. (2019) pointed out that MEP tends to overestimate evaporation for dry soil conditions. In our study, the largest overestimation was observed for lysimeter 3 (306%) in June, a period coincides with very dry conditions. As opposed to the other two lysimeters, no capillary rise can contribute to evaporation. Our results confirm that MEP overestimates evaporation for dry conditions. The problem is accentuated if the water table is below the extinction depth: During the dry period of June and July, the overestimation of evaporation using MEP is less important in lysimeter 1 and 2 as compared to lysimeter 3. In lysimeters 1 and 2 the water table is above the extinction depth and thus can contribute to maintaining a certain level of soil moisture. This is an important insight as it allows us to identify periods where MEP overestimates evaporation rates. A way to improve the performance of MEP during dry conditions could be the direct measurement of specific humidity (q_s). In our study, we estimated the specific humidity using equation (2.22) and (2.23), but a direct measurement (for example using iButton Hydrochron sensors) might increase the reliability of the results.

For certain periods, MEP underestimates the evaporation rates. We could not identify a systematic relation between the water table being above or below the extinction depth and the underestimation of the evaporation rates. As a first-order indication, MEP underestimated

evaporation rates during precipitation events.

In terms of overall performance, the FAO-56 skin method closely followed the MEP approach. As with the MEP method, the performance of the FAO-56 skin method is dependant on the water table concerning the extinction depth. If the water table is above the extinction depth (as is the case for lysimeter 1 throughout the experiment period), the FAO-56 skin method tends to underestimate the evaporation rate. This is consistent with previous findings: Allen (2011) pointed out that the FAO-56 skin method underestimated the evaporation because of capillary rise is not taken into account. On the other hand, we found that if the water table is consistently below the extinction depth (as is the case for lysimeter 3), the FAO-56 method systematically overestimated the evaporation rate (except for 2 months which do not significantly affect the trend to overestimate evaporation). The good overall, cumulative performance of lysimeter 2 is related to the fact that the periods of over- and underestimation compensate each other. As pointed out by Allen et al. (2005), critical parameters in the application of the FAO-56 method are the REW, TEW and K_{emax}. The implementation of this method was based on the parameter values found in the literature. It is possible that adaption of the parameters to field-specific conditions could further improve the performance (Mutziger et al. 2005).

Although the method of groundwater level fluctuation is relatively simple to implement, falling water tables are required. This can be a limiting factor in arid-and semi-arid regions, where the water table is often below the extinction depth. Another issue is related to the estimation of the specific yield. The estimation of evaporation based on the specific yield obtained through a pump test was not satisfactory as evaporation rates were overestimated significantly. However, the performance of this method increased significantly with our second estimate of the specific yield. The second method considered storage changes in the unsaturated zone, too, and is thus better suited for this kind of application. The estimation of specific yield will remain a problem for the application for this method. Estimating the specific yield is further complicated by effects such as plant growth (Logsdon et al. 2010), hysteresis (Nachabe 2002), and initial water table depth (Cheng et al. 2020).

Darcy's law is a method to estimate evaporation using field observations of soil moisture. Conceptually, the application of Darcy's law is straightforward. However, the problem is related to the parametrization of the soil-water characteristic curve. The application of the parameters obtained in the laboratory did not allow a sound estimation of the evaporation rates, even though a very good fit between pressure-head and soil moisture could be obtained. After the application of Darcy's law based on the laboratory parameters, we modified the soil

retention parameters to reduce the mismatch between observed and calculated evaporation rates. For all lysimeters, a very good fit could be obtained with one set of parameters. This clearly suggests that conceptually Darcy's law remains a very interesting approach, provided the soil-water characteristic curve is known. This, however, will not be the case in most situations.

2.5 Conclusions

The study explored the performance of four commonly used methods to estimate evaporation in semi-arid conditions. Different implementations of the methods were analysed. We used experimental data of three lysimeters with different water table depths. Based on the experimental data from sandy soil under the semi-arid climate condition, the following conclusions/recommendations can be drawn:

(1) The MEP method provided the best results in all lysimeters. MEP overestimated evaporation for dry conditions. If the water table is below the extinction depth, the largest biases are expected.

(2) The FAO-56 skin method could generally obtain good results. The method tended to underestimate the evaporation when the water table was above the extinction depth and overestimated the evaporation when the water table depth was larger than the extinction depth. We recommend to determine the extinction depth and measure the water table for a first-order indication of the performance of this method.

(3) Two approaches for the water table fluctuations were employed: GLF-G1 significantly overestimated the evaporation, due to uncertainties of the specific yield obtained from the pumping test. GLF-G2, which used a soil water balance for a better estimation of the specific yield could reproduce the bare soil evaporation across all groundwater depths. However, the water balance method requires falling water tables, which is only the case if the groundwater level is above the extinction depth. If the water table is below the extinction depth, a falling water table cannot be associated with evaporation.

(4) We could show that Darcy's law is in principle capable of reproducing evaporation dynamics very well. The issue, however, is that the required parameters for the soil-water characteristic curve at often not known. The parameters obtained in the laboratory resulted in a significant mismatch between observed and estimated evaporation rates. This is a serious limitation of the method which will undermine its applicability in most of the cases.

(5) Given the importance of the extinction depth in many of these methods, we suggest that the extinction depth is analyzed and the water table is measured as an integral part of evaporation studies. It provides a useful point of reference for the performance of the MEP and FAO-56 Skin method.

(6) Lysimeters were very well suited for this comparative analysis. We recommend the installation of lysimeters for areas where soil evaporation needs to be quantified. Ideally, weighing lysimeters are employed. Given the significant cost of such lysimeters, the soil-moisture balance based on soil moisture sensors is a pragmatic and useful alternative.

2.6 Acknowledgments

This study was supported by the National Natural Science Foundation of China (No. U1603243, 41230314, 41902249). The first author is grateful to Chang'an University Short-Term Study Abroad Program for Postgraduate Students (No.0021/300203110004) and Chinese Scholarship Council (No. 201906560022) for providing an opportunity to be a visiting student at the University of Neuchatel. The analysis was also partially supported by the SAFEA: High-End Foreign Experts Project (No. G20190027031). We thank Prof. Jingfeng Wang for his suggestion and assistance in the MEP method. We are also very grateful to Prof. Richard G. Allen who gave us a lot of help in using the FAO-56 skin method. We are grateful for the insightful comments and constructive suggestions from three anonymous reviewers and editors.

Chengcheng Gong's contributions to this paper:

Write the original draft, design the experiment, collect data, analyze data, as well as revise the paper.

References

Allen, R.G. 2011. Skin layer evaporation to account for small precipitation events—An enhancement to the FAO-56 evaporation model. Agricultural Water Management, 99(1): 8-18.

Allen, R.G., Pereira, L.S., Raes, D., Smith, M. 1998. Crop evapotranspiration-Guidelines for computing crop water requirements-FAO Irrigation and drainage paper 56. Fao, Rome, 300(9): D05109.

Allen, R.G., Pruitt, W.O., Raes, D., Smith, M., Pereira, L.S. 2005. Estimating evaporation from bare soil and the crop coefficient for the initial period using common soils information. Journal of irrigation and drainage engineering, 131(1): 14-23.

Alves, M., Music, B., Nadeau, D., Anctil, F. 2019. Comparing the Performance of the Maximum Entropy Production Model With a Land Surface Scheme in Simulating Surface Energy Fluxes. Journal of Geophysical Research: Atmospheres, 124(6): 3279-3300.

Bittelli, M., Ventura, F., Campbell, G.S., Snyder, R.L., Gallegati, F., Pisa, P.R. 2008. Coupling of heat, water vapor, and liquid water fluxes to compute evaporation in bare soils. Journal of Hydrology, 362(3-4): 191-205.

Bonan, G.B. 2008. Forests and climate change: forcings, feedbacks, and the climate benefits of forests. science, 320(5882): 1444-1449.

Brandes, D., Wilcox, B.P. 2000. EVAPOTRANSPIRATION AND SOIL MOISTURE DYNAMICS ON A SEMIARID PONDEROSA PINE HILLSLOPE 1. JAWRA Journal of the American Water Resources Association, 36(5): 965-974.

Buck A L. Buck research cr-1a user's manual[J]. Buck Research Instruments: Boulder, CO, USA, 1996, 5.

Brunner, Li, H., Kinzelbach, W., Li, W. 2007. Generating soil electrical conductivity maps at regional level by integrating measurements on the ground and remote sensing data. International Journal of Remote Sensing, 28(15): 3341-3361.

Brunner, Li, H., Kinzelbach, W., Li, W., Dong, X. 2008. Extracting phreatic evaporation from remotely sensed maps of evapotranspiration. Water Resources Research, 44(8).

Chen, L., Wang, W., Zhang, Z., Wang, Z., Wang, Q., Zhao, M., Gong, C. 2018. Estimation of bare soil evaporation for different depths of water table in the wind-blown sand area of the Ordos Basin, China. Hydrogeology Journal, 26(5): 1693-1704.

Cheng, D.-h., Li, Y., Chen, X., Wang, W.-k., Hou, G.-c., Wang, C.-l. 2013. Estimation of groundwater evaportranspiration using diurnal water table fluctuations in the Mu Us Desert, northern China. Journal of hydrology, 490: 106-113.

Cheng, D., Wang, W., Zhan, H., Zhang, Z., Chen, L. 2020. Quantification of transient specific yield considering unsaturated-saturated flow. Journal of Hydrology, 580: 124043. DOI:https://doi.org/10.1016/j.jhydrol.2019.124043

Chinnasamy, P., Maheshwari, B., Dillon, P., Purohit, R., Dashora, Y., Soni, P., Dashora, R. 2018. Estimation of specific yield using water table fluctuations and cropped area in a hardrock aquifer system of Rajasthan, India. Agricultural Water Management, 202: 146-155.

Cobos, D. R., Chambers, C. 2010. Calibrating ECH2O soil moisture sensors. Application note, 1-5.

Cooper, J., Gardner, C., Mackenzie, N. 1990. Soil controls on recharge to aquifers. Journal of Soil Science, 41(4): 613-630.

Crosbie, R.S., Binning, P., Kalma, J.D. 2005. A time series approach to inferring groundwater recharge using the water table fluctuation method. Water Resources Research, 41(1).

Davarzani, H., Smits, K., Tolene, R.M., Illangasekare, T. 2014. Study of the effect of wind speed on evaporation from soil through integrated modeling of the atmospheric boundary layer and shallow subsurface. Water resources research, 50(1): 661-680.

Dewar, R.C. 2005. Maximum entropy production and the fluctuation theorem. Journal of Physics A: Mathematical and General, 38(21): L371.

Flammini, A., Corradini, C., Morbidelli, R., Saltalippi, C., Picciafuoco, T., Giráldez, J.V. 2018. Experimental analyses of the evaporation dynamics in bare soils under natural conditions. Water resources management, 32(3): 1153-1166.

Freeze, R.A., Cherry, J.A. 1979. Groundwater prentice-hall. Englewood Cliffs, NJ, 176: 161-

177.
Gao, H., Cai, X., He, H. 2009. The Impact of Urbanization on the Surface Temperature in Xi'an. Acta Geographica Sinica, 64(9): 1093-1102.
Gardner, W. 1958. Some steady-state solutions of the unsaturated moisture flow equation with application to evaporation from a water table. Soil science, 85(4): 228-232.
Gardner, W., Fireman, M. 1958. Laboratory studies of evaporation from soil columns in the presence of a water table. Soil Science, 85(5): 244-249.
Hellwig, D. 1973a. Evaporation of water from sand, 1: Experimental set-up and climatic influences. Journal of hydrology, 18(2): 93-108.
Hellwig, D. 1973b. Evaporation of water from sand, 4: The influence of the depth of the water-table and the particle size distribution of the sand. Journal of Hydrology, 18(3-4): 317-327.
Henderson-Sellers, A., Irannejad, P., McGuffie, K., Pitman, A. 2003. Predicting land-surface climates-better skill or moving targets? Geophysical Research Letters, 30(14).
Hill, A.J., Durchholz, B. 2015. Specific yield functions for estimating evapotranspiration from diurnal surface water cycles. JAWRA Journal of the American Water Resources Association, 51(1): 123-132.
Huang, S.Y., Wang, J. 2016. A coupled force-restore model of surface temperature and soil moisture using the maximum entropy production model of heat fluxes. Journal of Geophysical Research: Atmospheres, 121(13): 7528-7547.
Kinzelbach, W., Bauer, P., Siegfried, T., Brunner, P. 2003. Sustainable groundwater management--Problems and scientific tool. Episodes-Newsmagazine of the International Union of Geological Sciences, 26(4): 279-284.
Kornejady, A., Ownegh, M., Bahremand, A. 2017. Landslide susceptibility assessment using maximum entropy model with two different data sampling methods. Catena, 152: 144-162.
Lautz, L.K. 2008. Estimating groundwater evapotranspiration rates using diurnal water-table fluctuations in a semi-arid riparian zone. Hydrogeology Journal, 16(3): 483-497.
Lawrence, D.M., Thornton, P.E., Oleson, K.W., Bonan, G.B. 2007. The partitioning of evapotranspiration into transpiration, soil evaporation, and canopy evaporation in a GCM: Impacts on land–atmosphere interaction. Journal of Hydrometeorology, 8(4): 862-880.
Lehmann, P., Assouline, S., Or, D. 2008. Characteristic lengths affecting evaporative drying of porous media. Physical Review E, 77(5): 056309.
Li, H., Brunner, P., Kinzelbach, W., Li, W., Dong, X. 2009. Calibration of a groundwater model using pattern information from remote sensing data. Journal of Hydrology, 377(1-2): 120-130.
Li, H., Kinzelbach, W., Brunner, P., Li, W., Dong, X. 2008. Topography representation methods

for improving evaporation simulation in groundwater modeling. Journal of Hydrology, 356(1-2): 199-208.

Li, N., Zhao, P., Wang, J., Deng, Y. 2020. The Long-Term Change of Latent Heat Flux over the Western Tibetan Plateau. Atmosphere, 11(3). DOI:10.3390/atmos11030262.

Liu, X., Xu, C., Zhong, X., Li, Y., Yuan, X., Cao, J. 2017. Comparison of 16 models for reference crop evapotranspiration against weighing lysimeter measurement. Agricultural Water Management, 184: 145-155.

Liu, Y., Hu, A. 2006. Changes of precipitation characters along Weihe Basin in 50 years and its influence on water resources. Journal of arid land resources and environment, 20(1): 85-87.

Logsdon, S., Schilling, K., Hernandez-Ramirez, G., Prueger, J., Hatfield, J., Sauer, T. 2010. Field estimation of specific yield in a central Iowa crop field. Hydrological Processes: An International Journal, 24(10): 1369-1377.

Loheide, S.P. 2008. A method for estimating subdaily evapotranspiration of shallow groundwater using diurnal water table fluctuations. Ecohydrology: Ecosystems, Land and Water Process Interactions, Ecohydrogeomorphology, 1(1): 59-66.

Loheide, S.P., Butler Jr, J.J., Gorelick, S.M. 2005. Estimation of groundwater consumption by phreatophytes using diurnal water table fluctuations: A saturated-unsaturated flow assessment. Water resources research, 41(7).

Ministry of Water Resources of China (MWR) (2010a), China water resources bulletin, Ministry of Water Resources of China, Beijing. [Available at http://www.mwr.gov.cn/].

Mualem, Y. 1976. A new model for predicting the hydraulic conductivity of unsaturated porous media. Water resources research, 12(3): 513-522.

Mutziger, A.J., Burt, C.M., Howes, D.J., Allen, R.G. 2005. Comparison of measured and FAO-56 modeled evaporation from bare soil. Journal of irrigation and drainage engineering, 131(1): 59-72.

Nachabe, M.H. 2002. Analytical expressions for transient specific yield and shallow water table drainage. Water resources research, 38(10): 11-1-11-7.

Qiao, G., Wang, W. 2014. Evaporation intensity of bare soil in a northwest arid inland basin. J Jilin Univ (Earth Sci Ed), 44(4): 1327-1332.

Quinn, R., Parker, A., Rushton, K. 2018. Evaporation from bare soil: Lysimeter experiments in sand dams interpreted using conceptual and numerical models. Journal of Hydrology, 564: 909-915.

Rianna, G., Reder, A., Pagano, L. 2018. Estimating actual and potential bare soil evaporation from silty pyroclastic soils: Towards improved landslide prediction. Journal of hydrology, 562: 193-209.

Ritchie, J., Johson, B. 1990. Soil and plant factors affecting evaporation. Agronomy(30): 363-390.

Saito, H., Šimůnek, J., Mohanty, B.P. 2006. Numerical analysis of coupled water, vapor, and heat transport in the vadose zone. Vadose Zone Journal, 5(2): 784-800.

Salvucci, G.D. 1993. An approximate solution for steady vertical flux of moisture through an unsaturated homogeneous soil. Water resources research, 29(11): 3749-3753.

Shah, N., Ross, M. 2009. Variability in specific yield under shallow water table conditions. Journal of Hydrologic Engineering, 14(12): 1290-1298.

Shahraeeni, E., Lehmann, P., Or, D. 2012. Coupling of evaporative fluxes from drying porous surfaces with air boundary layer: Characteristics of evaporation from discrete pores. Water Resources Research, 48(9).

Shanafield, M., Cook, P.G., Gutiérrez-Jurado, H.A., Faux, R., Cleverly, J., Eamus, D. 2015. Field comparison of methods for estimating groundwater discharge by evaporation and evapotranspiration in an arid-zone playa. Journal of Hydrology, 527: 1073-1083.

Shih, S.F. 1983. Soil surface evaporation and water table depths. Journal of irrigation and drainage engineering, 109(4): 366-376.

Shokri, N., Lehmann, P., Vontobel, P., Or, D. 2008. Drying front and water content dynamics during evaporation from sand delineated by neutron radiography. Water Resources Research, 44(6).

Shokri, N., Salvucci, G. 2011. Evaporation from porous media in the presence of a water table. Vadose Zone Journal, 10(4): 1309-1318.

Smits, K.M., Ngo, V.V., Cihan, A., Sakaki, T., Illangasekare, T.H. 2012. An evaluation of models of bare soil evaporation formulated with different land surface boundary conditions and assumptions. Water Resources Research, 48(12).

Sophocleous, M.A. 1991. Combining the soilwater balance and water-level fluctuation methods to estimate natural groundwater recharge: practical aspects. Journal of hydrology, 124(3-4): 229-241.

Stephens, D.B., Knowlton, J., Robert. 1986. Soil water movement and recharge through sand at a semiarid site in New Mexico. Water Resources Research, 22(6): 881-889.

Suleiman, A.A., Soler, C.M.T., Hoogenboom, G. 2007. Evaluation of FAO-56 crop coefficient procedures for deficit irrigation management of cotton in a humid climate. Agricultural water management, 91(1-3): 33-42.

Tran, D.T., Fredlund, D.G., Chan, D.H. 2015. Improvements to the calculation of actual evaporation from bare soil surfaces. Canadian Geotechnical Journal, 53(1): 118-133.

Trautz, A.C., Smits, K.M., Cihan, A. 2015. Continuum-scale investigation of evaporation from bare soil under different boundary and initial conditions: An evaluation of nonequilibrium phase change. Water Resources Research, 51(9): 7630-7648.

Valipour, M., Sefidkouhi, M.A.G., Raeini, M. 2017. Selecting the best model to estimate potential evapotranspiration with respect to climate change and magnitudes of extreme events. Agricultural Water Management, 180: 50-60.

Van Genuchten, M.T. 1980. A closed-form equation for predicting the hydraulic conductivity of unsaturated soils 1. Soil science society of America journal, 44(5): 892-898.

Veihmeyer, F., Brooks, F. 1954. Measurements of cumulative evaporation from bare soil. Eos, Transactions American Geophysical Union, 35(4): 601-607.

Wang, J., Bras, R. 2011. A model of evapotranspiration based on the theory of maximum entropy production. Water Resources Research, 47(3).

Wang, W., Zhang, Z., Duan, L., Wang, Z., Zhao, Y., Zhang, Q., Dai, M., Liu, H., Zheng, X., Sun, Y. 2018. Response of the groundwater system in the Guanzhong Basin (central China) to climate change and human activities. Hydrogeology Journal, 26(5): 1429-1441.

Wang, W., Zhang, Z., Yeh, T.-c.J., Qiao, G., Wang, W., Duan, L., Huang, S.-Y., Wen, J.-C. 2017. Flow dynamics in vadose zones with and without vegetation in an arid region. Advances in Water Resources, 106: 68-79.

Wang, W., Zhao, G., Li, J., Hou, L., Li, Y., Yang, F., 2011. Experimental and numerical study of coupled flow and heat transport, Proceedings of the Institution of Civil Engineers-Water Management. Thomas Telford Ltd, pp. 533-547.

Yang, Y., Yang, Y., Moiwo, J.P., Hu, Y. 2010. Estimation of irrigation requirement for sustainable water resources reallocation in North China. Agricultural Water Management, 97(11): 1711-1721.

Zhang, Z., Wang, W., Gong, C., Wang, Z., Duan, L., Yeh, T.c.J., Yu, P. 2019. Evaporation from seasonally frozen bare and vegetated ground at various groundwater table depths in the Ordos Basin, Northwest China. Hydrological Processes, 33(9): 1338-1348.

Zhang, Z., Wang, W., Wang, Z., Chen, L., Gong, C. 2018. Evaporation from bare ground with different water-table depths based on an in-situ experiment in Ordos Plateau, China. Hydrogeology Journal, 26(5): 1683-1691.

Zuo, D., Xu, Z., Cheng, L., Liu, X. 2011. Spatial-Temporal Variations and Mutations of Potential Evapotranspiration in the Weihe River Basin [J]. Resources Science, 33 (5): 975-982.

Chapter 3 *Salix psammophila* afforestations can cause a decline of the water table, prevent groundwater recharge and reduce effective infiltration

Chapter 3 has been published as: Zhang Z, Wang W, **Gong C**, Zhao M, Franssen H. J. H, Brunner P. *Salix psammophila* afforestations can cause a decline of the water table, prevent groundwater recharge and reduce effective infiltration[J]. Science of the Total Environment, 2021, 780: 146336.

Abstract

Afforestation can reduce desertification and soil erosion. However, the hydrologic implications of afforestation are not well investigated, especially in arid and semi-arid regions. China has the largest area of afforestation in the world, with one-third of the world's total plantation forests. How the shrubs affect evapotranspiration, soil moisture dynamics, and groundwater recharge remains unclear. We designed two pairs of lysimeters, one being 1.2 m deep and the other one 4.2 m deep. Each pair consists of one lysimeter with bare soil, while on the other one a shrub is planted. The different water table depths were implemented to understand how depth to groundwater affects soil moisture and water table dynamics under different hydrological conditions. Soil moisture, water table depth, sap flow, and rainfall were measured concurrently. Our study confirms that for the current meteorological conditions in the Ordos plateau recharge is reduced or even prohibited through the large-scale plantation *Salix psammophila*. Shrubs also raise the threshold of precipitation required to increase soil moisture of the surface ground. For the conditions we analyzed, a minimum of 6 mm of precipitation was required for infiltration processes to commence. In addition to the hydrological analysis, the density of root distribution is assessed outside of the lysimeters for different water table depths. The results suggest that the root-density distribution is strongly affected by water table depth. Our results have important implications for the determination of the optimal shrub-density in future plantations, as well as for the conceptualization of plant roots in upcoming numerical models.

***Keywords*:** *Salix psammophila*, Lysimeter, Groundwater recharge, Root distribution, Ecohydrology, Evapotranspiration; Soil moisture

3.1 Introduction

The Ordos plateau is a complex and sensitive ecotone in the semiarid zone of northern China (Chen et al., 2002). The Ordos Plateau is facing major environmental problems. One of the most important environmental problems is desertification. About 10,000 ha/year of land have become desert since the 1960s (Kamichika et al., 1989). To control and prevent desertification effectively, the Chinese government started a reforestation project called the "Three North Forest Shelterbelts" at the beginning of the 1980s (Zhang et al., 2016). In the year 2000, a policy called "Returning Farmland to Forest and Grassland" has been implemented in the Ordos plateau (Wang et al., 2010). In addition to combatting desertification, trees constitute carbon sinks (Baral and Guha 2004; Piao et al. 2009; Xu et al. 2007a). *Salix psammophila* is an important carbon pool. He et al. (2021) pointed out the total carbon sequestration (including the plant components, soil, and litter) of *Salix psammophila* reached 9.53 t hm^{-2} per year in alpine sandy land. The stand density for *Salix psammophila* was 355 ha^{-1} in the 1970s (Li et al. 2016), and 1600 ha^{-1} according to local farmers around 20 years ago (Zhao et al. 2021) in Southern Mu Us desert. *Salix psammophila* has been planted not only to halt shifting dunes (Heshmati et al., 2011), but also to provide fuel, and timber in the Mu-Us desert region (Ohte et al., 2003). *Salix psammophila* is a phreatophyte. Phreatophytes can take up water from the vadose zone as well as from the saturated zone and thus exert a significant influence on the hydrologic system (Naumburg et al., 2005; Le Maitre et al., 1999; Lubczynski, 2009; Banks et al., 2011; Schilling et al. 2014).

Since the 1990s water tables in the Ordos plateau have been dropping significantly, albeit not at the same rate throughout the basin. While the decline of water tables reduces non-productive phreatic evaporation rates (Brunner et al., 2008; Li et al., 2008) and therefore reduces the risk of salinization (Brunner et al. 2007), this decline caused several groundwater-dependent ecosystems to dry up, and the remaining lake-systems are in danger (Xu et al., 2007). With climate change, these problems could be accentuated (Yin et al. 2017). The decline of the water table also limits the development of the economy. Abundant mineral resources such as coal, petroleum, and natural gas have been found in the Mu Us desert. It is one of the largest regions for energy and chemical production in China (Yin et al., 2011). Mining these resources requires a significant amount of water. Concurrently, there is an increased push to expand the afforested areas in the project area by planting *Salix psammophila*, potentially increasing the pressure on groundwater resources.

A quantitative approach on how *Salix psammophila* affect groundwater is therefore required to develop water resources plans that consider desertification, ecological water use as

well as the requirements for the energy sector. Huang et al. (2016) calibrated a Hydrus-1D model taking into account the root water uptake of *Salix psammophila*. They found that the ratio of actual transpiration to potential transpiration decreased as a function of water table depth. Their study was based on a specific level of the groundwater table, fluctuations of the groundwater level were not considered. Groundwater level fluctuations can, however, be an important control of root development and growth (Rodriguez-Iturbe et al. 2007). Some studies have analyzed the influence of fluctuating water tables on the development of phreatophytes in this region. Yin et al. (2018) employed field and modeling approaches to study how native phreatophytes react to short-term pumping by carrying out a 23-day pumping test. They showed that the phreatophytes can recover from the stress induced by groundwater pumping as they can adapt to short periods of water stress using physiological and morphological traits. The rooting depth of trees is a basic tree functional trait determining resilience (Maeght et al., 2013) toward drought and changing groundwater conditions, However, rooting depth is difficult to measure. Fan et al. (2017) analyzed a global synthesis of 2,200 root observations. The results indicated a strong sensitivity and plasticity of root distribution to local soil water profiles. The depth to groundwater might be one of the most important environmental factors. Nevertheless, the current understanding of the growth of different types of roots and their role in taking up water in variable climatic conditions is still limited.

Precipitation is a major driver of biological processes in arid ecosystems (Zhao and Liu, 2010). When shrubs take up water from large rainfall events, the transpiration and respiration of the trees will increase (Schwinning and Sala, 2004). Consequently, the trees affect the water balance of the soil-groundwater (Huxman et al., 2004). Huang et al. (2020) showed that the reduction in recharge rates due to dense plantations was more than 90% below the surface ground 3 m in contrast with bare sandy soil, as deduced from chloride mass balance data in the Mu Us desert. Note that the application of the chloride mass balance is based on several assumptions, including that the system is in a steady-state. Assessing the influence on groundwater dynamics through e.g. lysimeters is a highly complementary approach to assess the conclusions of this previous study. Additionally, the influence on interception was, however, not quantified. Because of interception, small rainfall events might not necessarily lead to a significant increase in soil moisture or groundwater recharge. To fully understand the implications of *Salix psammophila* on the water cycle, the critical (i.e. the minimal) rainfall intensity and duration which leads to infiltration needs to be explored for the climatic conditions of the Ordos Basin.

Accurate experimental data are needed to quantify how the presence of *Salix psammophila*

affects infiltration and soil moisture as well as groundwater level dynamics. Therefore, a set of four lysimeters (two bare ground and two vegetated ground) was designed to study the relationship between evapotranspiration (ET), soil moisture- and groundwater dynamics in response to rainfall. Lysimeters constitute a powerful instrumental approach to carry out controlled experiments outside of the laboratory and under realistic conditions (Pütz et al. 2018). For areas where no surface runoff occurs, lysimeters account for all the relevant processes across the land-atmosphere interface. In our project area, the infiltration capacity of the sand is around 300 mm/h (Yair. 2001), while the most intense precipitation rates around 34.9 mm/h during the experiment period. Given that no surface runoff can occur, lysimeters constitute a holistic approach to observe infiltration, storage, and evaporation processes for this particular project area. The lysimeters were specifically designed to explore the role of groundwater levels in this context. Zhao et al. (2020) investigated the water use of *Salix psammophila* based on the two vegetated lysimeters. They used Darcy's law to estimate the soil evaporation based on data from April to November 2016. Their results showed that *Salix psammophila* can consume groundwater by extending the root length during the dry period. Additionally, they indicated that the infiltration of rainfall can be intercepted by the uptake of *Salix psammophila* root zone, and reduce groundwater recharge. To what extent interception will reduce the minimal amount of rainfall to increase soil moisture was not quantified, however. As discussed in Zhao et al. (2020), their approach had several shortcomings. A source of uncertainty is the application of Darcy's law. Hysteresis was not considered, and the soil water retention function is not well known. Besides, the data they used was only from the two vegetated lysimeters. However, to understand the relative importance on how *Salix psammophila* affects soil water and groundwater dynamics could thus not be fully established. The length of data in their research was from one growing season (April to November, 2016). The influence of *Salix psammophila* at the initial stage on the soil water and groundwater was also not analyzed.

This paper builds on this previous research and closes several important knowledge gaps. As opposed to the previous study by Zhao et al. (2020) this study makes use of two additional, non-vegetated lysimeters. This is important because it provides the information required on how planting *Salix psammophila* will change the soil water balance. This paper also considers two growing seasons (2015 and 2016), as opposed to only one by Zhao et al. (2020). Based on these important differences and expansions, the following questions are analysed: (1) the influence of *Salix psammophila* on groundwater recharge and water table dynamics under consideration of interception, (2) the influence of *Salix psammophila* on the soil water balance,

(3) the root adaptability to different water table depths. In addition to the previous study by Zhao et al. (2020), we also integrate root observations of two shrubs that were growing outside of the lysimeters.

From a methodological and data analysis point of view, our study differs significantly from the previous study by Zhao et al. (2020). The focus of Zhao et al. (2020) was on quantifying fluxes across the water table and the vadose zone to identify the relative contributions of groundwater and soil moisture to evaporation. Here we base our analysis on a mass balance approach, without the need of quantifying fluxes. Assumptions concerning the soil-water retention curve or the effects of hysteresis thus have not to be made.

3.2 Materials and methods

3.2.1 Study site description

The experimental site is located in the Mu Us Desert, Northwestern China. The climate is continental and semiarid. A hydrological station is located at the Henan town national weather station (Figure 3.1) and meteorological data were obtained from this station. There are 50 years of meteorological data (from 1957-2006), the long-term average annual air temperature is 8.0°C, and the observed extreme temperatures are -34.3 and 36.7°C in January 1958 and July 1959, respectively. The mean annual precipitation (1985-2008) is 340 mm, of which 70% falls as rain between July and September (Zhang et al., 2019). The mean annual potential evapotranspiration (PET) from 1985 to 2008 is 2266 mm. The growing season is from May to October and the dryness index (Potential ET divided by precipitation) is 6.7. The typical soil is sand, and highly susceptible to wind erosion. The landscape includes fixed, semi-fixed, and semi-mobile dunes, as well as inter-fixed dunes. The dominant vegetation type is *Salix psammophila*.

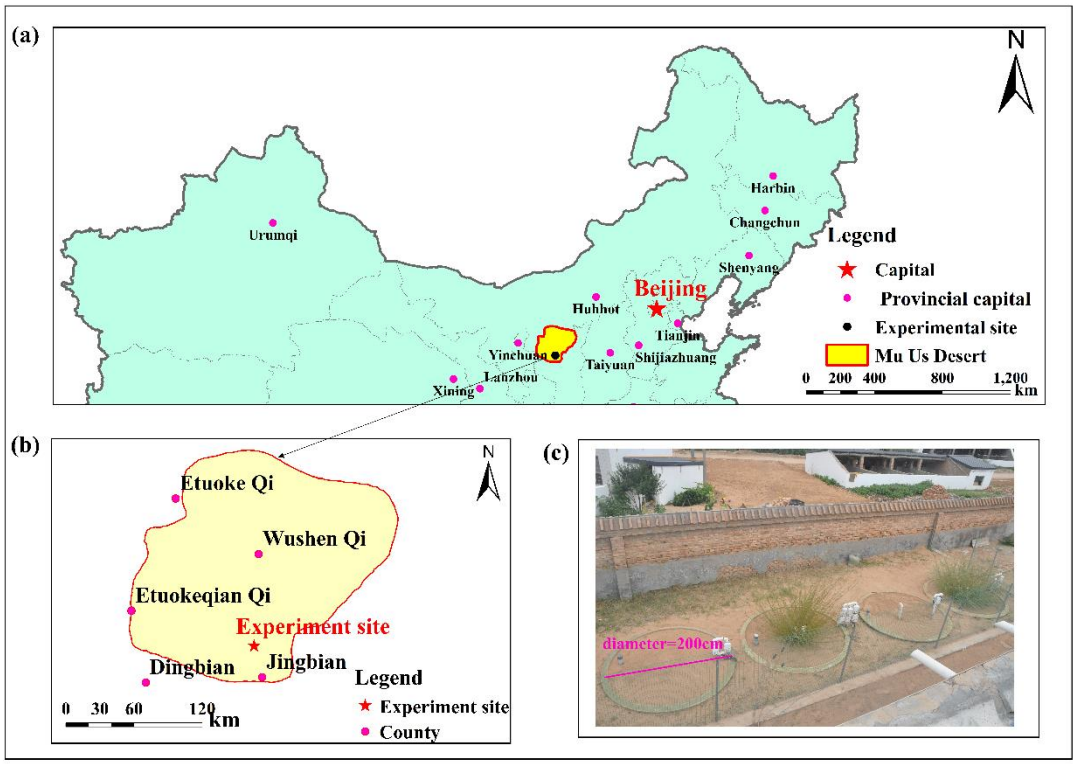

Figure 3.1 Location of the field site. (a) Location map of Mu Us desert in Northwest China; (b) Location map of the experimental site within Mu Us desert; (c) experimental site (there are four lysimeters built up with the same diameter of 200 cm). The boundary of Mu Us desert is from Liang and Yang (2016).

3.2.2 Field experiments with bare- and vegetated soil for two groundwater levels

To investigate how *Salix psammophila* responds to different water table depths, we designed two pairs of lysimeters filled with the soil material found locally with a bulk density of 1.55 g/cm^3. The results from a particle size analysis revealed that the sandy particles in the lysimeters account for more than 88% of the total particles. According to the United States Department of Agriculture textural soil classification, the soil can be classified as sand.

One pair of lysimeters is 1.2 m deep (subsequently labelled with the abbreviation *shal_*) and the other is 4.2 m deep (subsequently labelled with the abbreviation *deep_*). Water tables are monitored in all lysimeters. For each pair, one lysimeter features *Salix psammophila* and the other one is bare soil. We refer to these lysimeters as *shal_veg* and *shal_bare*, as well as *deep_veg* and *deep_bare*. The young *Salix psammophila* were dug out near the experimental site and planted for both vegetated lysimeters. They initially had the same rooting depths (30 cm). The two different groundwater depths for these pairs were implemented to assess the influence of the water table depth on the shrub behavior, soil water dynamics, and

evapotranspiration. The lysimeters are sealed at the lower end. In Mu Us desert, shallow water table depths are common (Chen et al. 2018; Li et al. 2012). Growing *Salix psammophila* at locations of shallow water table depths are also common practice (Huang et al. 2016; Cheng et al. 2013). Therefore, we set two initial water table depths: one pair equal to 1 m which is less than the extinction depth of this soil type (equal to 1.05 m (Ma et al., 2019)); and the other pair (about 2.5 m): one equal to about 2.5 m and the other equal to 2.8 m.

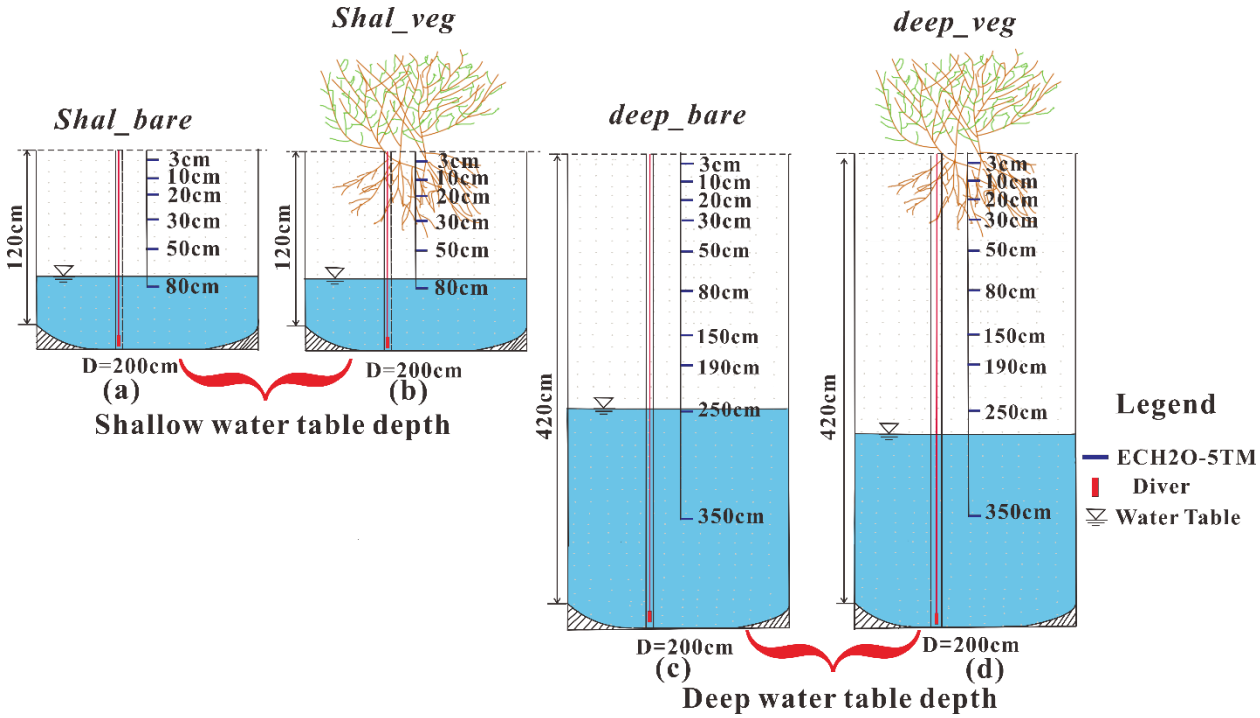

Figure 3.2 Two pairs of lysimeters with different water-table depths. (a) *shal_bare* has no vegetation and an initial water-table depth of about 1 m; (b) *shal_veg* has a *Salix psammophila* with an initial water-table depth of about 1 m; (c) *deep_bare* has no vegetation with a water-table depth of about 2.5 m; (d) *deep_veg* also has a *Salix psammophila* plant with water table depth about 2.8 m.

3.2.3 Data collection

We measured volumetric soil moisture content in the *shal_* lysimeters at the depths of 3, 10, 20, 30, 50, and 80 cm using ECH$_2$O-5TM probe (Decagon Inc., USA, ±1 ~ 2 %), and in the *deep_* lysimeters at the depths of 3, 10, 20, 30, 50, 80, 150, 190, 250 and 350 cm (Figure 3.2). Following the protocol of Cobos and Chambers (2010), we calibrated the sensors before installation. The data were logged with an interval of 5 min. At the Henan town national weather station, precipitation, wind speed and direction (around 10 m height), air pressure, relative humidity, and air temperature were measured and logged hourly. We also measured groundwater levels with an interval of 5 minutes for the two growing seasons from 1 July 2015

to 13 Oct 2015 (the first growing season) and from 23 April 2016 to 30 November 2016 (the second growing season) using CTD-diver installed at the bottom of the lysimeters. At the same time, we used another diver sensor Baro-Diver installed to measure the air pressure for correcting the measured groundwater level. Also, sap flow sensors EMS 62 (EMS Brno) with stem heat balance method (Lindroth et al. 1995) were installed in *deep_veg* to measure sap flow velocity from April to November 2016.

The root distributions under the different water table depths were measured at two nearby locations: one was from a dune depression with a low depth to groundwater, and the other was on a sand dune with a high depth to groundwater. The shrubs were dug out and the roots were sieved and washed at the sampling day. The cleaned roots of each sample were weighed.

3.2.4 Soil water balance and interception threshold

We estimated the water budgets for all the four lysimeters (Gong et al. 2020) using the following water balance equation:

$$\frac{dS}{dt} = P - ET - R \tag{3.1}$$

where dS/dt is the total water storage change in the lysimeters (cm/d), P is the total precipitation (cm/d), ET is the actual evapotranspiration (cm/d), and R is the surface runoff (cm/d). The surface runoff during the experiment can be neglected because no runoff occurs in the lysimeters, which is also the case in the project area (Wu et al. 2012; Zhang et al. 2018). The daily average soil moisture at the different depths was interpolated between the measurement points using linear interpolation (Figure 3.3). The total water storage in the lysimeter can be estimated as follows:

$$\frac{dS}{dt} = \Delta S_u + \Delta S_g \tag{3.2}$$

where S_u is the water storage in the unsaturated zone, and S_g is the water storage in the saturated zone. We can calculate S_u and S_g according to Figure 3.3.

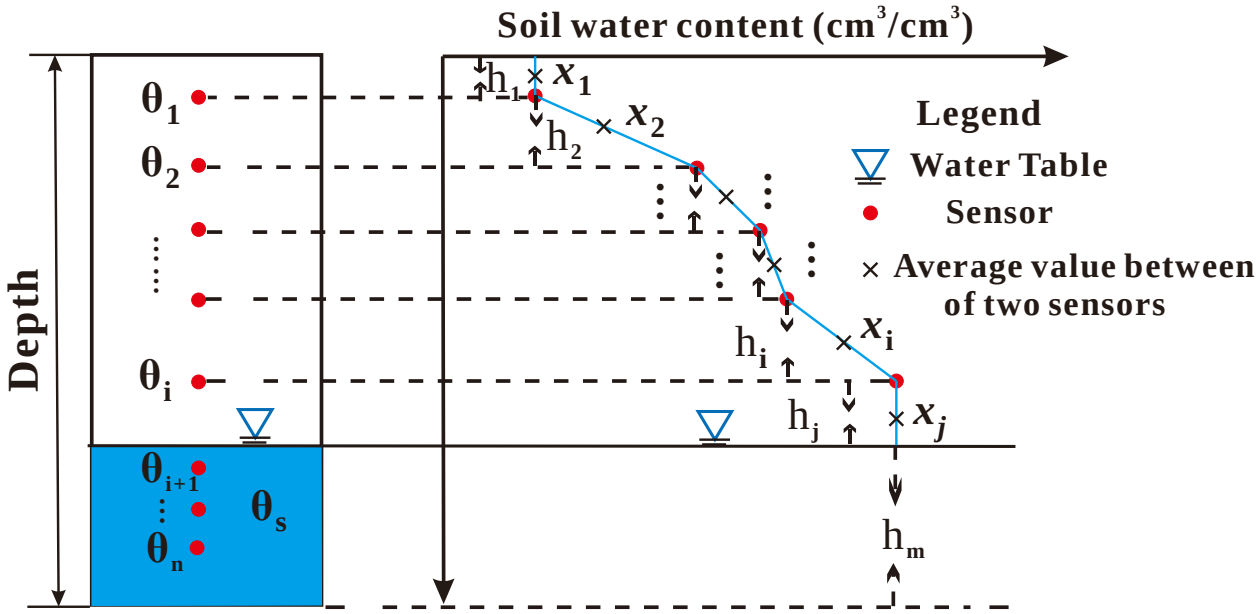

Figure 3.3 Schematic diagram of the sensors in the saturated and unsaturated zone and an example of soil water content profile (Gong et al. 2020). The change of storage and thus evapotranspiration can be estimated by comparing the soil moisture profiles and the groundwater levels between two periods in time (Daily, in this case). To calculate the water content on a specific day, the average values between two sensors (indicated with x_i in the diagram) were weighted by the distance between sensors (h_i).

Another aspect we can explore with our experimental setup is the identification of the critical threshold of precipitation required for infiltration to occur. The critical threshold corresponds to the interception capacity of the shrubs. By continuously comparing the changes of moisture content in the topmost soil zone with the measured precipitation rates, this threshold can be readily identified.

3.3 Results

3.3.1 Precipitation, potential evapotranspiration, and air temperature

During the two growing seasons (1 July, 2015 to 13 Oct, 2015 and from 1 April, 2016 to 30 November, 2016), there 93 rainfall events occurred, which resulted in a total of 508.1 mm. The average precipitation per event was 5.5 mm, with individual events ranging from 0.1 to 58.1 mm. In summary, light rainfall events (< 10.0 mm) were the most frequent, whereas heavy events (≥ 10.0 mm) were infrequent but constitute a major contribution to the total precipitation.

We used the Penman-Monteith equation (Allen et al., 1998) to calculate potential evapotranspiration (ET_0). The potential ET provides general information on the climatic forcing conditions in the project area. Note, however, that actual evapotranspiration rates were calculated using our lysimeter data (See section 3.2.4). Figure 3.4b depicts potential

evapotranspiration from July 1, 2015 to July 31, 2016. Potential evapotranspiration is closely following air temperature. The mean potential evapotranspiration was 3.4 mm/day with a standard deviation of 2.5 mm/day.

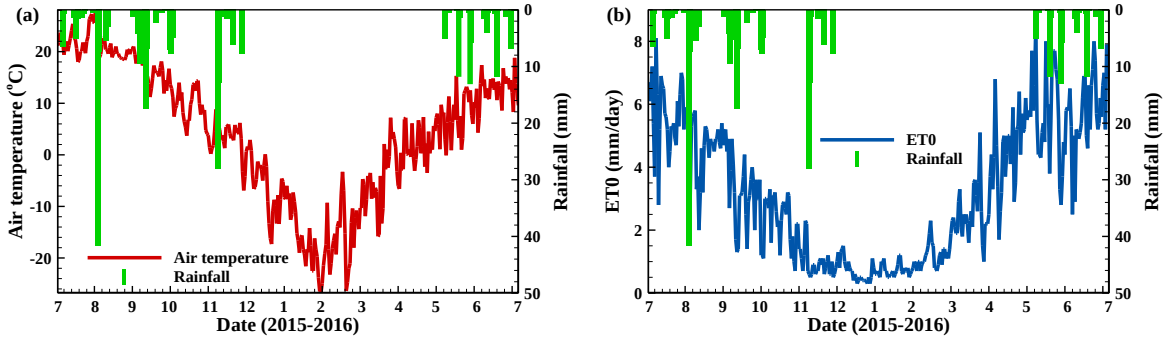

Figure 3.4 Rainfall and air temperature at the field site (a), potential evapotranspiration (ET_0), and rainfall (b).

3.3.2 Water Table Dynamics

The water table of the *shal_bare* and *shal_veg* showed a much more rapid response to rainfall and ET than that of the *deep_ bare* and *deep_veg*. The thicknesses of the vadose zone of *deep_ bare* and *deep_veg* were much larger than the extinction depth, and therefore the water table depth did not respond so rapidly as *shal_*. The water table of *deep_bare* and *deep_veg* showed a gradual rise in the first growing season (same amount of rainfall as *shall_* lysimeters), because ET was less than for *shal_bare* and *shal_veg* and there was a net recharge from the unsaturated zone.

In the first growing season (2015), groundwater levels in *shal_bare* and *shal_veg* declined due to ET (Figure 3.5a). From July 1 to August 31, the downward trends were basically the same for the two *shal_* lysimeters because transpiration was relatively small in the first growing season. After September 23, the water table depth in *shal_veg* was deeper than for *shal_bare.* This indicates that shrubs began to take up groundwater resources as a result of roots growing vertically. On the other hand, rainfall events smaller than 5 mm/day did not affect groundwater levels in the two *shal_* lysimeters. Rainfall events larger than 5 mm/day resulted in a response of the groundwater table. Its magnitude depended on rainfall amount and soil water content. Note that the shrubs were very small at this stage, so the effect of interception was not important.

In the second growing season (2016), groundwater levels for *shal_veg* and *shal_bare* started to deviate significantly as the shrubs grew larger with an increasing effect of root water uptake in *shal_veg*. The Diver sensor was placed 1 m below the ground surface to measure groundwater level (Figure 3.2b), and the recorded water table depth remained constant at 1 m depth in *shal_veg* after June 6, 2016, indicating that the water table depth was below 1 m

(Figure 3.5b). There was almost no groundwater in *shal_veg* as indicated by in-situ groundwater level measurements in the middle of June, 2016 and soil moisture measurements (Figure 3.6e). Besides, the water table depth decreased with ~0.63 cm/day in *shal_bare* after middle August 2016. In this case, evaporation from the bare ground caused the groundwater level to decrease (Figure 3.5b).

The initial water table depth of the *deep_bare* lysimeter was around 2.5 m, and the *deep_veg* lysimeter was about 2.8 m, respectively. Due to technical reasons, the water table depths could not be set to an equal level at the beginning of the experiment. The groundwater levels in *deep_veg* and *deep_bare* show similar dynamics during the first growing season (Figure 3.5c). The groundwater levels increased with 0.38 and 0.3 cm/day in *deep_veg* and *deep_bare*, respectively. It implies that root water uptake did not prevent groundwater recharge from occurring.

In the second growing season (2016), groundwater levels continuously decreased with ~0.70 cm/day in *deep_veg* from June 1 to November 30 (Figure 3.5d). The difference in groundwater levels of *deep_veg* compared to *deep_bare* is indicative of the rate of *Salix psammophila* to uptake soil moisture and groundwater. The groundwater level decline (0.95 cm/day) was larger in the dry period (from June 1 to August 11, 2016) than in the wet period (from August 12 to November 30, 2016) (0.53 cm/day). This indicates that heavy rainfall would slow down *Salix psammophila* consumption of groundwater. Groundwater levels still increased during the second growing season at a rate of ~0.13 cm/day for *deep_bare*.

Overall, our results show that the presence of vegetation affects the groundwater table in the following way: (1) in the first growing season (2015.7.1-2015.10.13), *Salix psammophila* had no effect on the water table depth of *deep_veg*, and a small effect (after September 23) on the *shal_veg*. (2) After the beginning of the second growing season (starting around May 2016 and finishing around November), *Salix psammophila* affected the groundwater levels. Firstly, *Salix psammophila* affected the shallow groundwater in *shal_veg* from May 1 (Figure 3.5b). While *Salix psammophila* influenced significantly the deep groundwater level in *deep_veg* from June 11 (Figure 3.5d). (3) Although heavy rainfall events occurred from August 12 to August 20, 2016 (the amount of rainfall was 150 mm), groundwater levels did not increase in *shal_veg* (Figure 3.5b) and *deep_veg* (Figure 3.5d). However, the groundwater level increased by 42.5 cm in *deep_bare*. This suggests that *Salix psammophila* absorbed the infiltrating water in *shal_veg* and *deep_veg*. While analyzing groundwater level dynamics provides insights into groundwater recharge, little can be said about soil moisture storage dynamics. The soil moisture loggers provide additional information on this aspect.

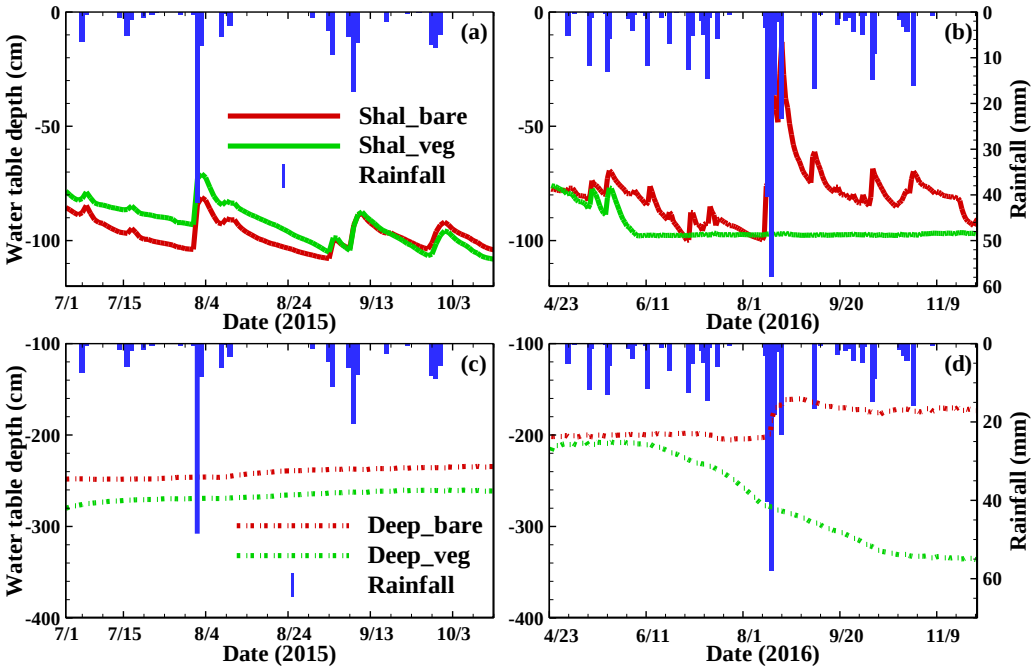

Figure 3.5 The fluctuation of water table depths during the experimental periods (2015.7.1-2015.10.13 and 2016.4.23-2016.11.30) for the four different lysimeters. (a) and (b) represent water table depth changes with time in the two growing seasons for the two *shal*_lysimeters (green and red lines indicate *shal_veg* and *shal_bare*, respectively); (c) and (d) show water table depth changes with time in two growing seasons for the two *deep*_lysimeters (green and red dotted lines are for *deep_veg* and *deep_bare*, respectively). The blue bar indicates that rainfall events occurred. Note, there is no groundwater in *shal_veg* lysimeter after the middle of June, 2016.

3.3.3 Soil Water Dynamics and critical precipitation threshold for infiltration

Figure 3.6 shows a comparison of soil moisture variations in the lysimeters with shrubs and without shrubs, illustrating the impact of soil water uptake by the *Salix psammophila* shrubs. Soil moisture kept relatively stable within the profile during the first growing season in *shal_veg* (Figure 3.6a). Compared to Figure 3.6b, *Salix psammophila* significantly affects the distribution of soil moisture content from the ground surface to 50 cm depth. In the spring of the second growing season of 2016, soil moisture at different depths slightly decreased in response to the transpiration demand. With the further growth of *Salix psammophila* and large transpiration demand in summer (from July to September 2016), soil moisture content significantly decreased from the ground surface to 80 cm depth. The soil moisture content at deeper depths did not directly respond to rainfall events during the experimental periods, except for a few heavy precipitation events (e.g., 13 August 2016). It can be seen that infiltrated water firstly increased soil moisture, which is subsequently consumed by *Salix psammophila.*

In *shal_bare*, the effects of soil surface evaporation only extend down to 20 cm depth (the left panel of Figure 3.6b). Below 20 cm depth in *shal_bare* in 2015, soil moisture content shows only very small fluctuations, while soil moisture content in the upper 20 cm falls and rises quickly in response to evaporation and infiltration of rainfall. During the second growing season (Figure 3.6f), evaporation could cause soil moisture to decrease until 70cm depth. However, when heavy rainfall events occurred (e.g., 13 August 2016), soil moisture content rapidly increased between the ground surface and a depth of 70 cm.

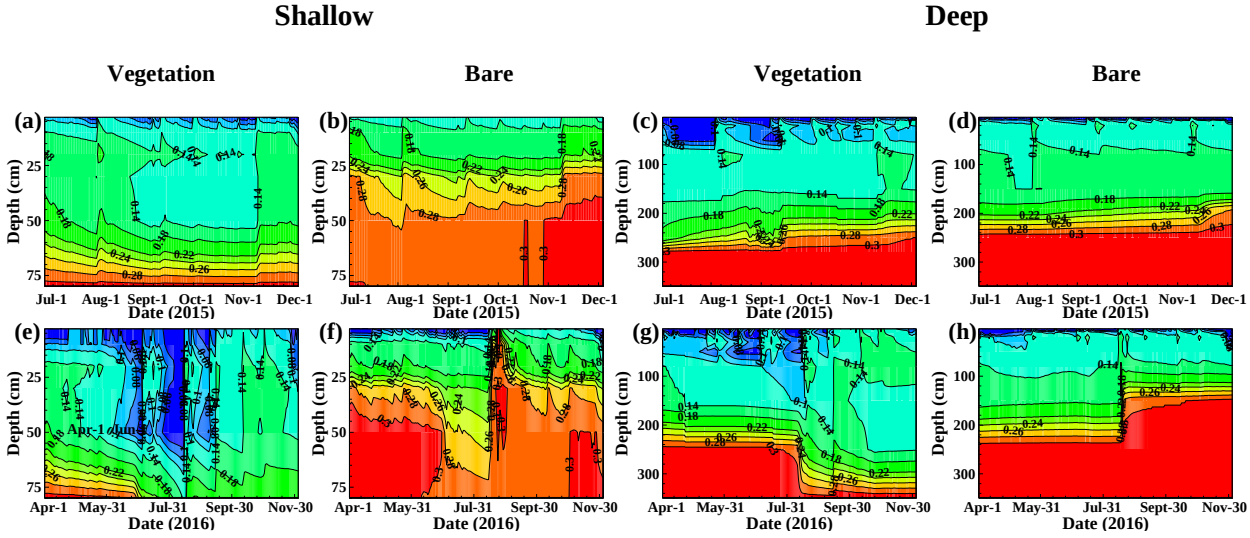

Figure 3.6 Variation of soil moisture content. (a) and (b), (c) and (d), (e) and (f), and (g) and (h) represent soil moisture changes in space and time in two growing seasons (2015.7.1-2015.11.30 and 2016.4.1-2016.11.30) in *shal_veg*, *shal_bare*, *deep_veg*, and *deep_bare*, respectively.

Unlike the *shal_veg* and *shal_bare*, the *deep_veg* features a relatively extended vadose zone (~ 2.8 m). Soil moisture content in the 0-60 cm soil layer was significantly lower than that for *shal_veg* from July, 2015 onwards. This is related to the deeper water table depth, thus capillary rise has a limited influence on the soil water content of the upper soil layer of 0-60 cm. Compared to the first growing season, the main difference was that from August 2016 onwards soil moisture decreased for the 160-350 cm layer. The abrupt decrease in soil moisture content by the end of the second growing season is consistent with a decrease in the groundwater level (Figure 3.5d).

Soil moisture content for the 0-10 cm soil layer (in *deep_bare*) was relatively low because of high atmospheric evaporative demand and limited or no capillary rise from the groundwater

during the experimental period (Figure 3.5d). Soil moisture content for the 150-250 cm layer showed an increasing trend as a result of the infiltration water during the period (Figure 3.6h). This demonstrates that groundwater recharge took place under bare soil conditions.

To identify how the presence of vegetation affects the critical threshold of precipitation for infiltration to occur, the precipitation data can be juxtaposed with soil moisture data. Only for rainfall events exceeding 6.0 mm, an increase of soil moisture was observed for vegetated conditions. Under vegetated conditions, smaller precipitation events did not change the soil moisture in an observable way. For precipitation events exceeding this critical threshold, vegetation still exerts a major influence on soil moisture dynamics. For example, around August 12, 2016, soil moisture at a depth of 50 cm in the shallow, vegetated system was around 0.035 cm^3/ cm^3, while for non-vegetated conditions soil moisture was 0.246 cm^3/ cm^3. The increase of soil moisture in response to a heavy precipitation event is also significantly affected by the presence of mature shrubs. For example, the change of soil moisture storage for non-vegetated conditions (5.98 cm) is larger than that of vegetated conditions (4.91 cm) during the same period.

3.3.4 Estimation of actual evapotranspiration (ET)

The cumulative ET estimation using the water balance equation for each lysimeter is shown in Figure 3.7 for the two growing seasons. Assuming that the shrubs do not significantly affect the soil surface energy budgets, the differences in ET between the *shal_veg* and *shal_bare,* and between the *deep_veg* and *deep_bare* are indicative of differences in transpiration for the two different water table depths. Without shrubs, *deep_bare* shows a net water gain as indicated by the rise of groundwater level at the end of the second growing season (see Figure 3.5d).

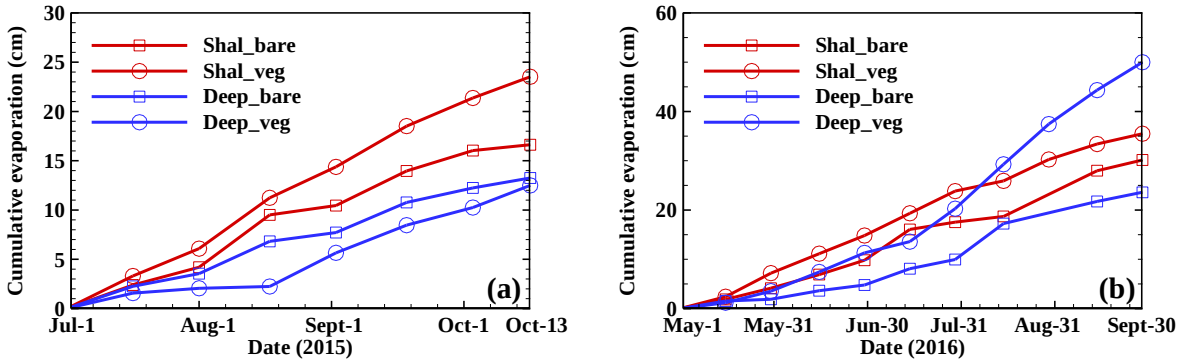

Figure 3.7 The cumulative evapotranspiration in *shal_veg* (red circle line), *shal_bare* (red square line), *deep_veg* (blue circle line), and *deep_bare* (blue square line) for the years 2015 (left) and 2016 (right)

It was found that the cumulative evapotranspiration in *deep_veg* was smaller than that in *deep_bare* in 2015. The reasons for this apparently surprising result might be: (1) Water table depth was deeper in *deep_veg* than that in *deep_bare.* That means that soil moisture along the profile in *deep_bare* was higher than that in *deep_veg* (Figure 3.6c and 3.6d); (2) *Salix psammophila* was small, it could not absorb much water from dry soil, and (3) surface ground obtained less water as a result of vegetation interception, for example, the change of soil moisture content at 3 cm depth in *deep_veg* and *deep_bare* were 0.019 cm^3/cm^3 and 0.038 cm^3/cm^3 respectively after a rainfall event (6.0 mm).

The sap velocity for one branch of *Salix psammophila* in *deep_* was 0.015 kg/h with a standard deviation of 0.028 kg/h (Figure 3.8). The value of sap velocity was highest in summer, followed by autumn, and the lowest in spring. It can be seen that heavy rainfall events caused sap flow to decrease even though heavy rainfall events effectively increased soil moisture for deep soil layers. That is because heavy rainfall is associated with less incoming radiation, higher relative air humidity and lower air temperature. Zhao and Liu (2010) obtained similar results.

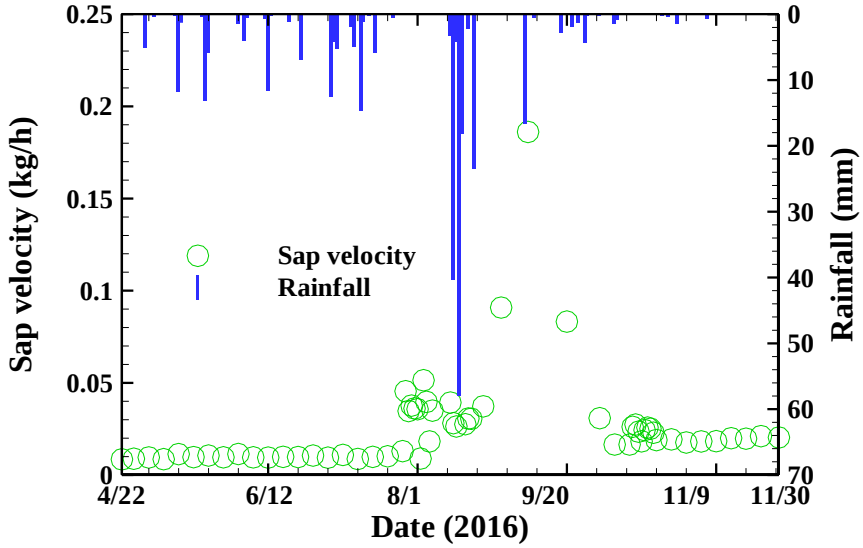

Figure 3.8 Sap velocity (Kg/h) in response to rainfall event in *deep_veg*

3.3.5 Root distribution

To understand how different water table depth conditions affect the development of the root system, we analyzed the root distribution of two *Salix psammophila* taken from places near the field site with different water table depths (one from a sand dune, and the other one from a dune depression). The root distributions are different as a function of the water table depth (Figure 3.9). The *Salix psammophila* in the dune depression has mainly roots between 0 and 60 cm depth. The root length density decreases with depth in this case, which is in correspondence to the findings of Zhu et al. (2016). When the *Salix psammophila* is located on the sand dune, the maxima of the root densities are located between 0-20 cm and 80-120 cm depth. The root length density decreases with depth going downwards to 20-60 cm depth, but increases again for the layer between 60 and 120 cm depth and decreases below 120 cm depth. The root distribution indicates that *Salix psammophila* may not only absorb shallow soil water but also consume deep soil water when the groundwater level is relatively deep.

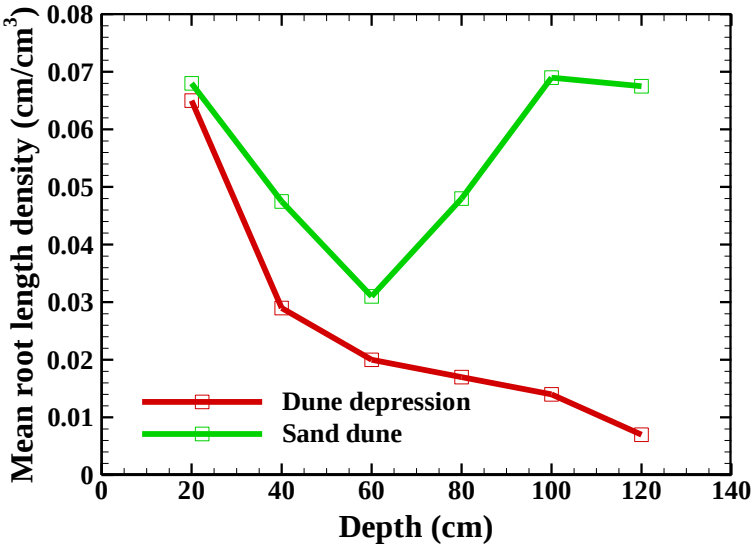

Figure 3.9 Mean root length density as a function of depth for *Salix psammophila* (red box and green box represent root length density for dune depression and sand dune, respectively. Water table depth of sand dune was larger than that of dune depression).

3.4 Discussion

The three questions raised in the introduction are discussed in the following sections.

3.4.1 Influence of vegetation on groundwater recharge and water table dynamics

In our experimental setup with the lysimeters, groundwater recharge can easily be identified through a rising water table. Whether or not groundwater recharge occurs in response to precipitation depends on the intensity and duration of precipitation (Owor et al., 2009), the depth to groundwater (Nazarieh et al., 2018), the hydraulic properties of the unsaturated zone（Wang et al., 2009) as well as the antecedent soil moisture conditions (Manfreda et al., 2005) which themselves are influenced by the presence of vegetation (see upcoming section 3.4.2). Many of these factors vary in time and it is thus not possible to define a “critical” precipitation amount that leads to groundwater recharge. However, our study clearly shows that the presence of mature shrubs greatly affects the potential groundwater recharge. In Figure 3.5a (shallow conditions and at that time where the shrubs are still very small and their influence thus less important) even small rainfall events result in groundwater recharge for both vegetated and non-vegetated conditions. However, later during the year (2016) when the shrubs have grown considerably, groundwater recharge exclusively occurs for the non-vegetated conditions (see

e.g. period after June 6, 2016). Not even the large precipitation event from August 15, 2016 of 58 mm resulted in groundwater recharge for the shallow, vegetated conditions.

During periods where no groundwater recharge occurs, the decline of the water table indicates a capillary rise, uptake through shrubs or phreatic (direct) evaporation. While the shrubs are still small (Figure 3.5a) no significant difference in the decline of the water table between vegetated and non-vegetated lysimeters can be observed. However, as the shrubs grow, their consumption of groundwater is evident in the increased rate of decline of the water table for both shallow and deep groundwater table conditions. For *shal_veg* the average decline rate was 1.5 cm/day between May 23 and June 3, 2016, but only 0.8 cm/day for *shal_bare*. For *deep_veg* and *deep_bare,* the decline rates were 0.5 cm/day for the vegetated and 0.1 cm/day for the non-vegetated conditions for the period between August 21 and November 26, 2016, respectively. These results suggest that *Salix psammophila* consumes groundwater by extracting groundwater from the capillary fringe. This is consistent with Ohte et al. (2003) who observed that *Salix psammophila* used both soil water and groundwater. Our results confirm this observation, as the vegetated conditions can result both in a decline of the water table as well as a reduction of soil moisture.

3.4.2 The influence of the presence of shrubs (versus bare soil) on the soil water balance

The presence of shrubs can influence if and how soil moisture increases in response to precipitation events. Interception, for example, can prevent soil moisture in the upper soil layers to increase in response to precipitation. Our data clearly indicate that the presence of shrubs reduces and sometimes prevents an increase in soil moisture. The presence of vegetation thus reduces the potential for groundwater recharge. For precipitation events exceeding the minimal threshold of 6 mm, vegetation still exerts a major influence on soil moisture dynamics - not unexpectedly so. This indicates that for soil water dynamics, the annual cumulative precipitation rates are not informative. Only precipitation events exceeding this threshold should be considered. For the meteorological conditions prevailing in the project area, this is of significant importance because of 23% the annual precipitation (for the year 2016, for example) is composed of events smaller than this critical threshold. The interception loss is likely to

increase with the growth of the shrubs.

3.4.3 Root growth and evapotranspiration under different water table conditions

Our previous analysis of soil moisture and water table dynamics suggests that *Salix psammophila* can consume groundwater (either directly or indirectly within the capillary zone above the water table), as well as soil water stored close to the surface. This requires an adaptation of the root system in response to the hydraulic conditions present. Based on the analysis of two shrub root densities, the root length density of *Salix psammophila* has two maxima if the depth to groundwater is large: one between 0 and 20 cm depth, and another between 80 and 120 cm depth. Similar results have been found in other studies. For example, Huang et al. (2016) also observed two maxima of the root length density of *Salix psammophila*. Fan et al. (2017) pointed out that the presence of a water table can draw roots deeper to tap its capillary rise. They also found that the dimorphic roots or deep roots are frequently observed in upland shrubs in season-dry climates when groundwater becomes accessible.

The field analysis of root densities where the water table is much closer to the surface indicated that there was only one maximum of root density. There are two possible reasons for this: Either, the precipitation and subsequent increase of soil moisture in the upper soil layer is sufficient to provide all water required by the shrub. It is also possible that the capillary rise of groundwater provides a sufficient supply of water (or a combination of both). The shrubs thus do not need to increase their root density additionally in the capillary zone. Figure 3.10 shows a conceptual model of root distributions for two different water table conditions.

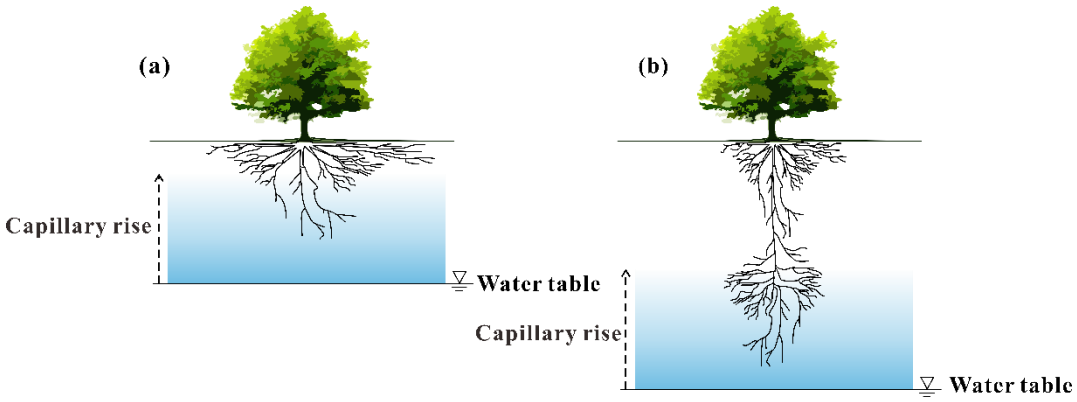

Figure 3.10 Conceptual model of shrub rooting density for two different depths to groundwater. (a) The uppermost soil layers are supplied with water through precipitation, as well as capillary rise. Only one maximum of root density can be observed. (b) deep water table depth conditions with two maxima: roots develop in the uppermost soil layers to efficiently uptake soil moisture originating from precipitation. A second maximum is observed in the capillary zone above the water table. Between the two maxima, soil moisture is consistently low and therefore the shrubs do not invest a lot of energy to grow their roots in this area.

To fully understand these adaptations of shrub roots in response to the hydraulic regime, more research is required. However, our results indicate that the distribution of roots significantly varies as a function of the hydraulic conditions. This is of outstanding importance and should be considered explicitly in any modeling attempt.

In this experimental setup, the total evapotranspiration rate of *Salix psammophila* under deep conditions was 6.0% higher than for the shallow one. This might be related to the fact that with a developed dimorphic root system water uptake is increasingly efficient. The roots in the upper layer absorb the incoming precipitation, while the roots close to the capillary fringe above the water table continuously tap the upward flux sustained through the capillary rise.

3.4.4 Implications for management

Our findings have important implications for the management of the *Salix psammophila* plantations in the Ordos plateau. To effectively control and prevent desertification, *Salix psammophila* has been planted in large areas. However, our results indicate that the presence of vegetation reduces or even prohibits groundwater recharge. Groundwater was consumed by

Salix psammophila. However, *Salix psammophila* plantations are indeed suitable for afforestation due to their low cost and the ease with which they are established under extremely desertified conditions (An et al., 2007). Besides, *Salix psammophila* is increasing carbon fixation (He et al. 2021). We recommend that the density of the planted *Salix psammophila* is carefully evaluated in the Mu Us desert region. Areas of bare ground between two *Salix psammophila* constitute an important area for recharge. If the shrub density is not too high, groundwater recharge is given for current climate conditions. Further studies regarding the role of optimal water table depth and distance between two *Salix psammophila* shrubs are needed. Numerical modeling approaches considering the influence of root distribution on both groundwater and soil water would be an efficient approach to identify the optimal planting density of *Salix psammophila* in the future.

Although there are some limitations for lysimeter installations, e.g. concerning monitoring lateral flow (Singh et al. 2018), lysimeters allow us to explore the complicated hydrological processes under realistic conditions in an excellent way. Two potential limitations regarding the application of lysimeters need to be discussed: (1) To a certain extent, lysimeters may limit root growth. It was thus important to analyze the root growth of plants outside of the lysimeter. The results were consistent. However, if the plants develop more roots, the limitation of the lysimeter could possibly become an issue. We thus recommend considering always the root structure of plants outside of the controlled setting of the lysimeter. (2) We have non-weighing lysimeters. Establishing the water balance is thus based on soil-moisture sensors, which have a certain measurement uncertainty. Moreover, soil moisture content needs to be estimated for the locations between the installed sensors. We used a simple linear interpolation approach because it is the most straightforward way to interpolate between the measurement points. As our sensor density was relatively high, this assumption is not expected to have any major implications for the results in contrast with other interpolation methods.

3.5 Conclusions

Four lysimeters were installed at the study site in the Mu Us desert of northwest China. Two of them were kept at a shallow water table depth and the other two at a relatively deep

water table depth. Each of the pairs had one lysimeter with bare soil (*shal_bare* and *deep_bare*) and one lysimeter vegetated by *Salix psammophila* (*shal_veg* and *deep_veg*). Key atmospheric and vegetation variables and soil conditions (i.e. air temperature, precipitation, sap velocity, soil moisture content and groundwater level) were measured throughout the experiments from July 1 to December 1, 2015, and April 1 to November 30, 2016. The following conclusions can be drawn:

(1) The presence of shrubs increases the critical threshold of precipitation required to increase soil moisture due to interception. In our study, we have quantified this amount. Precipitation events smaller than 6 mm did not lead to an increase of soil moisture on the surface ground. For the annual water balance, this means that precipitation rates are effectively reduced by around 23%. This critical threshold is dependent on the canopy, and more mature shrubs will likely increase this number.

(2) For the current climate conditions in the project area, the presence of *Salix psammophila* reduces groundwater recharge through the increase of interception and transpiration. This is in agreement with two previous studies (Huang et al. 2020; Zhao et al. 2020). Our experiments showed this reduction is independent of the depth to groundwater.

(3) Plants develop dimorphic systems to increase water uptake in the upper soil zone as well as from the capillary zone above the water table. The efficiency of water uptake and thus evapotranspiration rates are increased if dimorphic roots develop. Given that the lysimeters could potentially influence root growth, the additional observations of roots outside of the lysimeters were of critical importance.

(4) From a methodological point of view, the lysimeters allowed for controlled experiments outside of the laboratory. Our study is an example of how lysimeters provided quantitative insights and valuable information into complex processes, such as infiltration and soil moisture dynamics under vegetation and different water table conditions.

3.6 Acknowledgments

This study was supported by National Natural Science Foundation of China (No. 41902249, U1603243, 41230314), and the Key Research and Development Program of Shaanxi

(Program No. 2020SF-405). Gong Chengcheng is very grateful to the Chinese Scholarship Council (No. 201906560022) for providing an opportunity to be a visiting Ph.D. student at the University of Neuchâtel. The analysis was also partially supported by the SAFEA: High-End Foreign Experts Project (No. G20190027031). We greatly appreciate Qiangmin Wang, Li Chen, and Feng Yang in the field experimental work. We thank the editor and all anonymous reviewers for their valuable comments which have helped to improve the paper significantly.

Chengcheng Gong's contributions to this paper:

Collect data, analyze data, as well as revise the paper.

References

Allen, R. G., L. S. Pereira, D. Raes, and M. Smith (1998), Crop evapotranspiration-Guidelines for computing crop water requirements-FAO Irrigation and drainage paper 56, Fao, Rome, 300(9), D05109.

An, P., S. Inanaga, N. Zhu, X. Li, H. M. Fadul, and M. Mars (2007), Plant species as indicators of the extent of desertification in four sandy rangelands, African journal of ecology, 45(1), 94-102.

Banks, E., P. Brunner, and C. T. Simmons (2011), Vegetation controls on variably saturated processes between surface water and groundwater and their impact on the state of connection, Water Resources Research, 47(11).

Baral, A., Guha, G.S. (2004). Trees for carbon sequestration or fossil fuel substitution: the issue of cost vs. carbon benefit. Biomass and Bioenergy, 27(1): 41-55.

Brunner, P. Li, H.T., Kinzelbach, W. & Li W.P. (2007) Generating soil electrical conductivity maps at regional level by integrating measurements on the ground and remote sensing data, International Journal of Remote Sensing, 28:15, 3341-3361, DOI: 10.1080/01431160600928641

Brunner, P., H. Li, W. Kinzelbach, W. Li, and X. Dong (2008), Extracting phreatic evaporation from remotely sensed maps of evapotranspiration, Water Resources Research, 44(8).

Chen, Y. F., F. H. Yu, and M. Dong (2002), Scale-dependent spatial heterogeneity of vegetation in Mu Us sandy land, a semi-arid area of China, Plant Ecology, 162(1), 135-142.

Chen, L., Wang, W., Zhang, Z., Wang, Z., Wang, Q., Zhao, M., Gong, C. (2018). Estimation of bare soil evaporation for different depths of water table in the wind-blown sand area of the Ordos Basin, China. Hydrogeology Journal, 26(5): 1693-1704.

Cheng, D. H., Li, Y., Chen, X., Wang, W. K., Hou, G. C., & Wang, C. L. (2013). Estimation of groundwater evaportranspiration using diurnal water table fluctuations in the Mu Us Desert, northern China. Journal of Hydrology, 490, 106-113.

Cobos, D. R., Chambers, C. (2010). Calibrating ECH2O soil moisture sensors. Application note, 1-5.

Fan, Y., G. Miguez-Macho, E. G. Jobbágy, R. B. Jackson, and C. Otero-Casal (2017), Hydrologic regulation of plant rooting depth, Proceedings of the National Academy of Sciences, 114(40), 10572-10577.

Gong, C., Wang, W., Zhang, Z., Wang, H., Luo, J. and Brunner, P. (2020) Comparison of field methods for estimating evaporation from bare soil using lysimeters in a semi-arid area. Journal of Hydrology 590, 125334.

Heshmati, G. (2011), Biological models for protecting different land use in arid areas China, Journal of Rangeland Science, 1(3), 235-246.

He, L., Jia, Z., Li, Q., Zhang, Y., Wu, R., Dai, J., Gao, Y. (2021). Fine root dynamic characteristics and effect on plantation's carbon sequestration of three Salix shrub plantations in Tibetan Plateau alpine sandy land. Ecology and Evolution. DOI:10.1002/ece3.7221

Huang, J., Y. Zhou, J. Wenninger, H. Ma, J. Zhang, and D. Zhang (2016), How water use of Salixpsammophila bush depends on groundwater depth in a semi-desert area, Environmental Earth Sciences, 75(7), 556.

Huang, T., Pang, Z., Yang, S., Yin, L. (2020). Impact of Afforestation on Atmospheric Recharge to Groundwater in a Semiarid Area. Journal of Geophysical Research: Atmospheres, 125(9). DOI:10.1029/2019jd032185

Huxman, T. E., M. D. Smith, P. A. Fay, A. K. Knapp, M. R. Shaw, M. E. Loik, S. D. Smith, D. T. Tissue, J. C. Zak, and J. F. Weltzin (2004), Convergence across biomes to a common rain-use efficiency, Nature, 429(6992), 651.

Kamichika, M., T. Kobayashi, and A. Matsuda. (1989). Climate and environmental control technology. (In Japanese.] Pages 22–36 in Inner Mongolian Research Group, editor. Analysis of mechanism and movement of desertification in the arid land in China. Toyota Foundation project report 86-III-019.

Le Maitre, D. L., D. F. Scott, and C. Colvin (1999), Review of information on interactions between vegetation and groundwater, Water S.A, 25(2).

Li, H., W. Kinzelbach, P. Brunner, W. Li, and X. Dong (2008), Topography representation methods for improving evaporation simulation in groundwater modeling, Journal of Hydrology, 356(1-2), 199-208.

Li, W., Yan, M., Qingfeng, Z., Xingchang, Z. (2012). Groundwater use by plants in a semi-arid coal-mining area at the Mu Us Desert frontier. Environmental Earth Sciences, 69(3): 1015-1024. DOI:10.1007/s12665-012-2023-2.

Li, Y., Chen, W., Chen, J., Shi, H. (2016). Contrasting hydraulic strategies in Salix psammophila and Caragana korshinskii in the southern Mu Us Desert, China. Ecological Research, 31(6): 869-880. DOI:10.1007/s11284-016-1396-1.

Liang, P., Yang, X. (2016). Landscape spatial patterns in the Maowusu (Mu Us) Sandy Land, northern China and their impact factors. Catena, 145: 321-333. DOI:10.1016/j.catena.2016.06.023.

Lindroth, A., Cermak, J., Kucera, J., Cienciala, E., Eckersten, H. (1995). Sap flow by the heat balance method applied to small size Salix trees in a short-rotation forest. Biomass and bioenergy, 8(1): 7-15.

Lubczynski, M. (2009), The hydrogeological role of trees in water-limited environments, Hydrogeology Journal, 17(1), 247.

Maeght, J.-L., B. Rewald, and A. Pierret (2013), How to study deep roots—and why it matters, Frontiers in plant science, 4, 299.

Ma, Z., W. Wang, Z. Zhang, P. Brunner, Z. Wang, L. Chen, M. Zhao, and C. Gong (2019), Assessing bare-soil evaporation from different water-table depths using lysimeters and a numerical model in the Ordos Basin, China, Hydrogeology Journal, 27(7), 2707-2718.

Manfreda, S., M. Fiorentino, and V. Iacobellis (2005), DREAM: a distributed model for runoff, evapotranspiration, and antecedent soil moisture simulation, Advances in Geosciences, 2, 31–39.Naumburg, E., R. Mata-Gonzalez, R. G. Hunter, T. Mclendon, and D. W. Martin (2005), Phreatophytic vegetation and groundwater fluctuations: a review of current research and application of ecosystem response modeling with an emphasis on Great Basin vegetation, Environmental Management, 35(6), 726-740.

Nazarieh, F., H. Ansari, A. N. Ziaei, A. Izady, K. Davari, and P. Brunner (2018), Spatial and temporal dynamics of deep percolation, lag time and recharge in an irrigated semi-arid region, Hydrogeology journal, 26(7), 2507-2520.

Ohte, N., K. Koba, K. Yoshikawa, A. Sugimoto, N. Matsuo, N. Kabeya, and L. Wang (2003), Water utilization of natural and planted trees in the semiarid desert of Inner Mongolia, China, Ecological Applications, 13(2), 337-351.

Owor, M., R. Taylor, C. Tindimugaya, and D. Mwesigwa (2009), Rainfall intensity and groundwater recharge: empirical evidence from the Upper Nile Basin, Environmental Research Letters, 4(3), 035009.

Piao, S., Fang, J., Ciais, P., Peylin, P., Huang, Y., Sitch, S., Wang, T. 2009. The carbon balance of terrestrial ecosystems in China. Nature, 458(7241): 1009-13. DOI:10.1038/nature07944

Rodriguez‐Iturbe, I., P. D'Odorico, F. Laio, L. Ridolfi, and S. Tamea (2007), Challenges in humid land ecohydrology: Interactions of water table and unsaturated zone with climate, soil, and vegetation, Water Resources Research, 43(9).

Schilling, O., Doherty, J., Kinzelbach, W., Wang, H., Yang, P., Brunner, P. 2014. Using tree ring data as a proxy for transpiration to reduce predictive uncertainty of a model simulating groundwater–surface water–vegetation interactions. Journal of Hydrology, 519: 2258-2271.

Schwinning, S., and O. E. Sala (2004), Hierarchy of responses to resource pulses in arid and

semi-arid ecosystems, Oecologia, 141(2), 211-220.

Singh, G., Kaur, G., Williard, K., Schoonover, J., Kang, J. 2018. Monitoring of Water and Solute Transport in the Vadose Zone: A Review. Vadose Zone Journal, 17(1). DOI:10.2136/vzj2016.07.0058

Pütz, T., Fank, J. and Flury, M. (2018) Lysimeters in vadose zone research. Vadose Zone Journal 17(1), 1-4.

Wang, T., V. A. Zlotnik, J. Šimunek, and M. G. Schaap (2009), Using pedotransfer functions in vadose zone models for estimating groundwater recharge in semiarid regions, Water Resources Research, 45(4).

Wang, W., Zhang, Z., Duan, L., Wang, Z., Zhao, Y., Zhang, Q., Dai, M., Liu, H., Zheng, X., and Sun, Y. (2018). Response of the groundwater system in the Guanzhong Basin (central China) to climate change and human activities. Hydrogeology Journal 26, 1429-1441.

Wang, X., C. Zhang, E. Hasi, and Z. Dong (2010), Has the Three Norths Forest Shelterbelt Program solved the desertification and dust storm problems in arid and semiarid China?, Journal of Arid Environments, 74(1), 13-22.

Wu, Y., Hasi, E. and Wu, X. (2012) Characteristics of surface runoff in a sandy area in southern Mu Us sandy land. Chinese Science Bulletin 57(2-3), 270-275.

Xu, H.-l., Y. Mao, and J.-m. LI (2007a), Changes in groundwater levels and the response of natural vegetation to transfer of water to the lower reaches of the Tarim River, Journal of Environmental Sciences, 19(10), 1199-1207.

Xu, W., Yin, Y., Zhou, S. (2007b). Social and economic impacts of carbon sequestration and land use change on peasant households in rural China: a case study of Liping, Guizhou Province. J Environ Manage, 85(3): 736-45. DOI:10.1016/j.jenvman.2006.09.013

Yair A. Effects of biological soil crusts on water redistribution in the Negev Desert, Israel: A case study in longitudinal dunes. In: Belnap J, Lange O L, eds. Biological Soil Crusts: Structure, Function, and Management. Berlin: Springer-Verlag, 2001. 304–314.

Yin, J., He, F., Xiong, Y. J., & Qiu, G. Y. (2017). Effects of land use/land cover and climate changes on surface runoff in a semi-humid and semi-arid transition zone in northwest China. Hydrology and Earth System Sciences, 21(1), 183.

Yin, L., G. Hu, J. Huang, D. Wen, J. Dong, X. Wang, and H. Li (2011), Groundwater-recharge estimation in the Ordos Plateau, China: comparison of methods, Hydrogeology Journal, 19(8), 1563-1575.

Yin, L., Y. Zhou, D. Xu, J. Zhang, X. Wang, H. Ma, and J. Dong (2018), Response of phreatophytes to short‐term groundwater pumping in a semiarid region: Field experiments and numerical simulations, Ecohydrology, 11(4), e1948.

Zhang, Y., C. Peng, W. Li, L. Tian, Q. Zhu, H. Chen, X. Fang, G. Zhang, G. Liu, and X. Mu (2016), Multiple afforestation programs accelerate the greenness in the 'Three North'region of China from 1982 to 2013, Ecological Indicators, 61, 404-412.

Zhang, Z., W. Wang, C. Gong, Z. Wang, L. Duan, T. c. J. Yeh, and P. Yu (2019), Evaporation from seasonally frozen bare and vegetated ground at various groundwater table depths in the Ordos Basin, Northwest China, Hydrological Processes, 33(9), 1338-1348.

Zhang, Z., Wang, W., Wang, Z., Chen, L. and Gong, C. (2018) Evaporation from bare ground with different water-table depths based on an in-situ experiment in Ordos Plateau, China. Hydrogeology Journal 26(5), 1683-1691.

Zhao, M., Wang, W., Wang, Z., Chen, L., Ma, Z., Wang, Q. (2020), Water use of Salix in the variably unsaturated zone of a semiarid desert region based on in-situ observation. Journal of Hydrology, 591. DOI:10.1016/j.jhydrol.2020.125579

Zhao, W., and B. Liu (2010), The response of sap flow in shrubs to rainfall pulses in the desert region of China, Agricultural and Forest Meteorology, 150(9), 1297-1306.

Zhu, Y., G. Wang, and R. Li (2016), Seasonal dynamics of water use strategy of two salix shrubs in alpine sandy land, Tibetan Plateau, PloS one, 11(5).

Zhao, Y., Wang, L., Knighton, J., Evaristo, J., Wassen, M. 2021. Contrasting adaptive strategies by Caragana korshinskii and Salix psammophila in a semiarid revegetated ecosystem. Agricultural and Forest Meteorology, 300. DOI:10.1016/j.agrformet.2021.108323.

Chapter 4 On groundwater recharge in variably-saturated subsurface flow models

Chapter 4 has been published as: **Gong C**, Cook P G, Therrien R, Wang W, Brunner P. On groundwater recharge in variably saturated subsurface flow models[J]. Water Resources Research, 2023, 59(9): e2023WR034920.

Abstract

Groundwater models that simulate only saturated flow use groundwater recharge as an input parameter. In contrast, variably-saturated subsurface flow models, including integrated surface and subsurface hydrologic models, can jointly simulate the movement of water in the saturated and unsaturated zones. Instead of recharge, they require climate data such as precipitation and potential evapotranspiration. Given that the latter models represent hydrological processes operating throughout the unsaturated zone and at the water table, one might expect that recharge can be readily extracted from them. In this paper, we demonstrate that it is not the case. When the commonly used definitions of groundwater recharge are implemented in variably-saturated subsurface flow models, they do not yield meaningful results. Above all, the problems occur because of the storage dynamics in the capillary fringe above the water table. Despite this difficulty, variably-saturated subsurface flow models can provide the information required for water resources management directly.

Keywords: Capillary fringe; Groundwater recharge; Variably-saturated subsurface flow models; Water resources

4.1 Introduction

Groundwater recharge has long been of interest to water resources managers (Hund et al. 2018; Kinzelbach et al. 2010) as quantification of recharge is often considered essential for sustainable aquifer management (Healy 2010; Healy and Cook 2002; Scanlon et al. 2002). Numerous methods for estimating recharge exist (Healy 2010; Scanlon et al. 2002). As recharge is an important component of groundwater in the groundwater budget, hydrogeologists embed the concept of recharge in the way they think about groundwater systems. Understanding recharge dynamics is required to predict the impacts of land use/cover change and climate change on groundwater resources and to determine the risk of groundwater resource contamination by human activities. Groundwater managers often consider recharge rates to evaluate the sustainable level of extraction for a groundwater system.

Groundwater recharge is used in many analytical (Cuthbert 2010; Haitjema 1995; Lerner et al. 1990) and numerical solutions of groundwater flow equations (Rubin and Dagan, 1987), including numerical models. However, different types of models handle recharge in different ways. Groundwater models like MODFLOW (Harbaugh 2005; Harbaugh et al. 2000) simulate groundwater flow and require recharge as an input parameter (Sanford, 2002). They predict groundwater movement in response to recharge and groundwater pumping. In some cases, MODFLOW has been used to determine recharge using data such as hydraulic head, hydraulic conductivity and/or groundwater age (Baalousha, 2016; Knowling and Werner, 2016; Sanford et al., 2004; Zhu, 2000).

Variably-saturated subsurface flow models can simulate vadose zone processes by solving the Richards equation. Hydrus-1D (Šimůnek et al., 2005), a commonly-used variably saturated flow model, has been applied to estimate groundwater recharge (e.g., Hu et al., 2019, Hou et al., 2016, Batalha et al., 2018, Tonkul et al., 2019, Assefa and Woodbury, 2013). Typically, such models are set up as one-dimensional, essentially representing a lysimeter. The values extracted represent potential recharge (Healy 2010; Rushton 1997), as they focus on the unsaturated zone only and do not consider the position of the water table.

More holistic variably-saturated subsurface flow models which solve the three-

dimensional Richards equation in combination with Darcy's law for the saturated zone include HydroGeoSphere (Brunner and Simmons 2011; Aquanty 2018; Simmons et al. 2020), Parflow (Maxwell and Miller 2005), CATHY (Paniconi and Putti, 1994; Paniconi and Wood, 1993), and Hydrus-3D (Šimůnek et al., 2006). These models simulate infiltration processes through the unsaturated zone of the soil as well as saturated groundwater flow processes and the interactions and feedback mechanisms between the saturated and unsaturated zone. They, therefore, do not require recharge as an input, unlike fully saturated groundwater models such as MODFLOW. In fact, variably saturated subsurface flow models do not explicitly compute recharge internally. Instead, precipitation and evaporative forcing are used as input for simulations. As this type of model incorporates key hydrological processes, one might expect that groundwater recharge can be readily extracted from them. For example, Frei et al. (2009) explored recharge patterns and dynamics along rivers using Parflow. They calculated groundwater recharge as the difference between the infiltrating water flux and the vadose zone storage. Brandhorst et al. (2021) estimated recharge from Parflow based on the water table fluctuation method. Waldowski et al. (2023) estimated groundwater recharge by considering the water balance over the vertical extent of the water table fluctuations. Guay et al. (2013) referred to recharge in CATHY as the sum of vertical fluxes that cross a dynamically changing water table.

This paper explores to what extent variably-saturated subsurface flow models can be used to extract groundwater recharge. To extract recharge from variably-saturated subsurface flow models, a definition of groundwater recharge must be implemented in the postprocessing of the simulations and, to be scientifically sound, the results need to be unique, meaningful, and unambiguous. In this paper, we explore how different definitions of groundwater recharge can be implemented in variably-saturated subsurface flow models, and if they yield unique and meaningful results. We first briefly review the available definitions of groundwater recharge, and subsequently implement them in variably-saturated subsurface flow models and demonstrate that in fact these models cannot be used to estimate groundwater recharge in a unique way.

4.2 Definitions of recharge

Many definitions of groundwater recharge have been proposed. Healy (2010) defined groundwater recharge as "*the downward flow of water reaching the water table, adding to groundwater storage*". Several definitions along similar lines also have been proposed, for example by Schmoll et al. (2006), Delleur (2006), Sen (2008), de Vries and Simmers (2002), Sophocleous (1991), Singhal and Gupta (2010), Hillel (1998), Sophocleous and Perry (1985), Shamsudduha et al. (2011), Doble and Crosbie (2016), Carrera-Hernández et al. (2012), and Meixner et al. (2016). Given that the water table is defined as the surface where the pressure head is equal to zero, this type of definition can be implemented in physically based models, as the position of the water table can be tracked throughout the simulations, and the fluxes to and across it can be extracted through postprocessing the simulation results. Because the surface typically is not static, determining the flux across the surface can sometimes be non-trivial, especially if the water table is inclined. For the upcoming implementation of recharge definitions in numerical models, we label this approach *Recharge Definition I* (water crossing the pressure head equal to zero plane).

Others define groundwater recharge as "*the entry of water to the saturated zone*" (Freeze and Cherry, 1979). Note that the boundary between the saturated and unsaturated zones is the top of the capillary fringe, which is above the pressure head equal to zero plane. Definitions similar to that of Freeze and Cherry (1979) have been provided, for example by Nimmo et al. (2006), Tóth (2009), Simmers (2013), Sophocleous (2004), Fitts (2013), Lerner (1996), Poehls and Smith (2011), Haitjema (1995), Kresic and Stevanovic (2009), Sharp (2003), Xu and Beekman (2018), Gemitzi et al. (2017), and Dingman (2015). The boundary between fully saturated and unsaturated zones can in principle be tracked throughout the simulation and the fluxes to and across this boundary can be monitored. Likewise, fluxes at any other height above the water table can be monitored, no matter if it is a fixed or a dynamic height (such as the height of the capillary fringe). We label these definitions as *Recharge Definition II* (the entry of water to the saturated zone, crossing the boundary defined through the plane separating fully saturated and unsaturated conditions).

The definitions above are based on tracking a flux across a boundary. Other definitions of recharge are implicit in approaches that quantify recharge through the response of the system to infiltration and drainage. For example, the water table fluctuation (WTF) method relates a rise in the water table to groundwater recharge (Healy and Cook, 2002). Note that in some applications of the WTF method, a drainage term is also included to account for the discharge of the aquifer (Cuthbert 2010). This method therefore implicitly defines recharge using a mass balance approach as the change in an aquifer's saturated volume minus groundwater discharge. We label this approach as *Recharge Definition III* (recharge obtained from joint observations of the water table and groundwater discharge)

Some authors have defined recharge as net infiltration. For example, Dassargues (2018) defines recharge as "*The water that penetrates the soil flows deep underground (groundwater recharge) if it is not consumed by plants or humans*". Delleur (2006) refers to recharge as "*Deep soil water percolation, often referred to as groundwater recharge by soil scientists, is the water that has moved past the evaporative and root zones in the vadose zone and is no longer available to plants.*" Scanlon et al. (2002) pointed out that net infiltration, drainage, or percolation below the root zone are often equated to recharge in many vadose zone studies. Similarly, de Vries and Simmers (2002) state that "*all water that passes the root zone is assumed to have escaped evapotranspiration and could recharge the groundwater reservoir*". Cech (2009) defines groundwater recharge as "*Downward movement of water from the land surface into and through upper soil layers*". If recharge is defined as the net infiltration as proposed by these authors, in principle, one should also be able to extract this potential recharge by keeping track of the fluxes at a depth below the surface at which water can no longer be lost to the atmosphere (below the root extinction depth), provided the water table is below this extinction depth. Note, however, that net infiltration can significantly differ from recharge defined at or close to the water table, especially in systems with a large unsaturated zone. For the subsequent discussion, we label this approach as *Recharge Definition IV* (net infiltration below the extinction depth) This is also called *potential recharge*.

The four definitions of recharge are subsequently implemented in the numerical models

described in the following sections.

4.3 Methods

4.3.1 Numerical Model

Given that the formulation of vadose zone processes is essentially the same in all variably-saturated subsurface flow codes, the choice of a numerical code is not critical for this study as long as variably-saturated infiltration processes are represented. Therefore, we use HydroGeoSphere (Aquanty, 2018), a variably-saturated numerical model that uses the control volume finite-element method to solve 2D overland flow fully coupled with 3D subsurface flow described by Richards' equation. We simulate infiltration and drainage processes through simple 1D vertical columns.

We deliberately use simple models for the following reason: if the estimation of recharge cannot be obtained reliably from these simplest models, it will also be impossible to do so in more complicated models where, for example, the water table is inclined or complex catchment-scale processes are simulated.

We simulate one-dimensional vertical soil columns of 5 m in height. The surface area of the soil columns is 1 m^2. The soil columns are vertically discretized into 1000 finite element layers. The very fine vertical discretization ensures that there is no influence of grid discretization on the simulation results. The soil is assumed to be homogeneous for any given simulation. Different soil types (sand, loam, sandy loam, and loamy sand) are considered for some simulations and their soil water retention characteristics are described by the van Genuchten functions (van Genuchten 1980). Soil properties are presented in Table 4.1, where θ_s is the saturated water content, θ_r is the residual water content, K_s is the saturated hydraulic conductivity, and α and β are fitting parameters of the van Genuchten functions.

Table 4.1 The soil water retention characteristic parameters based on Carsel and Parrish (1988)

Soil type	θ_s (cm^3/cm^3)	θ_r (cm^3/cm^3)	α (m^{-1})	β (-)	K_s (m/d)
Sand	0.43	0.045	14.5	2.68	7.13
Loam	0.43	0.078	3.6	1.56	0.25
Sandy loam	0.41	0.065	3.7	1.89	1.06
Loamy sand	0.41	0.057	12.4	2.28	3.50

Initially, all models are in a hydrostatic equilibrium. A constant specified flux q_{inf} equal to 0.02 m/d is then applied to the upper boundary. Evapotranspiration is not simulated and so the specified flux represents a net infiltration rate. Depending on the simulation, the lower boundary is either a no-flow boundary or a drainage boundary. The water table is within the model domain. All models are run in a transient mode and model results are analyzed after a dynamic steady state is reached, for example, when the increase or decrease of the elevation of the water table has reached a constant rate. The specified flux at the upper boundary (q_{inf}) is applied from the 5th day and the total simulation time is 45 days. The bottom drainage boundary used for some models is shown by q_d in Figure 4.1. The initial and maximum time steps are 0.01 days and an adaptive time-stepping scheme is employed. Simulation results are written out daily and are post-processed with the Tecplot 360 2020 software (Tecplot, Inc, Bellevue, WA, USA).

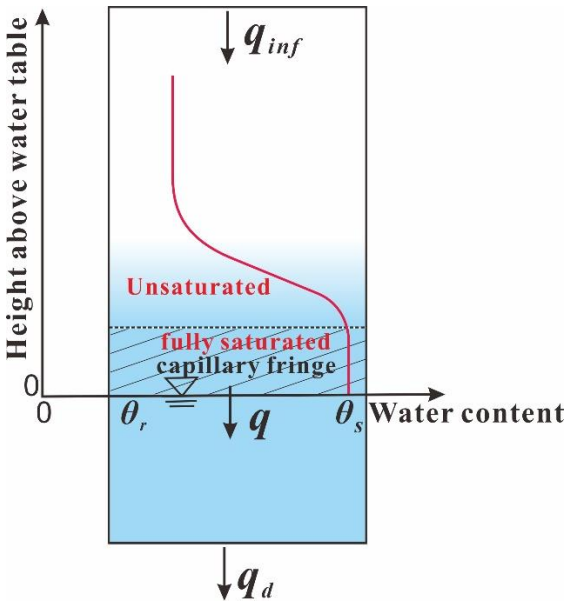

Figure 4.1 Schematic diagram of the imposed infiltration and drainage rates. The red line corresponds to the soil moisture profile above the water table. q_{inf} is the specified flux infiltrating the soil column, q is the flux across the water table, and q_d is the drainage flux. Several cases are simulated: In case 1, q_{inf}= q_d; in case 2, q_d=0 while $q_{inf} > 0$; and in case 3, q_d can either exceed or be smaller than q_{inf}.

Different cases are simulated: (1) a steady water table where the assigned infiltration flux at the top and drainage flux at the bottom are equal, which corresponds to a dynamic steady-state flow, (2) a rising water table due to infiltration but without drainage (q_d = 0) and therefore all the infiltrating water contributes to increasing the water table, and (3) constant but differing infiltration and drainage fluxes where, depending on the relative magnitudes of these fluxes, the water table rises or falls. Cases 1 and 2 are special cases of the more general case 3.

Case 1: The 1D dynamic steady-state system under infiltration conditions

We consider first a special case for steady-state flow where the specified infiltration flux is equal to the drainage flux (Figure 4.1). The constant drainage flux q_d is assigned as 0.02 m/d. Once the dynamic steady state is reached, the inflow flux is equal to the outflow, the water storage in the column does not change and therefore the water table remains at the same location.

Case 2: All infiltration contributes to the rise of the water table

Here, we focus on a one-dimensional column with a no-flow boundary at the bottom, which is equivalent to a closed lysimeter. Initially, the water table is below the surface,

infiltration is zero and the system is at a steady state (Figure 4.2(a)). Recharge is then triggered by infiltrating water, which leads to a rise in the water table (Figure 4.2 (b)). Because the bottom is impermeable, there is no groundwater flow below the water table and all infiltrating water contributes to raising the water table. Four different homogeneous soil columns, with properties described previously (sand, loam, sandy loam, and loamy sand) are employed in this case. The initial heads throughout the columns for the four soil columns are 1 m.

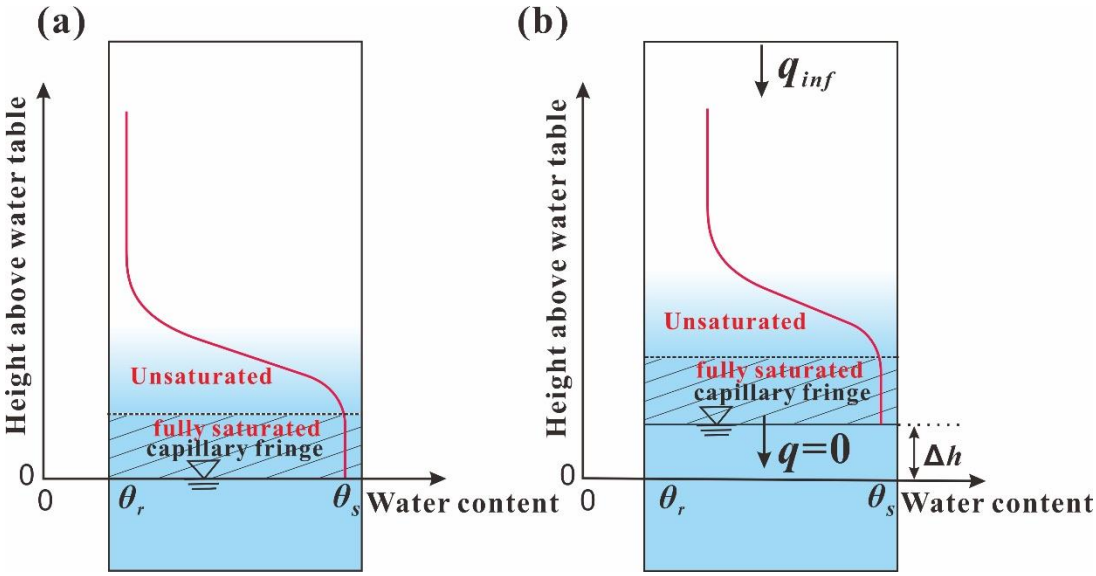

Figure 4.2 Schematic diagram of groundwater recharge (corresponding to case 2). (a) before infiltration (b) during infiltration. The infiltration causes a rise of the water table equal to Δh. The water content is shown on the x-axis and the height above the water table is on the y- axis. The red lines show the soil moisture profile above the water table. q_{inf} is the specified flux infiltrating the soil column, and q is the flux across the water table.

Case 3: Infiltration partially contributes to groundwater fluxes

In case 2, we examined a column equivalent to a closed lysimeter without any groundwater flow below the water table and towards the lower boundary, and therefore with all infiltrating water contributing to rising the water table. In case 3, we consider a more general case with drainage at the bottom boundary and where infiltrating water can contribute to raising the water table and also to vertical groundwater flow below the water table. Two soil columns were employed in this case and the material specified corresponds to sand. The initial heads throughout the columns are 2 m for both columns. Constant drainage fluxes q_d are assigned

to the lower boundary from the 5th day (Figure 4.1) with values equal to 0.01 and 0.025 m/d for the two columns, respectively. As before, a constant specified flux of 0.02 m/d is assigned to the top boundary. The special case where the drainage flux corresponds to the infiltration flux (and the system thus remains in a dynamic steady state) corresponds to case 1 and has already been discussed previously.

Based on the imposed drainage flux, the following situations will develop: (a) for $q_d = 0.01$ m/d, the water elevation increases in the soil column; (b) for $q_d = 0.025$ m/d, the water table decreases in the soil column.

4.3.2 Assessing the implementation of recharge definitions and the extraction of recharge

For the hydraulic configurations, the different definitions of recharge are implemented in the following way.

(1) Implementation of *Definition I* and recharge extraction

In *Definition I*, recharge is defined as the flux that crosses the water table vertically (with the water table defined as the iso-surface with pressure head h_p equal to zero). One can extract these fluxes by post-processing the output from the variably-saturated subsurface flow models by keeping track of the position of the $h_p = 0$ plane as a function of time and integrating fluxes across this plane. This definition of recharge is based on Healy (2010).

(2) Implementation of *Definition II* and recharge extraction

In *Definition II*, recharge is defined as the flux across the boundary between the saturated and the unsaturated zones (e.g. Freeze and Cherry 1979). Technically, the extraction plane is defined through the degree of saturation equal to 1 and is tracked throughout the simulation while the fluxes through this plane are extracted. Other boundaries, be it a fixed height above the water table or a fixed saturation, can be dynamically monitored in the same way.

(3) Implementation of *Definition III* and recharge extraction

In *Definition III,* recharge is defined through the response of the system to infiltration and drainage. To implement *Definition III*, we focus on the variations of the water table, but in some cases also consider the deep drainage as proposed by Cuthbert (2010). The water table fluctuation approach is a widely used field method to estimate groundwater recharge (Healy

and Cook 2002; Gong et al. 2021). Likewise, it can be employed in variably-saturated subsurface flow models jointly simulating groundwater levels and variably-saturated subsurface flow. A key assumption of this approach is that the rise of the water table is not related to horizontal fluxes, but instead to recharge, which is the case for the soil column with an impermeable bottom. In more complex 2- or 3-dimensional models with horizontal flow components, this contribution could be extracted through appropriate post-processing.

In its most basic application, only the specific yield and the temporal changes in the water table are required, and recharge R [L/T] is given by:

$$R = S_y \frac{dh}{dt} \tag{4.1}$$

where S_y [-] is specific yield, h [L] is the height of the water table, and t [T] is time. A commonly used formula to determine specific yield is given by (Freeze and Cherry 1979):

$$S_y = \theta_s - \theta_r \tag{4.2}$$

However, this expression for specific yield ignores the initial soil water content profile. As pointed out by multiple authors, e.g. Allison et al. (1990), Healy and Cook (2002), Crosbie et al. (2005), and Zhang et al. (2020), this simplification can result in a significant overestimation of recharge. Conversely, the addition of a small amount of water can cause a significant rise of the water table if the soil above the water table is close to saturation (Gillham 1984). If the initial soil water content above the water table is considered, a modified specific yield S_y^* can be employed:

$$S_y^* = \theta_s - \theta_i \tag{4.3}$$

where θ_i [cm^3/cm^3] is the initial soil water content, which varies with increasing height above the water table. Note that in the application of the water table fluctuation method as proposed by Cuthbert (2010), a drainage term is added to equation (4.1).

(4) Implementation of *Definition IV* and recharge extraction

Definition IV defined recharge as the net-infitration, i.e. the precipitation minus evapotranspiration. As opposed to *Definitions I* and *II* which define recharge at or above a certain height of the water table, *Definition IV* is evaluated at a depth below the land surface where the infiltrating water is no longer exposed to evapotranspiration. As in the current context

evapotranspiration is not simulated, the net-infiltration is equal to the specified infiltration flux imposed.

Table 4.2 Extracted values of recharge for all simulations and the different implementations of recharge definitions. Note that WTF means water table fluctuation method, and the unit in the table is m/d. The entries under *Definition I* (values above h_p=0 plane) and *Definition II* (saturation <1 plane) are additional simulations to illustrate the issues related to these definitions.

Definitions \ Cases			Case 1	Case 2				Case 3	
								Case 3 (a)	Case 3 (b)
			q_{inf}=0.02; q_d=0.02	q_{inf}= 0.02; q_d= 0				q_{inf}=0.02; q_d=0.01	q_{inf}=0.02; q_d=0.025
			Sand	Sand	Loam	Sandy loam	Loamy sand	Sand	Sand
Definition I	h_p=0 plane		0.02	0	0	0	0	0.01	0.025
	Above h_p=0 plane		0.02	0~0.02 (Figure 4.3)	0~0.02 (Figure 4.3)	0~0.02 (Figure 4.3)	0~0.02 (Figure 4.3)	0.01~0.02 (Figure 4.5)	0.02~0.025 (Figure 4.6)
Definition II	Saturation =1 plane		0.02	0	0	0	0	0.01	0.025
	Saturation <1 plane		0.02	0~0.02 (Figure 4.4)	0~0.02 (Figure 4.4)	0~0.02 (Figure 4.4)	0~0.02 (Figure 4.4)	0.01~0.02 (Figure 4.5)	0.02~0.025 (Figure 4.6)
Definition III	S_y	WTF only	0	0.027	0.127	0.047	0.031	0.013	—
		Discharge	0.02	0	0	0	0	0.01	0.025
	S_y^*	WTF only	0	0.003	0.012	0.002	0.004	0.0004	—
		Discharge	0.02	0	0	0	0	0.010	0.025
Definition IV			0.02	0.02	0.02	0.02	0.02	0.02	0.02

4.4 Results

The results of simulations and extraction of recharge are shown and analyzed in the subsequent section. Table 4.2 provides an overview of all simulations and the corresponding recharge definitions that were implemented to extract recharge.

4.4.1 Case 1: 1D dynamic steady-state system under infiltration conditions

For *Definitions I*, *II* and *IV*, the extracted recharge is equal to the specified infiltration flux (Table 4.2). For *Definition III* , the analysis based the water table fluctuation method yields a recharge flux of 0 as the water table is not moving. If the drainage term is considered, the extracted recharge is also equal to the specified infiltration flux. For this special case of a steady water table under infiltrating conditions, all definitions of recharge yield the same results, namely that recharge is equal to the net infiltration. Note, however, that if the water table fluctuation approach is employed this value is only obtained if the drainage term is considered.

4.4.2 Case 2: All infiltration contributes to the rise of the water table

1) Extraction recharge based on *Definition I*

For all soils, the flux directly across the water table is shown by the left-most bar for each type of soil in Figure 4.3 and it is equal to 0, see the histogram in Figure 4.3 (h_p= 0 plane; the left-most bar of each histogram). This result is related to the presence of a fully saturated zone, the so called capillary fringe above the water table (Figure 4.2 (a)). The result is also related to the impermeable boundary at the bottom, which causes infiltrating water to "pile up" on top of the water table. The strict application of the definition of recharge as being equal to the flux across the pressure head equal to zero plane thus provides an unrealistic estimate of recharge equal to 0 for this situation.

In principle, one could argue that, instead of extracting recharge across the pressure head equal to zero plane (the water table), recharge could be obtained by extracting vertical infiltration fluxes crossing a horizontal plane located at some height above the water table. This corresponds to the less strict definitions of recharge mentioned in the previous section (definitions of recharge), e.g. Scanlon et al. (2002). Therefore, fluxes crossing planes above the rising water table at heights of 0.1, 0.2, 0.3, 0.4, 0.5, 0.6, 0.7, and 0.8 m were also extracted as indicated in Figure 4.3. As expected, the extracted values increase from 0 to 0.02 m/d for an increasing height above the water table. With an increasing height, we approximate *Definition IV*, and the extracted fluxes tend towards the net specified flux imposed (q_{inf}= 0.02 m/d). However, there is no clear indication of how this height should be chosen. The extracted results are thus ambiguous.

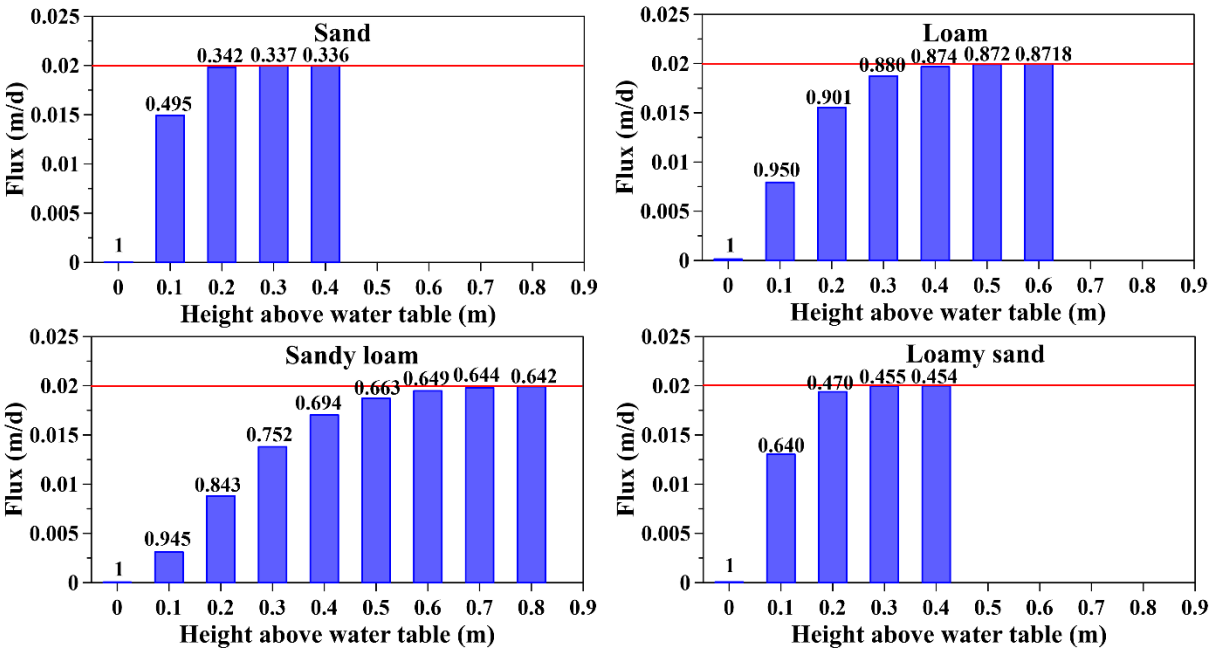

Figure 4.3 Fluxes across planes above the water table (pressure head equal to zero plane) and at constant heights above the water table for different soil types. The inverse of air-entry value (a proxy for the saturated height above the water table) is 0.069 m for sand, 0.278 m for loam, 0.270 m for sandy loam, and 0.081 m for loamy sand. The specified flux infiltrating all soil columns is equal to 0.02 m/ d (red line). The values above each column are the saturations at each height.

2) Extracting recharge based on *Definition II*

One could define recharge as the flux contributing to the saturated zone (*Definition II;* Freeze and Cherry, 1979). The integration plane would thus not be defined as the $h_p = 0$ plane, but rather as the plane above the water table where the saturation drops below 1. If the soil water retention curve is represented with the van Genuchten function, the exact numerical location of this plane corresponds to the pressure equal to zero plane as opposed to, for example, the Brooks-Corey function (1964) where a specific height above the water table, corresponding to the inverse of the air-entry pressure, marks the boundary between the saturated and the unsaturated zones. However, even with the van Genuchten approach one can define a saturation value smaller than 1 for which the soil can reasonably be considered to be fully saturated (Silliman et al. 2002). Figure 4.4 shows how the extracted fluxes vary when computed across a plane defined by a saturation value rather than the pressure head equal to zero plane. The planes

(h_p= 0 or a given saturation) move according to the simulation results. The results clearly indicate that the definition of a cutoff for saturation has a major influence on extracted recharge rates.

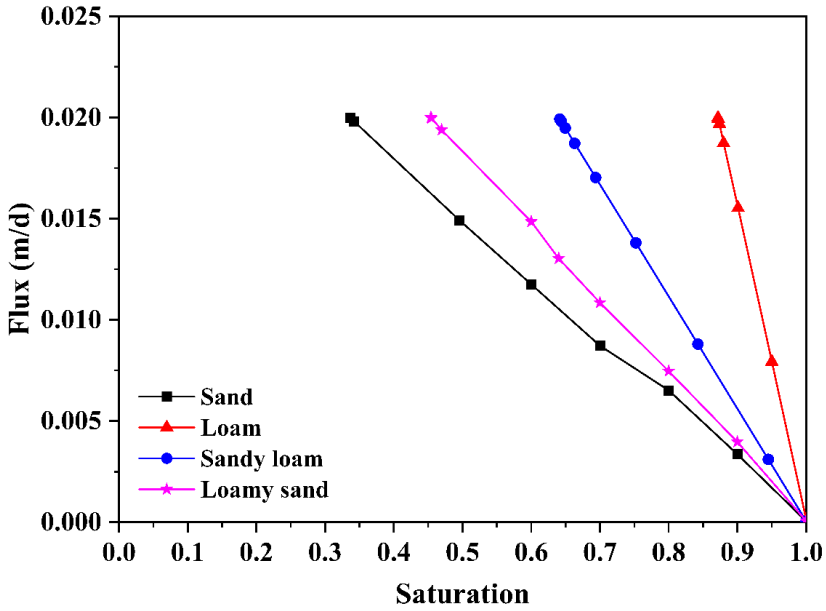

Figure 4.4 The fluxes across planes defined by the degree of saturation for sand, loam, sandy loam, and loamy sand. The infiltration flux is 0.02 m/d.

3) Extraction of recharge based on *Definition III*

Definition III relates recharge to the changing water level fluctuations (see equations (4.2) and (4.3) for the different notations of the specific yield. Note that, in some applications of the water table fluctuation method, a drainage term is considered and added to equation (4.1), as suggested by Cuthbert (2010). As in this specific simulation case there is no drainage, this additional term is not considered.

By using equation (4.1) (the change of the water table is extracted with daily timestep) and assuming a static value of the specific yield (equation (4.2)), the estimated recharge rate is 0.127 m/d, which is greater than the infiltration rate. This overestimation is easily explained. The water table rises at a rate of 0.359 m/d and the rate is then multiplied by the specific yield S_y, which is the difference between saturated and residual water contents. Using values shown in Table 4.1 for loam, its specific yield is equal to 0.352. The specific yield in this formulation does not consider the initial water content above the water table, as opposed to the approach

where the initial water content above the water table is considered and a modified specific yield S_y^* is defined (see equation (4.3) and entry for S_y^* in Table 4.2). The consideration of the initial water content to estimate recharge with the water table fluctuation method is feasible through appropriate post-processing of the model output. A problem with this approach is that the estimation of recharge rates will heavily depend on the temporal discretization used for the simulations. If the change in the height of the water table (dh) in one timestep is less than the height of the capillary fringe, then the initial soil water content (θ_i) will be equal to or very close to the saturated water content. The modified specific yield according to equation (4.3) is therefore equal to zero, which leads to a recharge equal to zero. Therefore, applying the water table fluctuation method to estimate recharge yields ambiguous results that depend on the time step size.

4) Extraction of recharge based on *Definition IV*

As in this context evapotranspiration is not simulated explicitly, the imposed infiltration flux corresponds to net-infiltration and thus *Definition IV.* The graphs in Figure 4.3 show that for an increasing evaluation height above the water table, the corresponding extracted recharge approximates the net infiltration and thus *Definition IV*. The factors influencing at what height above the water table the extracted recharge corresponds to the net-infiltration is influenced by the infiltration rate, the hydraulic conductivity, and the air-entry pressure.

4.4.3 Case 3: Infiltration partially contributes to groundwater fluxes

4.4.3.1 Case 3(a) $q_d = 0.01$ m/d, $q_{inf} = 0.02$ m/d: the drainage flux is smaller than the infiltration flux and the water table rises in the soil column.

In this case, the infiltrating water will both contribute to rising the water table and to groundwater flow below the water table. The extracted flux across the water table plane (*Definition I*) is equal to q_d (0.01 m/d). Likewise, the extracted flux across the saturation equal to 1 plane (*Definition II*) is also equal to q_d (0.01 m/d). In analogy to the previous section recharge values extracted from planes above the water table and above the full saturation plane were also extracted, see Figure 4.5.

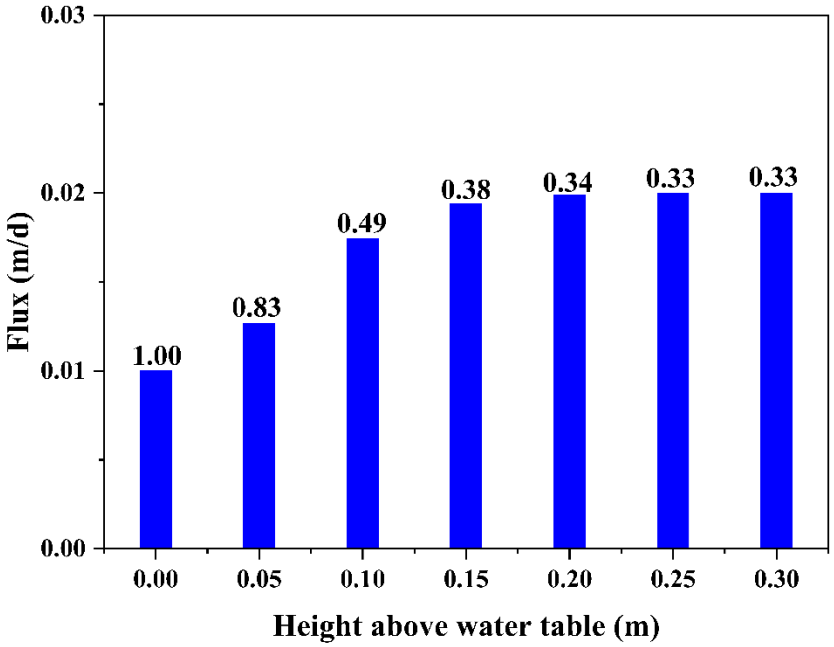

Figure 4.5 Fluxes across planes across the water table (h_p=0) and at constant heights above the water table for sand for imposed infiltration rates of 0.02 m/d. The values above the columns represent the saturations on the planes. The drainage rate is 0.01 m/d, the water table rises.

In employing *Definition III*, the rise of the water table is related to groundwater recharge. One can also consider the drainage rate (0.01m/d), in addition to the recharge estimated based on the increase of the water table. As before, the calculation of the specific yield has a significant influence on the results. The result is 0.013 m/d if the specific yield is based on equation (4.2), and 0.0004 m/d equation (4.3) is used.

The results of recharge using *Definition IV* (net infiltration) can also be found in Figure 4.5. With the increasing height above the water table, the extracted recharge rate approximates the infiltration rate (q_{inf}= 0.02 m/d).

4.4.3.2 Case 3(b) $q_d = 0.025$ m/d, $q_{inf} = 0.02$ m/d: the drainage flux is greater than the infiltration flux, and the water table elevation decreases in the soil column.

If recharge is extracted based on *Definition I*, the flux across the pressure head equal to zero plane is equal to q_d (0.025 m/d), see Figure 4.6. As before, results from different heights above the water table are also plotted. The infiltrating water arrives above the capillary fringe and thus the flux across the water table is equal to the drainage flux.

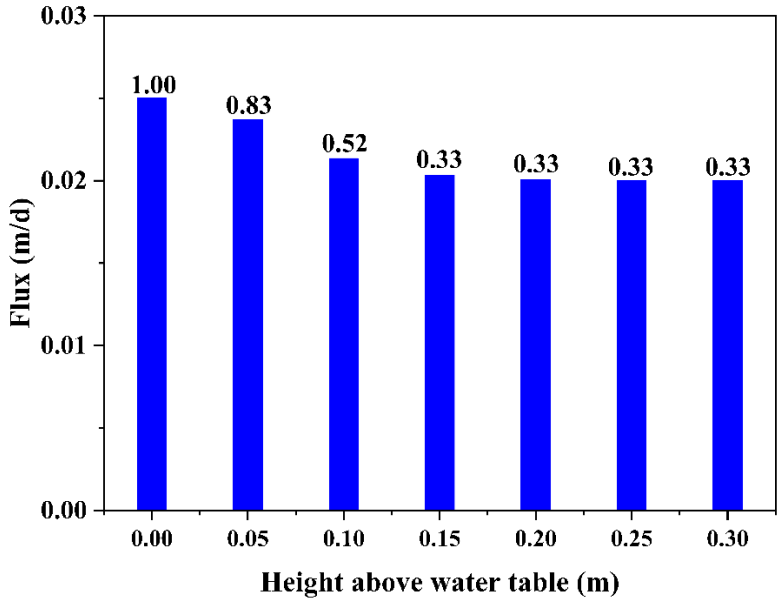

Figure 4.6 Fluxes across planes across the water table (h_p=0) and at constant heights above the water table for sand for imposed infiltration rates of 0.02 m/d. The values above the columns represent the saturations on the planes. The drainage rate is 0.025 m/d, water level decreases.

Employing *Definition II,* the flux across the saturation equal to 1 plane is equal to q_d (0.025 m/d). The application of *Definition III* yields zero (numerically below zero) recharge as the water table is decreasing. As before, the drainage rate can be considered (0.025 m/d).

The results based on *Definition IV* can also be found in Figure 4.6 where fluxes extracted at different heights above the h_p= 0 plane are shown. As the height increases (approximating *Definition IV*), the extracted flux tends towards the specified infiltration flux in the soil column (0.02 m/d).

4.5 Discussion

4.5.1 Discussion of the modeling approach

The simulations described in this paper are based on homogenous 1D systems with constant boundary conditions. If more complex, 2 or 3- dimensional systems are considered, two additional factors can further complicate the analysis: (1) the water table might be inclined and not flat as in the 1D case; and (2) horizontal fluxes will affect the water table dynamics. Both of these complications can in principle be considered through appropriate post-processing of the simulation results. The analysis is further complicated if transient boundary conditions, hysteresis, or heterogeneity are considered. In addition, for simple 1D models, the drainage flux

can be easily considered in the context of the water fluctuation method. However, in the more complex, 2 or 3- dimensional setting, it is very difficult to associate the drinage fluxes to rivers or other discharge points to a specific recharge event or period, as the temporal dynamics of groundwater level change and drainage can be very different. While all of these aspects can be accounted for through an adequate model setup and appropriate post-processing, all the issues highlighted above remain, thus preventing the unambiguous assessment of groundwater recharge.

4.5.2 Implications for exacting groundwater recharge from variably-saturated subsurface flow models

It is becoming increasingly popular to examine how recharge changes under future climates (Crosbie et al. 2013; Ghazavi and Ebrahimi 2019; McCallum et al. 2010; Mileham et al. 2009; Moeck et al. 2016). Variably-saturated subsurface flow models, especially integrated surface and subsurface models, such as HydroGeoSphere represent all relevant hydrological processes and are thus, until closer examination, expected to be suitable to extract and observe recharge processes for current and future conditions. However, our analysis has clearly demonstrated that extracting groundwater recharge from physically based models yields ambiguous results even for very simple systems. The fundamental challenge is that the definition of recharge is anything but clear and thus cannot be implemented in a unique way in the postprocessing process of physically-based models.

Hillel (1998, p480) eloquently highlighted the problems with identifying the water table and thus recharge: *"Groundwater is sustained (recharged) by percolation through the unsaturated zone, and the position of its surface (the water table) is determined by the relative rates of recharge versus outflow. Reciprocally, the position of the water table affects the moisture profile and flow conditions above it. One problem encountered in attempting to distinguish between the unsaturated and saturated zones is that the boundary between them may not be exactly at the water table but at some elevation above it, corresponding to the upper extent of the capillary fringe (at which the suction is equal to the air-entry value for the soil). Frequently, this boundary is diffuse and scarcely definable, particularly when affected by*

hysteresis."

A quantity that can be uniquely quantified with variably-saturated subsurface flow models is the flux below the root zone or extinction depth. Water below the root zone or extinction depth will not transpire or evaporate, the extinction depth is thus clearly defined, and can thus be used in an unambiguous way. This flux corresponds to the potential recharge and can be very useful. However, this approach does not work if the water table is above the extinction depth. Also, if the water table is very deep, as is typically the case in arid- and semi-arid areas, the time lag between deep infiltration and recharge can be very long (Nazarieh et al. 2018; Rossman et al. 2014). The potential recharge will eventually contribute to groundwater.

Another quantity that can be uniquely extracted and which is of direct use to many water resources management questions is the dynamics of the saturated volume. Note, however, that as illustrated above and previously highlighted in the literature (Gillham, 1984), the response of the water table and thus the dynamics of the saturated volume to infiltrating water will significantly depend on the antecedent soil moisture conditions above the water table (Gillham, 1984).

4.6 Conclusions

Recharge cannot always be unambiguously extracted from variably-saturated subsurface flow models and so care should be taken when such models are employed to extract it. However, infiltration fluxes below the extinction depth can be extracted uniquely, for example, to analyze how land use/cover or climate change affects the potential contribution to groundwater. Changes of saturated volumes can be easily extracted and provide direct and relevant information for water resources management. Since recharge is only of indirect interest to water resource management, the difficulty in accurately quantifying recharge in variably-saturated subsurface flow models is not of concern. Rather, since the models simulate both surface water, unsaturated and saturated zone flows, they are able to accurately predict groundwater declines caused by land surface activities. They, therefore, are ideally suited to addressing water resource problems.

Conflict of Interest：

The authors declare that they have no conflicts of interest relevant to this research.

Data Availability Statement:

The input files of models in this research are available at: https://doi.org/10.6084/m9.figshare.23791467.v1 (Gong et al., 2023). A softeware HydroGeoSphere license would be required to run the models (cotact sales@aquanty.com).

Acknowledgments:

Chengcheng Gong is very grateful to the Chinese Scholarship Council (No. 201906560022) for providing an opportunity to be a visiting Ph.D. student at the University of Neuchâtel. This research was also partially supported by the SAFEA: High-End Foreign Experts Project (No. G20200027030). We appreciate the insightful comments and constructive suggestions from anonymous reviewers and editors.

Chengcheng Gong's contributions to this paper:

Write the original draft, set up models, analyze the results from models, and revise the paper.

References

Allison, G., Cook, P., Barnett, S., Walker, G., Jolly, I., Hughes, M. 1990. Land clearance and river salinisation in the western Murray Basin, Australia. Journal of Hydrology, 119(1-4): 1-20.

Aquanty Inc., 2018. HydroGeoSphere: A three-dimensional numerical model describing fully-integrated subsurface and surface flow and solute transport. Waterloo, Ontario, Canada. https://www.aquanty.com/hgs-download.

Assefa, K.A., Woodbury, A.D., 2013. Transient, spatially varied groundwater recharge modeling. Water Resources Research, 49(8): 4593-4606.

Baalousha, H.M., 2016. Development of a groundwater flow model for the highly parameterized Qatar aquifers. Modeling Earth Systems and Environment, 2(2).

Batalha, M.S., Barbosa, M.C., Faybishenko, B., van Genuchten, M.T., 2018. Effect of temporal averaging of meteorological data on predictions of groundwater recharge. Journal of Hydrology and Hydromechanics, 66(2): 143-152.

Brandhorst, N., Erdal, D., Neuweiler, I., 2021. Coupling saturated and unsaturated flow: comparing the iterative and the non-iterative approach. Hydrology and Earth System Sciences, 25(7): 4041-4059.

Brooks, R.H. and Corey, A.T. 1964. Hydraulic Properties of Porous Media. Hydrology Paper, Vol. 3, Colorado State University, Fort Collins.

Brunner, P., Simmons, C., 2011. HydroGeoSphere: A Fully Integrated, Physically Based Hydrological Model, 50, 170-6 pp. DOI:10.1111/j.1745-6584.2011.00882.x.

Carrera-Hernández, J.J., Smerdon, B.D., Mendoza, C.A. 2012. Estimating groundwater recharge through unsaturated flow modelling: Sensitivity to boundary conditions and vertical discretization. Journal of Hydrology, 452-453: 90-101. DOI:10.1016/j.jhydrol.2012.05.039.

Carsel, R.F., Parrish, R.S. 1988. Developing joint probability distributions of soil water retention characteristics. Water resources research, 24(5): 755-769.

Cech, T.V., 2009. Principles of water resources: history, development, management, and policy. John Wiley & Sons.

Crosbie, R.S., Binning, P., Kalma, J.D. 2005. A time series approach to inferring groundwater recharge using the water table fluctuation method. Water Resources Research, 41(1). DOI:10.1029/2004wr003077.

Crosbie, R.S., Scanlon, B.R., Mpelasoka, F.S., Reedy, R.C., Gates, J.B., Zhang, L. 2013. Potential climate change effects on groundwater recharge in the High Plains Aquifer, USA. Water Resources Research, 49(7): 3936-3951. DOI:10.1002/wrcr.20292.

Cuthbert, M.O. 2010. An improved time series approach for estimating groundwater recharge from groundwater level fluctuations. Water Resources Research, 46(9). DOI:10.1029/2009wr008572.

Dassargues, A., 2018. Hydrogeology: groundwater science and engineering. CRC Press.

de Vries, J.J., Simmers, I. 2002. Groundwater recharge: an overview of processes and challenges. Hydrogeology Journal, 10(1): 5-17. DOI:10.1007/s10040-001-0171-7.

Delleur, J.W., 2006. The handbook of groundwater engineering. CRC press.

Dingman, S.L., 2015. Physical hydrology. Waveland press.

Doble, R.C., Crosbie, R.S. 2016. Review: Current and emerging methods for catchment-scale modelling of recharge and evapotranspiration from shallow groundwater. Hydrogeology Journal, 25(1): 3-23. DOI:10.1007/s10040-016-1470-3.

Fitts, C.R., 2013. Groundwater, Groundwater Science, pp. 1-22. DOI:10.1016/b978-0-12-384705-8.00001-7.

Freeze, R.A., Cherry, J.A., 1979. Groundwater.

Frei, S., Fleckenstein, J.H., Kollet, S.J., Maxwell, R.M., 2009. Patterns and dynamics of river–aquifer exchange with variably-saturated flow using a fully-coupled model. Journal of Hydrology, 375(3-4): 383-393. DOI:10.1016/j.jhydrol.2009.06.038.

Gemitzi, A., Ajami, H., Richnow, H.-H. 2017. Developing empirical monthly groundwater recharge equations based on modeling and remote sensing data – Modeling future groundwater recharge to predict potential climate change impacts. Journal of Hydrology,

546: 1-13. DOI:10.1016/j.jhydrol.2017.01.005.

Ghazavi, R., Ebrahimi, H. 2019. Predicting the impacts of climate change on groundwater recharge in an arid environment using modeling approach. International Journal of Climate Change Strategies and Management, 11(1): 88-99. DOI:10.1108/ijccsm-04-2017-0085.

Gillham, R. 1984. The capillary fringe and its effect on water-table response. Journal of Hydrology, 67(1-4): 307-324.

Gong, C., Zhang, Z., Wang, W., Duan, L., Wang, Z. 2021. An assessment of different methods to determine specific yield for estimating groundwater recharge using lysimeters. Science of The Total Environment, 788. DOI:10.1016/j.scitotenv.2021.147799.

Gong, C., Cook, P.G., Therrien, R., Wang, W., Brunner, P. 2023. Models for "On groundwater recharge in variably-saturated subsurface flow models" [dataset]. DOI:10.6084/m9.figshare.23791467.v1.

Guay, C., Nastev, M., Paniconi, C., Sulis, M., 2013. Comparison of two modeling approaches for groundwater-surface water interactions. Hydrological Processes, 27(16): 2258-2270. DOI:10.1002/hyp.9323.

Haitjema, H.M., 1995. Analytic element modeling of groundwater flow. Elsevier.

Harbaugh, A.W., 2005. MODFLOW-2005, the US Geological Survey modular ground-water model: the ground-water flow process. US Department of the Interior, US Geological Survey Reston, VA.

Harbaugh, A.W., Banta, E.R., Hill, M.C., McDonald, M.G. 2000. Modflow-2000, the u. s. geological survey modular ground-water model-user guide to modularization concepts and the ground-water flow process. Open-file Report. U. S. Geological Survey(92): 134.

Healy, R.W., 2010. Estimating groundwater recharge. Cambridge University Press.

Healy, R.W., Cook, P.G. 2002. Using groundwater levels to estimate recharge. Hydrogeology Journal, 10(1): 91-109. DOI:10.1007/s10040-001-0178-0.

Hillel, D., 1998. Environmental soil physics: Fundamentals, applications, and environmental considerations. Elsevier.

Hou, L., Wang, X.-S., Hu, B.X., Shang, J., Wan, L., 2016. Experimental and numerical investigations of soil water balance at the hinterland of the Badain Jaran Desert for groundwater recharge estimation. Journal of Hydrology, 540: 386-396.

Hu, W., Wang, Y.Q., Li, H.J., Huang, M.B., Hou, M.T., Li, Z., She, D.L., Si, B.C., 2019. Dominant role of climate in determining spatio-temporal distribution of potential groundwater recharge at a regional scale. Journal of Hydrology, 578.

Hund, S.V., Allen, D.M., Morillas, L., Johnson, M.S. 2018. Groundwater recharge indicator as tool for decision makers to increase socio-hydrological resilience to seasonal drought. Journal of Hydrology, 563: 1119-1134. DOI:10.1016/j.jhydrol.2018.05.069.

Kinzelbach, W., Brunner, P., von Boetticher, A., Kgotlhang, L., Milzow, C., 2010. Sustainable

water management in arid and semi-arid regions, 119-130 pp. DOI:10.1017/CBO9780511760280.009.

Knowling, M.J., Werner, A.D., 2016. Estimability of recharge through groundwater model calibration: Insights from a field-scale steady-state example. Journal of Hydrology, 540: 973-987.

Kresic, N., Stevanovic, Z., 2009. Groundwater hydrology of springs: Engineering, theory, management and sustainability. Butterworth-heinemann.

Lerner, D.N., Issar, A.S., Simmers, I. 1990. Groundwater recharge. A Guide to Understanding and Estimating Natural Recharge. International Contributions to Hydrogeology. International Association of Hydrogeologists, 8.

Lerner, D.N., 1996, Groundwater recharge: in Geochemical processes, Weathering and Groundwater Recharge in Catchments (Saethe, O.M., and de Caritat, P., eds.), Balkema, Rotterdam, p. 109-150.

Maxwell, R.M., Miller, N.L. 2005. Development of a coupled land surface and groundwater model. Journal of Hydrometeorology, 6(3): 233-247.

McCallum, J.L., Crosbie, R.S., Walker, G.R., Dawes, W.R. 2010. Impacts of climate change on groundwater in Australia: a sensitivity analysis of recharge. Hydrogeology Journal, 18(7): 1625-1638. DOI:10.1007/s10040-010-0624-y.

Meixner, T., Manning, A.H., Stonestrom, D.A., Allen, D.M., Ajami, H., Blasch, K.W., Brookfield, A.E., Castro, C.L., Clark, J.F., Gochis, D.J., Flint, A.L., Neff, K.L., Niraula, R., Rodell, M., Scanlon, B.R., Singha, K., Walvoord, M.A. 2016. Implications of projected climate change for groundwater recharge in the western United States. Journal of Hydrology, 534: 124-138. DOI:10.1016/j.jhydrol.2015.12.027.

Mileham, L., Taylor, R.G., Todd, M., Tindimugaya, C., Thompson, J. 2009. The impact of climate change on groundwater recharge and runoff in a humid, equatorial catchment: sensitivity of projections to rainfall intensity. Hydrological Sciences Journal, 54(4): 727-738. DOI:10.1623/hysj.54.4.727.

Moeck, C., Brunner, P., Hunkeler, D. 2016. The influence of model structure on groundwater recharge rates in climate-change impact studies. Hydrogeology Journal, 24(5): 1171-1184. DOI:10.1007/s10040-016-1367-1.

Nazarieh, F., Ansari, H., Ziaei, A.N., Izady, A., Davari, K., Brunner, P. 2018. Spatial and temporal dynamics of deep percolation, lag time and recharge in an irrigated semi-arid region. Hydrogeology Journal, 26(7): 2507-2520. DOI:10.1007/s10040-018-1789-z.

Nimmo, J.R., Healy, R.W., Stonestrom, D.A. 2006. Aquifer recharge. Encyclopedia of hydrological sciences.

Paniconi, C., Putti, M., 1994. A comparison of Picard and Newton iteration in the numerical solution of multidimensional variably saturated flow problems. Water Resources Research, 30(12): 3357-3374.

Paniconi, C., Wood, E.F., 1993. A detailed model for simulation of catchment scale subsurface hydrologic processes. Water Resources Research, 29(6): 1601-1620.

Poehls, D., Smith, G.J., 2011. Encyclopedic dictionary of hydrogeology. Academic press.

Rossman, N.R., Zlotnik, V.A., Rowe, C.M., Szilagyi, J. 2014. Vadose zone lag time and potential 21st century climate change effects on spatially distributed groundwater recharge in the semi-arid Nebraska Sand Hills. Journal of Hydrology, 519: 656-669. DOI:10.1016/j.jhydrol.2014.07.057.

Rubin, Y., Dagan, G., 1987. Stochastic identification of transmissivity and effective recharge in steady groundwater flow: 1. Theory. Water Resources Research, 23(7): 1185-1192.

Rushton K (1997) Recharge from permanent water bodies. In: Simmers I (ed) Recharge of phreatic aquifers in (semi)arid areas. AA Balkema, Rotterdam, pp 215–255.

Sanford, W., 2002. Recharge and groundwater models: an overview. Hydrogeology Journal, 10(1): 110-120.

Sanford, W., Plummer, L.N., McAda, D., Bexfield, L., Anderholm, S., 2004. Hydrochemical tracers in the middle Rio Grande Basin, USA: 2. Calibration of a groundwater-flow model. Hydrogeology Journal, 12(4).

Scanlon, B.R., Healy, R.W., Cook, P.G. 2002. Choosing appropriate techniques for quantifying groundwater recharge. Hydrogeology Journal, 10(1): 18-39. DOI:10.1007/s10040-001-0176-2.

Schmoll, O., Howard, G., Chilton, J., Chorus, I., 2006. Protecting groundwater for health: managing the quality of drinking-water sources. World Health Organization.

Sen, Z., 2008. Wadi hydrology. Crc Press.

Shamsudduha, M., Taylor, R.G., Ahmed, K.M., Zahid, A. 2011. The impact of intensive groundwater abstraction on recharge to a shallow regional aquifer system: evidence from Bangladesh. Hydrogeology Journal, 19(4): 901-916. DOI:10.1007/s10040-011-0723-4.

Sharp, J.M., 2003. A glossary of hydrogeological terms. Department of Geological Sciences, The University of Texas.

Simmers, I., 2013. Estimation of natural groundwater recharge, 222. Springer Science & Business Media.

Simmons, C. T., Brunner, P., Therrien, R., Sudicky, E. A., 2020. Commemorating the 50th anniversary of the Freeze and Harlan (1969) Blueprint for a physically-based, digitally-simulated hydrologic response model, Journal of Hydrology, vol 584, 124309.

Silliman S E, Berkowitz B, Simunek J, et al. Fluid flow and solute migration within the capillary fringe[J]. Groundwater, 2002, 40(1): 76-84.

Singhal, B.B.S., Gupta, R.P., 2010. Applied hydrogeology of fractured rocks. Springer Science & Business Media.

Šimůnek, J., Van Genuchten, M.T., Sejna, M., 2005. The HYDRUS-1D software package for

simulating the one-dimensional movement of water, heat, and multiple solutes in variably-saturated media. University of California-Riverside Research Reports, 3: 1-240.

Šimůnek, J., Van Genuchten, M.T., Šejna, M., 2006. The HYDRUS software package for simulating two-and three-dimensional movement of water, heat, and multiple solutes in variably-saturated media. Technical manual, version, 1: 241.

Sophocleous, M., 2004. Groundwater recharge. Oxford, UK.

Sophocleous, M., Perry, C.A. 1985. Experimental studies in natural groundwater-recharge dynamics: the analysis of observed recharge events. Journal of Hydrology, 81(3-4): 297-332.

Sophocleous, M.A. 1991. Combining the soilwater balance and water-level fluctuation methods to estimate natural groundwater recharge: practical aspects. Journal of hydrology, 124(3-4): 229-241.

Tonkul, S., Baba, A., Simsek, C., Durukan, S., Demirkesen, A.C., Tayfur, G., 2019. Groundwater recharge estimation using HYDRUS 1D model in Alasehir sub-basin of Gediz Basin in Turkey. Environ Monit Assess, 191(10): 610.

Tóth, J., 2009. Gravitational systems of groundwater flow: theory, evaluation, utilization. Cambridge University Press.

van Genuchten, M.T. 1980. A closed-form equation for predicting the hydraulic conductivity of unsaturated soils. Soil science society of America journal, 44(5): 892-898.

Waldowski, B. et al., 2023. Estimating Groundwater Recharge in Fully Integrated pde-Based Hydrological Models. Water Resources Research, 59(3). DOI:10.1029/2022wr032430.

Xu, Y., Beekman, H.E. 2018. Review: Groundwater recharge estimation in arid and semi-arid southern Africa. Hydrogeology Journal. DOI:10.1007/s10040-018-1898-8.

Zhang, Z., Wang, W., Gong, C., Zhang, M. 2020. A comparison of methods to estimate groundwater recharge from bare soil based on data observed by a large-scale lysimeter. Hydrological Processes, 34(13): 2987-2999.

Zhu, C., 2000. Estimate of recharge from radiocarbon dating of groundwater and numerical flow and transport modeling. Water Resources Research, 36(9): 2607-2620.

Chapter 5 An assessment of different methods to determine specific yield for estimating groundwater recharge using lysimeters

Chapter 5 has been published as: **Gong C**, Zhang Z, Wang W, Duan L, Wang Z. An assessment of different methods to determine specific yield for estimating groundwater recharge using lysimeters[J]. Science of the Total Environment, 2021, 788: 147799.

Abstract

Estimation of groundwater recharge is considered crucial for the management of groundwater resources. The groundwater level fluctuation method (GLF) is a widely used approach to estimate groundwater recharge due to its simplicity and ease of implementation. However, the main source of uncertainty is the specific yield for the GLF method. Although there have been some methods for determining specific yield, the influence of specific yield on the estimation of recharge remains unclear. We set up three lysimeters with different water table depths in the Guanzhong Basin, China. Soil moisture content along with the soil profile, water table depths, and rainfall data were measured continuously. These data provide us with accurately observed recharge and allow us to analyze the performance of specific yield from different methods in estimating recharge. The main results are: (1) The constant specific yield from the pumping tests, which is equal to the ultimate specific yield, significantly overestimated the observed recharge rates independent of water table depths. (2) The constant specific yield obtained from saturated soil moisture content minus field capacity tended to overestimate the recharge under the shallow water table depths (less than 2 m), and vice versa; (3) The depth-dependent specific yield using the measured soil moisture content along with soil profile can obtain reliable recharge across all water table depths. (4) The accuracy of the depth-dependent specific yield obtained by the soil water retention curve relies on reliable parameters. The parameters α and n have to be taken into account carefully for determining the specific yield. Our results are important for the application of the GLF method to estimate recharge. More importantly, it is valuable for the sustainable management of groundwater recourses.

Keywords: Groundwater level fluctuation method; Lysimeter; Specific yield; Water table depth; Soil moisture content

5.1 Introduction

Groundwater recharge is an important process in the hydrological cycle (Wang et al. 2015). Understanding the groundwater recharge mechanism and accurately estimating recharge are not only essential for sustainable management of groundwater resources (de Vries and Simmers 2002; Gleeson et al. 2016; Healy and Cook 2002; Sophocleous 1991), but also are important in the analysis of agriculture contamination (Böhlke 2002; Healy and Scanlon 2010). Unfortunately, there are still challenges in estimating groundwater recharge, as recharge is affected by many factors, such as vegetation, soil properties, soil thickness, precipitation duration and intensity (Zhang et al. 2021; Moeck et al. 2020). Moreover, the recharge is difficult to directly observe (Cheng et al. 2017; Moeck et al. 2020; Moeck et al. 2018). The relationship between precipitation and groundwater recharge is characterized by high spatial heterogeneity and temporal variability (Baker et al., 2021; Wang et al. 2015). Also, highly variable lag-times between precipitation and recharge have been observed (Nazarieh et al. 2018).

Generally speaking, there are three approaches to estimate groundwater recharge, including physical methods, numerical modeling methods, and tracer methods (Healy and Scanlon 2010; Scanlon et al. 2002). Numerical modeling and tracer methods have been used to estimate recharge in recent years (Cartwright et al. 2017; Lu et al. 2020; Moeck et al. 2016; Moeck et al. 2017; Zhang et al. 2020a; Zhang et al. 2020b). However, the numerical modeling methods are sensitive to boundary conditions (Carrera-Hernández et al. 2012; Xu and Beekman 2019) and require reliable parameters (Brunner et al. 2012). Tracer methods, e.g., the chloride mass balance method can provide information on recharge sources (Scanlon et al., 2002; Huang et al., 2020). Nevertheless, estimating recharge is based on several assumptions, including that the system is in a steady-state (Zhang et al., 2021; Huang et al. 2020). Physical methods can obtain recharge with high temporal resolution (Scanlon et al. 2002), and these methods mainly include direct measurements (lysimeter) and indirect measurements (e.g., zero flux plane,

Darcy's law, and groundwater level fluctuation (GLF) method) (Jafari et al. 2019). Among these physical methods, the GLF method is the most commonly used (Healy and Cook 2002).

The GLF method was proposed as early as the 1920s (Meinzer 1923). This method only requires data on groundwater level fluctuations and specific yield (Crosbie et al. 2005; Crosbie et al. 2019). As it is easy to implement, the GLF method is a highly attractive and widely used method for estimating groundwater recharge (Healy and Cook 2002; Labrecque et al. 2020). For example, Yin et al. (2011) used the GLF method to estimate recharge in the Ordos Plateau, China. Rama et al. (2018) used the GLF method to estimate recharge in the coastal shallow aquifer of Santa Catarina Island. Koïta et al. (2018) proposed a method combined GLF method with magnetic resonance soundings to estimate changes in groundwater storage in hard rock. Besides that, another advantage of the GLF method is that we can obtain recharge with a high temporal resolution (e.g., hourly or daily) (Jie et al. 2011).

The difficulty in applying the GLF method is to obtain an accurate value of specific yield (Crosbie et al. 2019; Maréchal et al. 2006). Because specific yield is related to many factors, such as time, water table depth and soil texture (Lv et al. 2021; Cheng et al. 2020; Cheng et al., 2015; Nachabe, 2002). To obtain a reliable specific yield, a range of approaches have been proposed (Cheng et al. 2020; Crosbie et al. 2005; Duke 1972; Sophocleous 1991). Firstly, the specific yield can be determined by pumping tests using the type-curve method (Wenzel 1936) and drainage experiment (Cheng et al., 2015). The second approach to estimate specific yield is obtained from the soil moisture characteristic curve, which is equal to saturated soil moisture content minus residual soil moisture content. Duke (1972) considered this specific yield to be the ultimate specific yield. Zhang et al. (2020a) estimated recharge using the GLF method based on the ultimate specific yield. They found that using the ultimate specific yield significantly overestimated groundwater recharge compared to lysimeter data. Gillham (1984) considered that a reasonable specific yield is the saturated soil moisture content minus the field capacity. Shah and Ross (2009) pointed out that this approach can obtain reliable specific yield under deep water table depths (> 2 m). However, whether this value (saturated moisture content minus field capacity) can be used to estimate recharge under deep water table depth remains to be

examined. Childs (1960) emphasized that the value of specific yield is not constant, but as a function of the water table depth. dos Santos Júnior and Youngs (1969) extended the work of Childs (1960) and defined the specific yield that accounted for time and water table depth. They pointed out that the water table depth and time are the main factors influencing the specific yield. Duke (1972) suggested that the specific yield is equal to the saturated soil moisture content minus the average soil moisture content in a layer of thickness (dz) at the ground surface. This method requires the measured soil moisture content. Afterwards, Crosbie et al. (2005) proposed a formula for determining the depth-dependent specific yield that used the van Genuchten model (van Genuchten, 1980) to describe the soil moisture content as a function of the water table depth. Loheide et al. (2005) pointed out that the dependence of the specific yield on the water table depth should be taken into account when the water table depths are less than 1 m. In reality, the specific yield is usually considered to be a constant value for estimating recharge (Pan et al. 2017; Yin et al. 2011; Zhang et al. 2019). Few studies have used the depth-dependent specific yield to estimate groundwater recharge (Crosbie et al. 2005; Fan et al. 2014). Additionally, although the GLF method is widely used to estimate recharge at the field sites (Callahan et al. 2012; Wang et al. 2014; Zhang et al. 2019), studies have rarely examined the performance of specific yield on estimating recharge in contrast with the observed recharge.

Given the specific yield is the main source of uncertainty in estimating recharge using the GLF method (Delottier et al. 2018), the purpose of this study is to analyze the performances of the specific yield from different methods on estimating recharge compared to observed recharge. Lysimeters provide an effective tool for observing recharge, which can be used to explore complicated environmental processes under realistic conditions (Pütz et al. 2018). To this end, we built three lysimeters with different water table depths in the Gunzhong Basin, China. While there have been some studies analyzing the dynamics of specific yield, our study is probably the most comprehensive as it directly compared different lysimeters for a wide range of soil moisture and water table conditions. The novelty of this study is also that the depth-dependent specific yield was systematically analyzed for estimating the groundwater recharge under different water table depths.

5.2 Materials and Methods

5.2.1 Study area

We carried out a field experiment in the Gunzhong Basin, China (latitude is $34^0$22’14’’ N and longitude is $108^0$54’11’’ E) (Figure 5.1). The average annual air temperature is 14.9 ℃, the average annual rainfall is 545 mm, and the average annual potential evaporation is 990 mm (Su et al. 2019). The rainy season occurs from May to October and accounts for 80% of the annual rainfall (Wang et al. 2018).

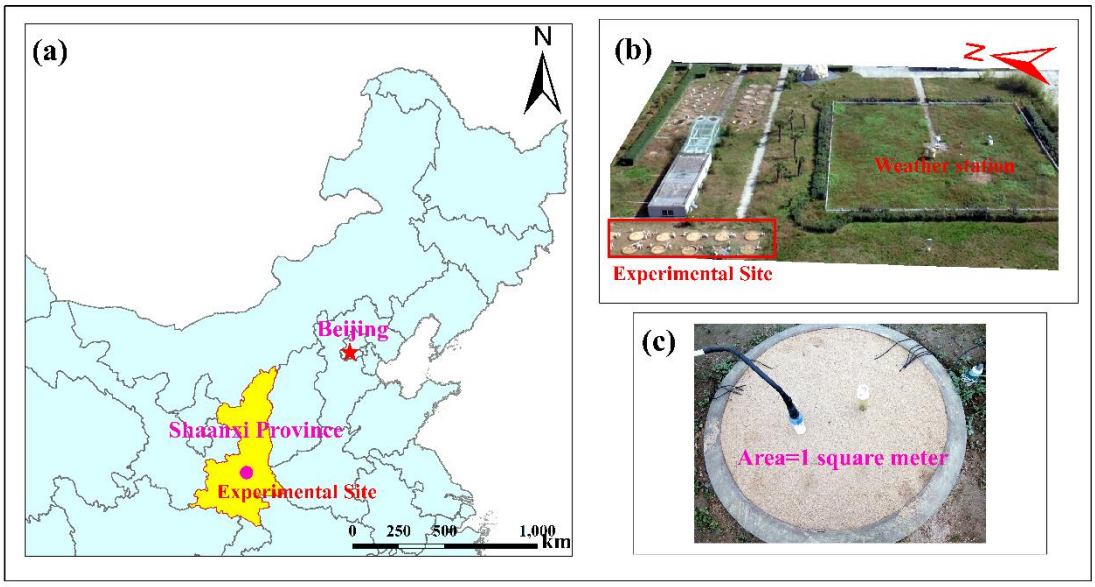

Figure 5.1 (a) Location of the field site in the Guanzhong Basin, China. (b) and (c) are the photos of the field experiment and lysimeter. The figure was modified from Gong et al. (2020).

5.2.2 Experimental design and collection of data

Three lysimeters with different depths were set up on the field site. The depths of these three lysimeters are 220 cm, 320 cm and 420 cm, and the surface area of all lysimeters is 1 m^2. The bottom of the lysimeter is sealed and the water tables fluctuate due to rainfall and evaporation. The initial water table depths were about 180 cm (Lysimeter 1), 280 cm (Lysimeter 2) and 380 cm (Lysimeter 3) on October 1, 2016. The lysimeters were filled with homogeneous sand from the Mu Us desert. The groundwater levels were monitored with DI271 CTD-Diver (Diver Inc., ±0.5 cm H2O) in each lysimeter, while Diver DI500 (Baro-Diver) was used to measure the air pressure to correct groundwater level. Meteorological data, such as wind speed,

rainfall, air temperature, and relative humidity were automatically measured by the weather station located at the experiment site (Figure 5.1). The soil moisture content was observed using the ECHO-5TM sensors (Decagon Inc., ±2%) at depths of 3, 10, 20, 40, 80, 130 and 180 cm in lysimeter 1, and 3, 10, 20, 40, 80, 130, 180, 230 and 280 cm in lysimeter 2, as well as 3, 10, 20, 40, 80, 130, 180, 230, 280 and 350 cm in lysimeter 3 (Figure 5.2). All sensors were calibrated following the steps from Cobos and Chambers (2010) before they were installed. All data were collected at 5 min intervals. The experimental period in this study was from October 1, 2016 to September 30, 2017.

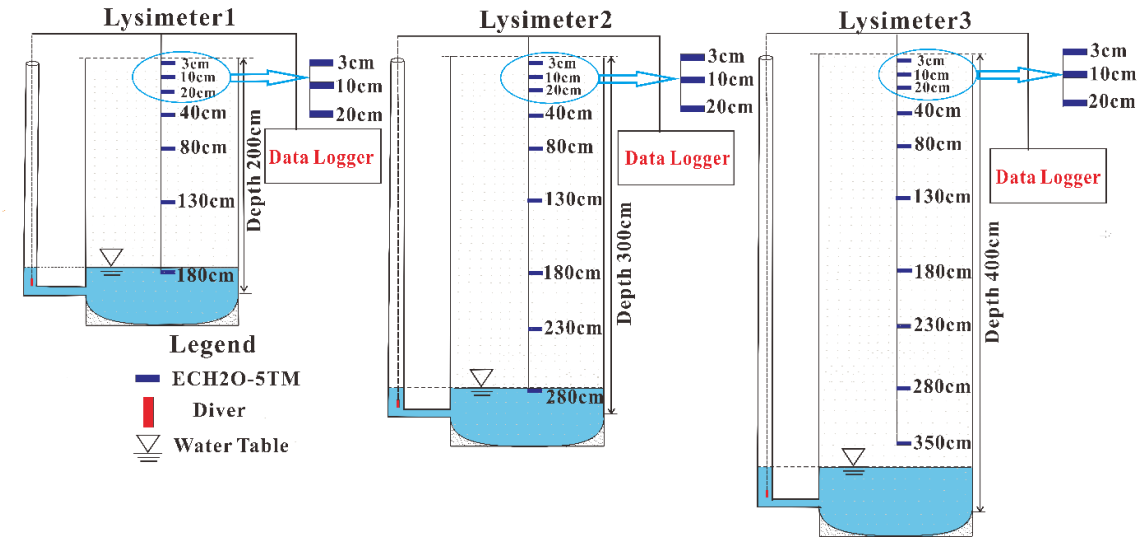

Figure 5.2 Schematic diagram of the lysimeters with different water table depths. The initial water table depth was around 180 cm in lysimeter 1, around 280 cm in lysimeter 2, and around 380 cm in lysimeter 3. The figure is similar to the diagram presented by Gong et al. (2020).

5.2.3 Methods

5.2.3.1 Observed groundwater recharge

As lysimeters in the field site are non-weighing lysimeters, groundwater recharge can be obtained by equation (5.1) (Zhang et al. 2020a) as follows:

$$GR = (\theta_s - \theta_i)\,\Delta GW \tag{5.1}$$

where, GR (cm) is the groundwater recharge, θ_s (cm^3/cm^3) is the saturated soil moisture content, θ_i (cm^3/cm^3) is the soil moisture content at the observation point, and ΔGW (cm) is the change of the water table. The observed groundwater recharge obtained from equation (5.1)

is considered as the reference value. Note that the uncertainties concerning the measurement instruments are very small less than 2 % according to the producer of the sensors. We have thus not considered the influence of instrument uncertainty in the subsequent analysis of our data.

5.2.3.2 Groundwater level fluctuation method (GLF)

The GLF method is based on the assumption that the increase in groundwater levels is the result of infiltration water arriving at the water table (Nimmo et al. 2015). Based on the change in water table and specific yield, the recharge can be calculated as follows:

$$GR = S_y \, dh/dt \tag{5.2}$$

where S_y (-) represents the specific yield, h (cm) represents the height of the water table, and t (day) represents the time.

In this study, S_y was determined using four commonly used approaches:

(1) Based on a constant value from the pumping test

In general, the specific yield can be determined by the pumping test. In this study, pumping tests were performed in all lysimeters. The detailed steps of pumping tests were described in Gong et al. (2020). According to the concept, the specific yield is the volume of water that can be released from storage per unit of surface area of porous medium per unit of the decreased water table (Freeze and Cherry 1979). The specific yield in lysimeter 1 was 0.31, in lysimeter 2 was 0.30, and in lysimeter 3 was also 0.30.

(2) Based on a constant value from saturated moisture content minus field capacity (FC)

A widely used method for estimating specific yield is equation (5.3) as follows:

$$S_y = \theta_s - S_r \tag{5.3}$$

where, S_r represents specific retention (cm^3/cm^3). S_r can be equal to residual soil moisture content (Crosbie et al. 2005) or field capacity (Gillham 1984). Zhang et al. (2020a) used the residual soil moisture content to calculate the specific yield, and the estimation of recharge significantly overestimated the observed recharge. In this paper, the field capacity is used to determine specific yield and estimate recharge. The value of the field capacity from sand used in Gong et al. (2020) is 0.12 cm^3/cm^3.

(3) Based on the depth-dependent method using measured soil moisture (SM)

Duke (1972) suggested that the specific yield accounting for water table depths can be determined by equation (5.4). Equation (5.4) is based on two assumptions: (1) the initial soil profile is in static equilibrium, and (2) the steady-state can be instantaneously reattained after the system is drained.

$$S_y = \theta_s - \theta(H) \tag{5.4}$$

where, $\theta(H)$ represents the average soil moisture observed in a layer of thickness dz at the soil surface, and H (cm) is the water table depth. We used three methods to obtain the value of $\theta(H)$: (1) using the observed soil moisture content at 3 cm below the ground surface (SM-3); (2) using the observed soil moisture content at 20 cm below the ground surface (SM-20), and (3) using the averaged soil moisture content along with the profile of vadose zone (SM-average).

(4) Based on the depth-dependent method using soil water retention curve (DM)

Crosbie et al. (2005) suggested a formula that used the van Genuchten model (van Genuchten 1980) to describe the soil moisture content as the function of pressure head to determine specific yield. The method is based on the assumption that the pressure head distribution is hydrostatic along with the soil profile at equilibrium. The formula can be expressed as follows:

$$S_y = S_{yu} - \frac{S_{yu}}{[1+(\alpha d_i)^n]^{(1-\frac{1}{n})}} \tag{5.5}$$

where, S_{yu} denotes the ultimate specific yield, which is equal to $(\theta_s - \theta_r)$; d_i represents the water table depth at time i; and α and n are soil-specific parameters of the van Genuchten model (van Genuchten 1980). Firstly, we used these parameters obtained from the laboratory experiment. The detailed procedure on the laboratory experiment can be found in Gong et al. (2020). The estimated parameters θ_s, θ_r, α and n are 0.32 cm^3/cm^3, 0.022 cm^3/cm^3, 0.022 1/cm, and 4.14, respectively.

Equation (5.5) includes four parameters, in which θ_s and θ_r can be obtained by the field or laboratory experiments, while α (inversely related to air entry value) and *n* (depending on pore size distribution) have to be obtained from measured data (soil moisture content and pressure head) fitting the soil-water characteristic curve. There is a great uncertainty related to

the parameters α and n (Calamak and Yanmaz 2017), which will lead to uncertainty in the estimation of recharge directly. Therefore, we calibrated the parameters α and n by minimizing the root mean square error between the estimation of cumulative recharge and the observed cumulative recharge in lysimeter 1. The calibrated parameters α and n were 0.035 1/cm and 1.68, respectively. In lysimeters 2 and 3, we determined the specific yields based on the calibrated parameters. Using the parameters from the laboratory to obtain the specific yield by DM method, we called it DM-La, while based on the calibrated parameters, we called it DM-Ca.

5.2.3.3 Parameter uncertainty analysis for the DM method

Given the significant uncertainty from the parameters α and n for determining the specific yield in the DM method, we analyzed the uncertainty of the parameters α and n in estimating recharge as follows:

$$R = S_y \frac{\Delta h}{\Delta t} \tag{5.6}$$

Equation (5.6) can be expanded to Taylor series on mean values of parameters, and by neglecting the second-order and higher order terms (Sun et al. 2013), the perturbation of groundwater recharge can be written as follows:

$$R \approx \left[\frac{\partial R}{\partial n}\right] \Delta n + \left[\frac{\partial R}{\partial \alpha}\right] \Delta \alpha \tag{5.7}$$

If the perturbations of α and n are mutually independent, the cross-covariance of R and α, and that of R and n can be given as follows:

$$\sigma_{Rn}^2 = \frac{\partial R}{\partial n}\sigma_n^2 \text{ and } \sigma_{Rn}^2 = \frac{\partial R}{\partial \alpha}\sigma_\alpha^2 \tag{5.8}$$

where, $\frac{\partial R}{\partial n}$ and $\frac{\partial R}{\partial \alpha}$ are the sensitivity of R at the given time concerning the change in α and n. σ_n^2 and σ_α^2 are the variances of n and α, which represent the recharge uncertainties associated with n and α. The corresponding groundwater recharge variance can be obtained by equation (5.9):

$$\sigma_R^2 = \left[\frac{\partial R}{\partial n}\right]^2 \sigma_n^2 + \left[\frac{\partial R}{\partial \alpha}\right]^2 \sigma_\alpha^2 \tag{5.9}$$

$$\frac{\partial R}{\partial n} = -\frac{(\theta_s - \theta_r)\Delta h}{\Delta t}(1 + {x_1}^n)^{\left(\frac{1}{n}-1\right)}\left[\frac{{x_1}^n\left(\frac{1}{n}-1\right)\log(x_1)}{1+{x_1}^n} - \frac{\log(1+{x_1}^n)}{n^2}\right] \tag{5.10}$$

$$\frac{\partial R}{\partial \alpha} = -\frac{(\theta_s - \theta_r)\Delta h d_i n}{\Delta t} {x_1}^{(n-1)}(1 + {x_1}^n)^{\left(\frac{1}{n}-2\right)}\left(\frac{1}{n} - 1\right) \quad (5.11)$$

where, $x_1 = \alpha d_i$ and let $\sigma_n^2 = b\sigma_\alpha^2$ (b is constant). Then, the cross-covariance σ_{Rn}^2 and $\sigma_{R\alpha}^2$ are normalized by the square root of the product of the variances of R and n and σ_n^2, or those of R and α and σ_α^2 to obtain their corresponding cross-correlations ρ_{Rn} and $\rho_{R\alpha}$ at time *t*.

$$\rho_{Rn} = \frac{\sigma_{Rn}^2}{\sqrt{\sigma_R^2 \sigma_n^2}} = \frac{\frac{\partial R}{\partial n}}{\sqrt{\left[\frac{\partial R}{\partial n}\right]^2 + \frac{1}{b}\left[\frac{\partial R}{\partial \alpha}\right]^2}} \quad (5.12)$$

$$\rho_{R\alpha} = \frac{\sigma_{R\alpha}^2}{\sqrt{\sigma_R^2 \sigma_\alpha^2}} = \frac{\frac{\partial R}{\partial \alpha}}{\sqrt{b\left[\frac{\partial R}{\partial n}\right]^2 + \left[\frac{\partial R}{\partial \alpha}\right]^2}} \quad (5.13)$$

5.3 Results

5.3.1 The observed groundwater recharge in all lysimeters

The amount of rainfall during the entire experimental period was 566 mm (Figure 5.3a). Most of the rainfall events were less than 10 mm/day. The largest rainfall event was 70.0 mm/day and occurred on July 28, 2017. Figure 5.3a also illustrates the daily water table depth of the three lysimeters and the daily rainfall from October 1, 2016 to September 30, 2017. The water table depths in all lysimeters increased during the experimental period. The initial water table depths were 176.3 cm (lysimeter 1), 277.5 cm (lysimeter 2) and 384.2 cm (lysimeter 3). During the experimental period, the water table depths increased by 141.2 cm (lysimeter 1), 171.7 cm (lysimeter 2) and 179.2 cm (lysimeter 3). The dynamics of the water table depth in all lysimeters can be divided into two periods. The first period was from October, 2016 to March, 2017, and the second from April to September, 2017. In the first period, the water table depth slowly increased because only small rainfall events occurred (The amount of rainfall was equal to 108.7 mm). The increased rate was 0.18, 0.20, and 0.28 cm/day in lysimeters 1, 2, and 3, respectively. In the second period, the water table depth exhibited a larger increase compared to the first period. The average rising rate was 0.54, 0.67, and 0.64 cm/day in lysimeters 1, 2, and 3, respectively.

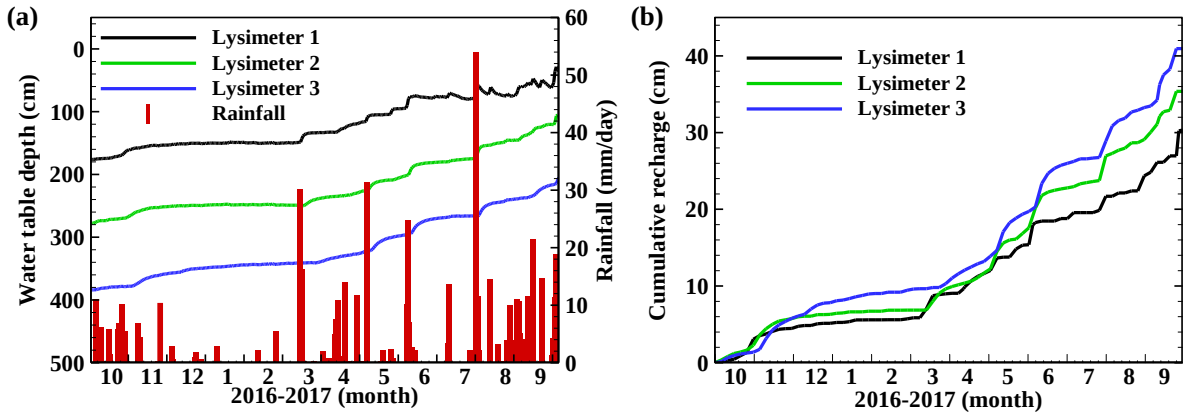

Figure 5.3 (a) The dynamics of water table depth in lysimeter 1 (black line), lysimeter 2 (green line), and lysimeter 3 (blue line). (b) The cumulative groundwater recharge in lysimeters 1, 2, and 3 during the experimental period.

The cumulative observed groundwater recharge in lysimeters 1, 2, and 3 are presented in Figure 5.3b. The total groundwater recharge in lysimeters 1, 2, and 3 were 30.3, 35.4, and 40.9 cm at the end of the experimental period, respectively.

Table 5.1 The determination of specific yield from different methods. Note that the specific yields from SM to DM method are the average value in this table.

Method / Lysimeters	Pumping test	FC	DM-La	DM-Ca	SM-average	SM-3	SM-20
Lysimeter 1	0.31	0.20	0.27	0.14	0.17	0.24	0.20
lysimeter 2	0.30	0.20	0.30	0.20	0.20	0.26	0.25
lysimeter 3	0.30	0.20	0.30	0.22	0.22	0.25	0.23

5.3.2 Results of specific yield from different methods

The results of specific yields from different methods are shown in Table 5.1. It should be noted that the specific yield from the DM and SM methods are concerned with water table depth in all lysimeters. Table 5.1 shows the average specific yield of the DM and SM methods. The dynamics of specific yield over time are shown in Figure 5.4. The variability in the specific yield is larger under the shallow water table depth than that under the deep water table depth.

For example, the specific yield determined by the DM-Ca method varies from 0.05 to 0.18 in lysimeter 1, while the fluctuation of specific yield varied from 0.19 to 0.23 in lysimeter 3.

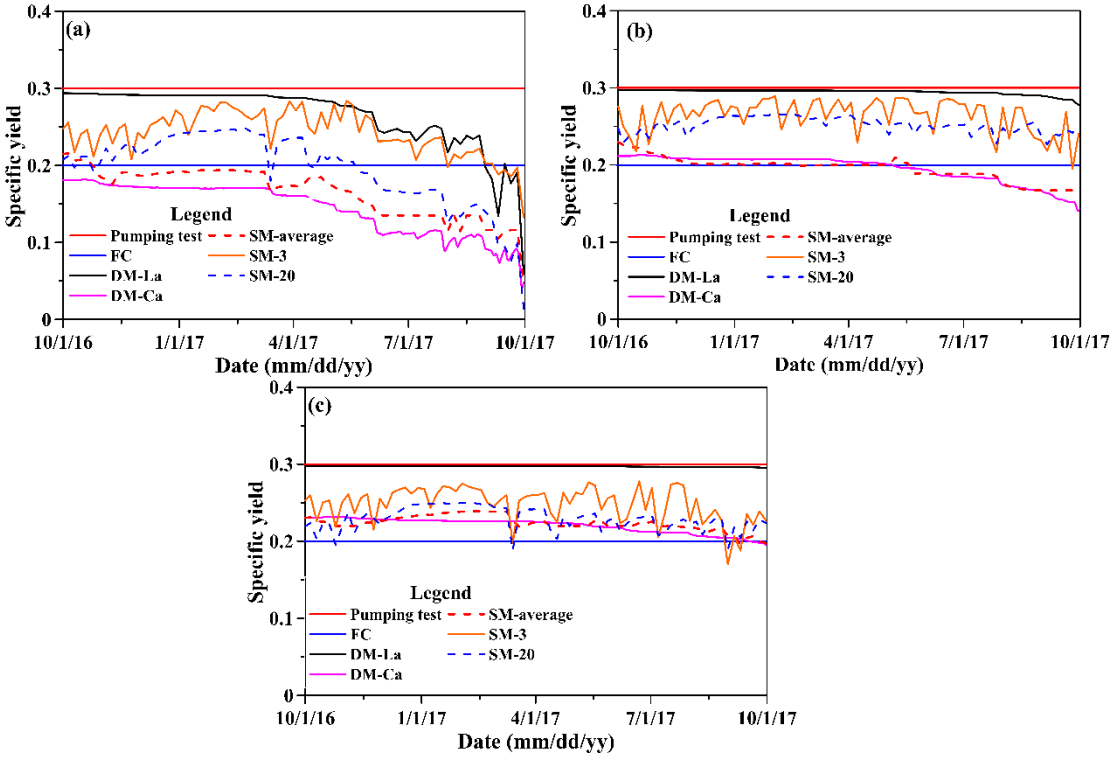

Figure 5.4 The values of specific yield from pumping test (average specific yield of three lysimeters), FC (saturated moisture content minus field capacity) method, DM (depth-dependent) method using the parameters from the laboratory (DM-La) and calibrated parameters (DM-Ca), and SM (saturated soil moisture content minus the measured soil moisture content) method based on the average measured soil moisture content of the vadose zone (SM-average), at 3 cm (SM-3) and 20 cm (SM-20) below the surface ground in lysimeter 1(a), lysimeter 2 (b), lysimeter 3 (c), respectively.

5.3.3 Groundwater recharge from the GLF method based on different S_y determination approaches

5.3.3.1 The estimation of recharge based on specific yield from pumping tests

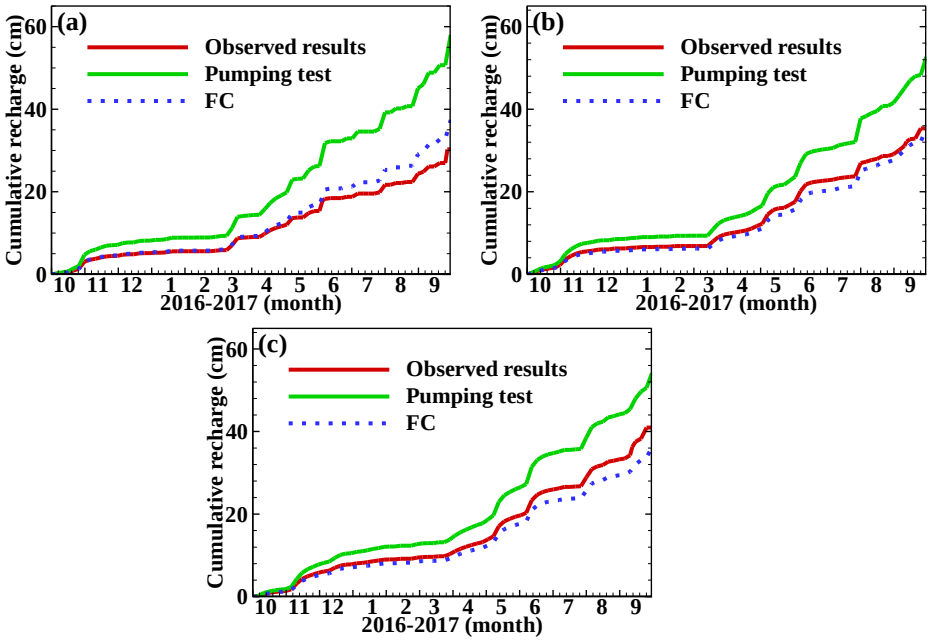

Figure 5.5 The estimation of cumulative groundwater recharge in lysimeter 1 (a), 2 (b), and 3 (c) based on the specific yield from pumping test and FC method.

The estimation of cumulative recharge based on the specific yield from the pumping tests was 57.9 cm in lysimeter 1, 52.7 cm in lysimeter 2, and 54.1 cm in lysimeter 3. The results significantly overestimated the observed recharge in all lysimeters (see Figure 5.5).

5.3.3.2 The estimation of recharge based on the specific yield from FC method

The estimation of cumulative recharge based on the specific yield from the FC method (equation 5.3) was 37.4 cm in lysimeter 1. It can obtain satisfactory results from October, 2016 to April, 2017. After April 2017, the difference between the estimated and observed results is large. At the end of the experiment, the estimation of results showed an overestimation of 23.4% in contrast with the observed recharge in lysimeter 1. However, the estimation of recharge was 35.1 cm in lysimeter 2, which was consistent with the observed result (35.4 cm). The estimation of recharge in lysimeter 3 was underestimated 12.0% of the observed results.

5.3.3.3 The estimation of recharge based on the specific yield from SM method

The estimation of recharge based on the specific yield from the SM-average method (equation (5.4)) was 25.7 cm, 33.1 cm, and 39.4 cm in lysimeters 1, 2, and 3. This method underestimated the observed recharge by 15.2% in lysimeter 1, 6.5% in lysimeter 2, and 3.7% in lysimeter 3 (Figure 5.6). The estimation of recharge with specific yield from SM-3 method

was 40.6 cm in lysimeter 1, 45.8 cm in lysimeter 2, and 39.4 cm in lysimeter 3. In lysimeter 1 and 2, the estimation of recharge overestimated the observed results, while reliable recharge can be obtained in lysimeter 3. The specific yield from SM-20 method can obtain satisfactory recharge at the end of the experiment in lysimeter 1 (28.8 cm) and lysimeter 3 (40.8 cm). However, the estimation of recharge in lysimeter 2 (43.7 cm) overestimated the observed results by 23.5%.

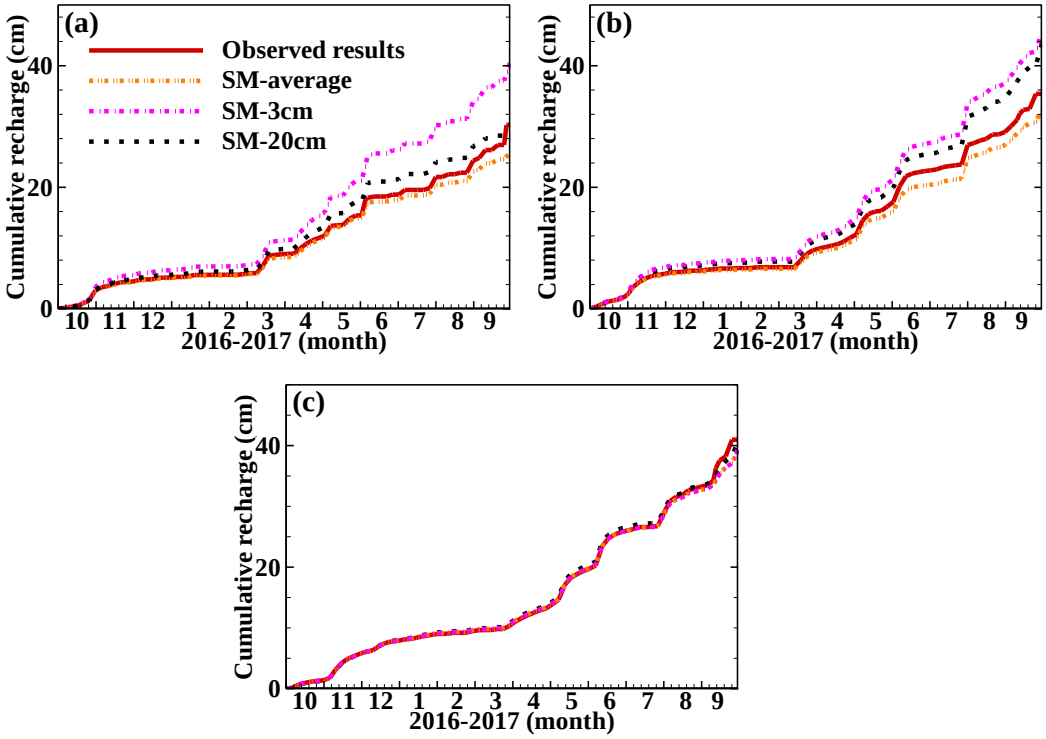

Figure 5.6 The estimation of cumulative recharge in lysimeter 1 (a), 2 (b), and 3 (c) based on the specific yield from the SM method.

5.3.3.4 The estimation of recharge based on the specific yield from DM method

The estimation of recharge based on the specific yield from DM method with the laboratory parameters were 42.1 cm, 51.3 cm, and 53.5 cm in lysimeters 1, 2, and 3, respectively (Figure 5.7). This approach overestimated the observed results in all lysimeters. However, the estimation of recharge based on the specific yield from DM method with the calibrated parameters could obtain satisfactory results for all lysimeters. The estimation results were 29.8 cm (lysimeter 1), 37.5 cm (lysimeter 2), and 42.5 cm (lysimeter 3), which were basically equal to the observed results.

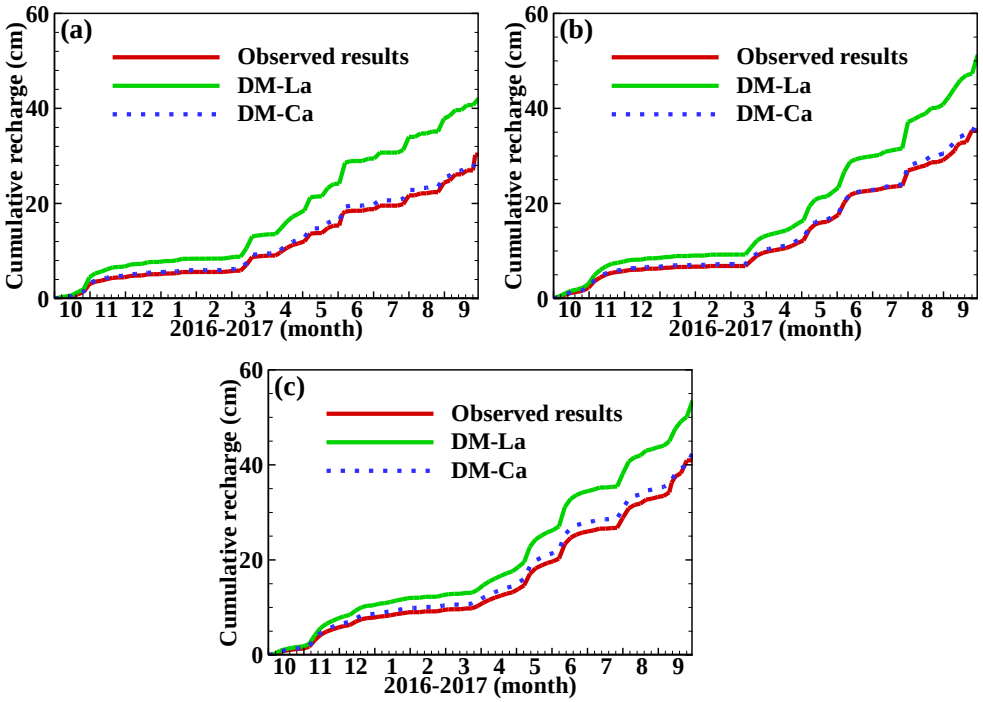

Figure 5.7 The estimation of cumulative groundwater recharge in lysimeter 1 (a), 2 (b), and 3 (c) based on the specific yield from DM method (DM-La and DM-Ca mean the laboratory and calibrated parameters are used).

5.3.4 Parameter uncertainty analysis for DM method

The cross-correlations between groundwater recharge and α, and those between groundwater recharge and n (i.e., equation (5.12) and (5.13)) are plotted as a function of the water table depth in Figure 5.8. As illustrated by the black and red lines, when the water table depth is shallow, the groundwater recharge is positively correlated with n, and negatively correlated with α. Afterward, the value of ρ_{Rn} continuously increases and approaches 1, and the $\rho_{R\alpha}$ value also increases while approaching 0.

The influence of the magnitude of b (ratio of σ_n^2 to σ_α^2) on cross-correlations are also shown in Figure 5.8. The higher the value of b, the larger value of ρ_{Rn}, and the faster it rises to 1. For the $\rho_{R\alpha}$, the larger value of b, the higher the starting value of $\rho_{R\alpha}$ and the earlier it rises to 0. The value of b determines the rate of reaching the maximum values of $\rho_{R\alpha}$ and ρ_{Rn} over the water table depth.

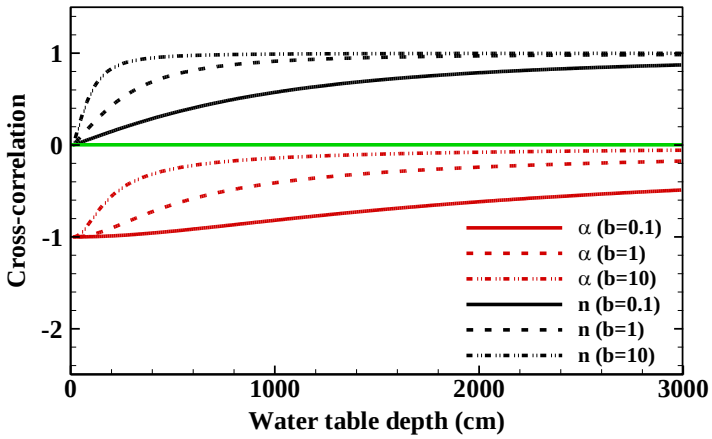

Figure 5.8. Cross-correlation between the groundwater recharge and soil parameters α and *n* as a function of water table depth for different *b* values (the ratio of σ_n^2 to σ_α^2).

5.4 Discussion

We estimated groundwater recharge based on the GLF method using specific yield from four commonly used methods. The estimation of recharge was compared with the observed recharge from three lysimeters under different water table depths. The performance of specific yield in estimating the recharge, and how the specific yield influences the estimation of recharge are discussed in this section.

Among all methods, the specific yield from the DM-Ca method can obtain the best estimation of recharge in all lysimeters (Figure 5.5-5.7). This indicates that the specific yield from the DM-Ca method is reliable. Therefore, we considered the specific yield from the DM-Ca method as the reference value in analyzing the influence of specific yield in estimating recharge under different water table depths.

The constant specific yield from pumping tests overestimated the observed recharge significantly in all lysimeters. The average specific yield (0.3) in all lysimeters was equal to the ultimate specific yield (saturated soil moisture minus residual soil moisture). This is in agreement with previous studies that have indicated that the use of the ultimate specific yield can overestimate the recharge in the GLF method (Zhang et al. 2020a; Crosbie et al., 2005). It should be noted that the specific yield from the pumping tests differs from the aquifer pumping tests in the field. The performance of the specific yield from the aquifer pumping tests is not in the scope of this study and is thus not discussed here.

The estimation of recharge based on specific yield from FC method was more accurate than that from the pumping test. Shah and Ross (2009) pointed out that the FC method can obtain reasonable specific yield under deep water table depth (large than 2m). However, our data clearly shows that the specific yield from the FC method underestimated the reference specific yield (DM-Ca) under deep water table depth (Figure 5.4c). Under the condition of water table depth less than about 2 m (lysimeter 1 and the period after June in lysimeter 2), the FC method tends to overestimate the specific yield in contrast with DM-Ca method (Figure 5.4 (a) and (b)). This is related to the soil moisture content along with soil profile under the shallow water table depth is larger than that under the deep water table depth due to the effect of capillary fringe (Crosbie et al. 2005; Gillham 1984). In lysimeter 2, the water table depth covered the period over 2 m and under 2 m. We can obtain satisfactory recharge as the estimation of recharge is over- and underestimation compensates each other (Figure 5.6 (b)).

The specific yield from the SM-average method is nearly equal to the specific yield from the DM-Ca method. However, the SM-average method requires high-density sensors for measuring the soil moisture along with soil profile. In reality, the application of the SM-average method is challenging, especially under deep water table depth. Alternatively, the specific yield from SM-3 and SM-20 can obtain reliable recharge under deep water table depths (Figure 5.6 (c)). However, the better choice is the SM-20 method as the specific yield is closer to the specific yield obtained from SM-average and DM-Ca method (Figure 5.4 (c)). The soil moisture content at 3 cm below the surface ground varied rapidly in response to the rainfall and evaporation. At a short time scale, the SM-3 method may yield large errors in estimating recharge. It is thus to suggest the SM-20 method to determine specific yield under deep water table depth in our case.

DM method can obtain the specific yield as a function of water table depth. However, the potential problem related to this method is the uncertainty of parameters for the soil water retention curve. The parameters from the laboratory cannot obtain a reliable specific yield. Results of the uncertainty analysis in the parameters α and n show that both α and n can affect the specific yield on estimating recharge if the water table depth is shallow. If the water

table depth is deep, the main source of the uncertainty is the parameter n. It is critical to obtain reliable parameters using DM method. Besides the parameters from the laboratory, another popular method for obtaining parameters is to use pedotransfer functions (PTFs) (da Silva et al. 2017). Wang et al. (2009) used PTFs in vadose zone models to estimate the groundwater recharge in semiarid regions. They found that the uncertainty in recharge estimation is greatly influenced by the parameter n. Consequently, the parameters should be carefully considered when estimating the recharge based on the DM method.

5.5 Conclusions

In this study, three lysimeters with different water table depths were set up in the Guangzhong Basin, China. Rainfall, water table depths, and soil moisture content along with the soil profile were continuously monitored from October 1, 2016 to September 30, 2017. Based on these observed data, we systematically analyzed the influence and performance of the specific yield from methods on the estimation of recharge. Several key conclusions can be drawn as follows:

(1) Using the specific yield based on pumping tests does not allow to obtain a reliable estimation of recharge independent of the water table conditions.

(2) Using the specific yield obtained from FC method (saturated water content minus field capacity), a satisfactory estimation of recharge cannot be obtained. Under the shallow water table depth (less than 2 m), the estimation of recharge tends to overestimate, while the estimation of recharge tends to underestimate if the water table depth is larger than 2 m.

(3) The specific yield based on the SM-average method can obtain reliable estimations of groundwater recharge. However, this method requires measured soil moisture content along with the soil profile. In our case, as an alternative, the observed soil moisture content at 20 cm below the ground surface can be used to obtain reliable specific yield under the deep water table depth.

(4) The specific yield based on the DM method heavily relies on the parameters α and n. The uncertainty analysis of these two parameters showed that both α and n affect the specific

yield under the shallow water table depths. Only the parameter n has a great influence on the specific yield under deep water table depths.

The analysis of the specific yield can improve the estimation of recharge by the groundwater level fluctuation method. This study is based on observed data from the homogeneous sandy soil without vegetation in a semi-arid region. For area covered y vegetation and heterogeneous soil, further investigations of the specific yield need to indicates that the approach to determine specific yield can provide very different results. Our study also suggests that the depth to water table is an important factor in the estimation of specific yield. We thus strongly recommend to employ, if possible, multiple approaches to estimate specific yield. The differences in estimated recharge provide important indications concerning the reliability of the recharge estimates.

Acknowledgements

This study is supported by the National Natural Science Foundation of China (No.U1603243, 41230314). Chengcheng Gong is grateful to the Chinese Scholarship Council (No. 201906560022) for providing an opportunity to be a visiting student at the University of Neuchâtel. We greatly appreciate Dr. Yanwei Lu who read the manuscript and gave valuable suggestions. We are grateful for the insightful comments and constructive suggestions from two anonymous reviewers and the editor.

Chengcheng Gong's contributions to this paper:

Write the original draft, design the experiment, collect data, analyze data, as well as revise the paper.

References

Böhlke J-K (2002) Groundwater recharge and agricultural contamination. Hydrogeology Journal 10: 153-179. doi: 10.1007/s10040-001-0183-3.

Brunner P, Doherty J, Simmons CT (2012) Uncertainty assessment and implications for data acquisition in support of integrated hydrologic models. Water resources research.

Calamak M, Yanmaz AM (2017) Uncertainty Quantification of Transient Unsaturated Seepage through Embankment Dams. International Journal of Geomechanics 17: 04016125. doi: doi:10.1061/(ASCE)GM.1943-5622.0000823.

Callahan TJ, Vulava VM, Passarello MC, Garrett CG (2012) Estimating groundwater recharge in lowland watersheds. Hydrological Processes 26: 2845-2855. doi: https://doi.org/10.1002/hyp.8356.

Carrera-Hernández JJ, Smerdon BD, Mendoza CA (2012) Estimating groundwater recharge through unsaturated flow modelling: Sensitivity to boundary conditions and vertical discretization. Journal of Hydrology 452-453: 90-101. doi: 10.1016/j.jhydrol.2012.05.039.

Cartwright I, Cendón D, Currell M, Meredith K (2017) A review of radioactive isotopes and other residence time tracers in understanding groundwater recharge: Possibilities, challenges, and limitations. Journal of Hydrology 555: 797-811. doi: https://doi.org/10.1016/j.jhydrol.2017.10.053.

Cheng D, Wang W, Zhan H, Zhang Z, Chen L (2020) Quantification of transient specific yield considering unsaturated-saturated flow. Journal of Hydrology 580: 124043. doi: https://doi.org/10.1016/j.jhydrol.2019.124043.

Cheng Y, Zhan H, Yang W, Dang H, Li W (2017) Is annual recharge coefficient a valid concept in arid and semi-arid regions? Hydrology and Earth System Sciences 21: 5031.

Childs E (1960) The nonsteady state of the water table in drained land. Journal of Geophysical Research 65: 780-782.

Cobos D, Chambers C (2010) Calibrating ECH2O soil moisture sensors, application note. Available at:(accessed 29 November 2014).

Crosbie RS, Binning P, Kalma JD (2005) A time series approach to inferring groundwater recharge using the water table fluctuation method. Water Resources Research 41. doi: 10.1029/2004wr003077.

Crosbie RS, Doble RC, Turnadge C, Taylor AR (2019) Constraining the magnitude and uncertainty of specific yield for use in the water table fluctuation method of estimating recharge. Water Resources Research.

da Silva AC, Armindo RA, Brito AdS, Schaap MG (2017) An Assessment of Pedotransfer Function Performance for the Estimation of Spatial Variability of Key Soil Hydraulic Properties. Vadose Zone Journal 16: vzj2016.2012.0139. doi: https://doi.org/10.2136/vzj2016.12.0139.

de Vries JJ, Simmers I (2002) Groundwater recharge: an overview of processes and challenges. Hydrogeology Journal 10: 5-17. doi: 10.1007/s10040-001-0171-7.

Delottier H, Pryet A, Lemieux JM, Dupuy A (2018) Estimating groundwater recharge uncertainty from joint application of an aquifer test and the water-table fluctuation method. Hydrogeology Journal 26: 2495-2505. doi: 10.1007/s10040-018-1790-6.

dos Santos Júnior AG, Youngs EG (1969) A study of the specific yield in land-drainage situations. Journal of Hydrology 8: 59-81. doi: https://doi.org/10.1016/0022-1694(69)90031-6.

Duke HR (1972) Capillary properties of soils-influence upon specific yield. Transactions of the ASAE 15: 688-0691.

Fan J, Oestergaard KT, Guyot A, Lockington DA (2014) Estimating groundwater recharge and evapotranspiration from water table fluctuations under three vegetation covers in a coastal sandy aquifer of subtropical Australia. Journal of Hydrology 519: 1120-1129. doi: https://doi.org/10.1016/j.jhydrol.2014.08.039.

Freeze RA, Cherry JA (1979) Groundwater prentice-hall. Englewood Cliffs, NJ 176: 161-177.

Gillham RW (1984) The capillary fringe and its effect on water-table response. Journal of Hydrology 67: 307-324. doi: https://doi.org/10.1016/0022-1694(84)90248-8.

Gleeson T, Befus KM, Jasechko S, Luijendijk E, Cardenas MB (2016) The global volume and distribution of modern groundwater. Nature Geoscience 9: 161-167. doi: 10.1038/ngeo2590.

Gong C, Wang W, Zhang Z, Wang H, Luo J, Brunner P (2020) Comparison of field methods for estimating evaporation from bare soil using lysimeters in a semi-arid area. Journal of Hydrology 590: 125334. doi: https://doi.org/10.1016/j.jhydrol.2020.125334.

Healy RW, Cook PG (2002) Using groundwater levels to estimate recharge. Hydrogeology journal 10: 91-109.

Healy RW, Scanlon BR (2010) Estimating groundwater recharge. Cambridge University Press.

Huang T, Pang Z, Yang S, Yin L (2020) Impact of Afforestation on Atmospheric Recharge to Groundwater in a Semiarid Area. Journal of Geophysical Research: Atmospheres 125. doi: 10.1029/2019jd032185.

Jafari H, Sudegi A, Bagheri R (2019) Contribution of rainfall and agricultural returns to groundwater recharge in arid areas. Journal of Hydrology 575: 1230-1238. doi: https://doi.org/10.1016/j.jhydrol.2019.06.029.

Jie Z, van Heyden J, Bendel D, Barthel R (2011) Combination of soil-water balance models and water-table fluctuation methods for evaluation and improvement of groundwater recharge calculations. Hydrogeology Journal 19: 1487-1502.

Koïta M, Yonli HF, Soro DD, Dara AE, Vouillamoz J-M (2018) Groundwater Storage Change Estimation Using Combination of Hydrogeophysical and Groundwater Table Fluctuation Methods in Hard Rock Aquifers. Resources 7: 5.

Labrecque G, Chesnaux R, Boucher M-A (2020) Water-table fluctuation method for assessing aquifer recharge: application to Canadian aquifers and comparison with other methods. Hydrogeology Journal 28: 521-533. doi: 10.1007/s10040-019-02073-1.

Loheide SP, Butler Jr JJ, Gorelick SM (2005) Estimation of groundwater consumption by phreatophytes using diurnal water table fluctuations: A saturated-unsaturated flow assessment. Water resources research 41.

Lu YW, Li HJ, Si BC, Li M (2020) Chloride tracer of the loess unsaturated zone under sub-humid region: A potential proxy recording high-resolution hydroclimate (vol 700, 134465, 2020). Science of the Total Environment 710: 1. doi: 10.1016/j.scitotenv.2019.135511.

Lv M, Xu Z, Yang Z-L, Lu H, Lv M (2021) A comprehensive review of specific yield in land surface and groundwater studies. Journal of Advances in Modeling Earth Systems n/a. doi: https://doi.org/10.1029/2020MS002270.

Maréchal JC, Dewandel B, Ahmed S, Galeazzi L, Zaidi FK (2006) Combined estimation of specific yield and natural recharge in a semi-arid groundwater basin with irrigated agriculture. Journal of Hydrology 329: 281-293. doi: 10.1016/j.jhydrol.2006.02.022.

Meinzer OE (1923) The occurrence of ground water in the United States with a discussion of principles. University of Chicago.

Moeck C, Brunner P, Hunkeler D (2016) The influence of model structure on groundwater recharge rates in climate-change impact studies. Hydrogeology Journal 24: 1171-1184. doi: 10.1007/s10040-016-1367-1.

Moeck C, Grech-Cumbo N, Podgorski J, Bretzler A, Gurdak JJ, Berg M, Schirmer M (2020) A global-scale dataset of direct natural groundwater recharge rates: A review of variables, processes and relationships. Science of The Total Environment 717: 137042. doi: https://doi.org/10.1016/j.scitotenv.2020.137042.

Moeck C, Radny D, Popp A, Brennwald M, Stoll S, Auckenthaler A, Berg M, Schirmer M (2017) Characterization of a managed aquifer recharge system using multiple tracers. Science of The Total Environment 609: 701-714. doi: https://doi.org/10.1016/j.scitotenv.2017.07.211.

Moeck C, von Freyberg J, Schirmer M (2018) Groundwater recharge predictions in contrasted climate: The effect of model complexity and calibration period on recharge rates. Environmental Modelling & Software 103: 74-89. doi: https://doi.org/10.1016/j.envsoft.2018.02.005.

Nazarieh F, Ansari H, Ziaei AN, Izady A, Davari K, Brunner P. Spatial and temporal dynamics of deep percolation, lag time and recharge in an irrigated semi-arid region. Hydrogeology Journal 2018; 26: 2507-2520.

Nimmo JR, Horowitz C, Mitchell L (2015) Discrete-storm water-table fluctuation method to estimate episodic recharge. Groundwater 53: 282-292.

Pan Y, Gong H, Sun Y, Wang X, Ding F (2017) Distributed estimation and analysis of precipitation recharge coefficient in strongly-exploited Beijing plain area, China. Chinese geographical science 27: 88-96.

Pütz T, Fank J, Flury M (2018) Lysimeters in Vadose Zone Research. Vadose Zone Journal 17. doi: 10.2136/vzj2018.02.0035.

Rama F, Miotlinski K, Franco D, Corseuil HX (2018) Recharge estimation from discrete water-table datasets in a coastal shallow aquifer in a humid subtropical climate. Hydrogeology Journal 26: 1887-1902. doi: 10.1007/s10040-018-1742-1.

Scanlon BR, Healy RW, Cook PG (2002) Choosing appropriate techniques for quantifying groundwater recharge. Hydrogeology journal 10: 18-39.

Shah N, Ross M (2009) Variability in Specific Yield under Shallow Water Table Conditions. Journal of Hydrologic Engineering 14: 1290-1298. doi: doi:10.1061/(ASCE)HE.1943-5584.0000121.

Sophocleous MA (1991) Combining the soilwater balance and water-level fluctuation methods to estimate natural groundwater recharge: practical aspects. Journal of hydrology 124: 229-241.

Su D, Zhang Q, Ngo H, Dzakpasu M, Guo W, Wang X (2019) Development of a water cycle management approach to Sponge City construction in Xi'an, China. Science of the Total Environment 685: 490-496.

Sun R, Yeh T-CJ, Mao D, Jin M, Lu W, Hao Y (2013) A temporal sampling strategy for hydraulic tomography analysis. Water Resources Research 49: 3881-3896. doi: https://doi.org/10.1002/wrcr.20337.

van Genuchten MT (1980) A closed-form equation for predicting the hydraulic conductivity of unsaturated soils 1. Soil science society of America journal 44: 892-898.

Wang P, Grinevsky SO, Pozdniakov SP, Yu J, Dautova DS, Min L, Du C, Zhang Y (2014) Application of the water table fluctuation method for estimating evapotranspiration at two phreatophyte-dominated sites under hyper-arid environments. Journal of Hydrology 519: 2289-2300. doi: https://doi.org/10.1016/j.jhydrol.2014.09.087.

Wang T, Franz TE, Zlotnik VA (2015) Controls of soil hydraulic characteristics on modeling groundwater recharge under different climatic conditions. Journal of Hydrology 521: 470-481. doi: https://doi.org/10.1016/j.jhydrol.2014.12.040.

Wang T, Zlotnik VA, Šimunek J, Schaap MG (2009) Using pedotransfer functions in vadose zone models for estimating groundwater recharge in semiarid regions. Water Resources Research 45.

Wang W, Zhang Z, Duan L, Wang Z, Zhao Y, Zhang Q, Dai M, Liu H, Zheng X, Sun Y (2018) Response of the groundwater system in the Guanzhong Basin (central China) to climate change and human activities. Hydrogeology Journal 26: 1429-1441.

Wenzel LK (1936) The Thiem method for determining permeability of water-bearing materials and its application to the determination of specific yield, results of investigations in the Platte River valley, Nebraska.

Xu Y, Beekman HE (2019) Review: Groundwater recharge estimation in arid and semi-arid southern Africa. Hydrogeology Journal 27: 929-943. doi: 10.1007/s10040-018-1898-8.

Yin L, Hu G, Huang J, Wen D, Dong J, Wang X, Li H (2011) Groundwater-recharge estimation in the Ordos Plateau, China: comparison of methods. Hydrogeology Journal 19: 1563-1575.

Zhang J, Wang W, Wang X, Yin L, Zhu L, Sun F, Dong J, Xie Y, Robinson NI, Love AJ (2019) Seasonal variation in the precipitation recharge coefficient for the Ordos Plateau, Northwest China. Hydrogeology journal 27: 801-813.

Zhang Z, Wang W, Gong C, Zhang M (2020a) A comparison of methods to estimate groundwater recharge from bare soil based on data observed by a large-scale lysimeter. Hydrological Processes.

Zhang Z, Wang W, Gong C, Zhao M, Franssen H-JH, Brunner P (2021) *Salix psammophila* afforestations can cause a decline of the water table, prevent groundwater recharge and reduce effective infiltration. Science of The Total Environment: 146336. doi: https://doi.org/10.1016/j.scitotenv.2021.146336.

Zhang Z, Wang W, Gong C, Zhao M, Wang Z, Ma H (2020b) Effects of non-isothermal flow on groundwater recharge in a semi-arid region. Hydrogeology Journal. doi: 10.1007/s10040-020-02217-8.

Chapter 6 Conclusions and Outlook

6.1 Summary of main contributions

The work presented in this thesis aimed at improving the understanding of infiltration and recharge processes under bare ground and vegetated conditions, and increasing the robustness of recharge estimation. In particular, the infiltration and recharge process under different water table depths were systematically analyzed. We used multiple non-weighing lysimeters in combination with numerical models to accomplish the goal of this thesis. Some key findings and contributions can be summarized as follows:

(1) The commonly used methods for estimating evaporation under different water table depth conditions were evaluated in Chapter 2. The results show that the extinction depth can be an important reference indicator for the performance of estimating evaporation for MEP and FAO-56 skin methods. The MEP method provided the best results under different water table depth conditions. However, the MEP method overestimated evaporation under dry conditions. This research suggests that the water table depths and moisture conditions should be considered if soil evaporation is estimated in field settings. In addition, the findings presented in Chapter 2 provide valuable insights for selecting an appropriate method for estimating bare soil evaporation, taking into account the specific water table depth conditions, which can enhance the accuracy of potential recharge estimation.

(2) The influence of *Salix psammophila* on the infiltration- and recharge process was investigated in Chapter 3. The results show that *Salix psammophila* reduces groundwater recharge through the increase of interception and transpiration. *Salix psammophila* can develop dimorphic systems to increase water uptake in the upper soil zone as well as from the capillary zone above the water table if the water table depth is larger than the extinction depth. We put forth a conceptual model of root distribution density in response to varying water table depths, which can provide important impetus for upcoming root distribution models.

(3) Having established an increased understanding of the infiltration process, variably saturated subsurface flow models were explored to extract groundwater recharge in Chapter 4. These models represent all relevant hydrologic processes, but a systematic analysis of how these

models can be employed to estimate recharge is outstanding. We implemented numerous definitions of recharge in a variably saturated model and extracted recharge for a wide range of boundary conditions. The results show that recharge cannot be unambiguously extracted from variably saturated surface flow models due to the storage dynamics of the capillary zone. However, potential recharge can be uniquely extracted.

(4) Actual recharge is frequently regarded as a mere indication for water resource managers, with the water table fluctuation method being a widely employed technique globally. To better assess the performance of the water table fluctuation method, Chapter 5 examined various methods for determining specific yield, with a focus on the estimation of actual recharge, particularly the evaluation of depth-dependent specific yield. The results show that the water table depth is an important factor for determining the specific yield, and using the depth-dependent can obtain the best recharge values, however, it depends on a robust parametrization of the soil retention curve. Since the uncertainty of the specific yield is considerable, we suggest multiple approaches should be used to conceptualize the specific yield for the subsequent application of the water table fluctuation method. The findings presented in this chapter offer valuable insights for estimating actual recharge.

(5) From a methodological point of view, the thesis clearly demonstrated that lysimeters offer a high degree of precision in tracking the dynamics of soil water content, evapotranspiration rates, and groundwater levels. This renders them a particularly effective tool for understanding the complex interactions that occur between vegetation, soil, and groundwater systems under real-world conditions. This capacity is of paramount importance for the quantitative assessment of infiltration and recharge rates.

6.2 Outlook and Suggestions for Future Research

(1) Improving the estimation of evaporation under dry conditions in arid and semi-arid conditions.

In Chapter 2, we showed that the MEP method can provide the best estimation of evaporation under different water table depth conditions. However, it overestimated the actual evaporation for dry conditions. Therefore, it is very important to improve the MEP method for

the estimation of evaporation under dry conditions, especially in arid and semi-arid regions where the water is limited. Future studies can explore if using the direct measurement of specific humidity (mass of water vapor in a unit mass of moist air) can improve the accuracy of MEP under dry conditions.

Understanding evaporation under dry conditions is a prerequisite for improving the estimation of evaporation. For example, it should be clear that the process of evaporation for dry conditions is controlled by capillary flow, vapor flow, or film flow under different stages. Film flow is often ignored in the previous studies. In addition, the consideration of vapor flow would be important to further increase the robustness of evaporation estimates in arid and semi-arid regions. Other methods need to be developed to improve the estimation of evaporation by considering film flow or vapor flow so that the potential recharge can be accurately quantified.

(2) Developing a dynamic root system model taking into account water table depths and exploring the impact of large-scale afforestation on the groundwater recharge.

A limitation of Chapter 3 is that the key factors of the plant properties, such as leaf area index and sap flow were not observed continuously. Future studies should consider the influence of those factors on recharge. Moreover, the lysimeter may influence the root growth of *Salix psammophila*. Further studies should document the roots outside of lysimeters over time. Given the water table depth is influencing the root length density distribution significantly, models of the root density distribution need to be developed considering the water table depths and soil water dynamics. In addition, only individual shrubs studied, and the afforestation at large scales should be investigated in order to establish an optimal density of *Salix psammophila*. Only one type of plant was investigated in this thesis, and the influence of other native plants on the recharge and infiltration process should be further explored.

(3) Analyzing the pathway of water flow under the vegetation conditions.

The presence of vegetation may lead to preferential flow paths caused by plant roots. In this work, only the dynamics of the water level, soil water content and evapotranspiration are explored under the *Salix psammophila* condition, and the paths of water movement are not observed and simulated. Understanding the path of infiltrated water is vital for improving the

ability of the model to predict groundwater recharge. Further research can explore if there is a preferential pathway using the noninvasive electrical resistivity tomography method under the vegetation condition.